Delft University of Technology

FIELDWORK COASTAL ENGINEERING - CT5318

OCTOBER 2004

Participants

Bos, Carline

Burgers, Joppe Jort

Van Dijk, Merijn

Heeringa, Evan

Van den Hengel, David

Lausman, Robert

Oortman, Niek

Poot, Ronnie

Segboer, Tom

De Sonneville, Ben

Preface

The study Civil Engineering at Delft University of Technology (DUT) mainly consists of theoretical courses. A few opportunities are given to explore the practical side as well. One of the practical courses is “fieldwork coastal engineering (ct 5318)” in the fifth year which focuses on analyzing coastal structures and processes. In this course a trip is made to Varna, Bulgaria, to do hydraulic measurements on the beach and the coastal structures. The data was processed in Varna and analyzed once returned to Holland. To get acquainted with some other facets of coastal engineering fieldtrips are made to the trailing suction dredger “Ham 310”, to the quarries of Marciana and Sini Vir, the harbor of Burgas and Varna and a tourist trip to the northern oilfields.

This report describes the measured data, the used methods and the technical interpretation of the results.

Ir. Henk Jan Verhagen organizes the subject every year with great enthusiasm. In Varna he is assisted by ir. Boyan Savov and prof. Kristjo Daskalov. Their efforts are highly appreciated. Also the support of Eskana SA is appreciated. Thanks to them we could visit two quarries. Finally we would like to thank dredging company “van Oord” for their financial support.

Table of contents

Table of contents 4

List of figures 8

List of tables 10

1 Introduction 11

2 Analysis of the Tetra pods on breakwater of the "Sunny Day Marina" 12

2.1 Tetra pod Measurement 12

2.2 Calculation of the design wave 15

2.2.1 Hudson: 15

2.2.2 Van der Meer: 16

2.2.3 Hanzawa: 17

2.3 Maximum depth-limited wave 18

2.4 Wave transmission 18

2.5 Calculation expected breakage 20

2.6 Counted number of broken Tetrapods 21

2.7 General Analysis & Conclusions 21

2.8 Additional: The Parapet Structure 24

3 Beach measurements 25

3.1 Beach line 25

3.2 Comparison between two measuring systems 26

3.3 Beach profiles 26

3.4 Comparison between two measuring systems 32

3.5 Volume Calculation 32

3.6 Report on the sampling of beach sand on Sirius Beach and sieve analysis at TU Delft 38

3.6.1 Sampling 38

3.6.2 Sieve analysis 39

3.6.3 Conclusions from D50 values 40

3.6.4 Recommendations 41

4 Wave Measurements 42

4.1 Introduction 42

4.2 Approach: Visual observations 42

4.3 Approach: Pressure measurements 43
4.4 Results 43
4.4.1 Visual observations 43
4.5 Analysis of the observations with CRESS 45
4.5.1 Refraction 45
4.5.2 Shoaling and breaking 45
4.6 Cress calculation 46
4.7 Pressure measurements 48
5 Profile measurements of a groin 51
5.1 Introduction 51
5.1.1 Van der Meer 51
5.2 Location of measurements 52
5.3 Method used to measure profiles 53
5.4 Results of the measured profiles 53
5.5 Displacement of rocks 53
5.6 Change of total volume 55
5.7 Remarks 56
5.7.1 Accuracy 56
5.7.2 Differences of water level 56
6 Quarry Exercise 57
6.1 Introduction 57
6.2 The Quarries 57
6.3 Measurements 59
6.3.1 Small rocks 59
6.3.2 Large rocks 60
6.4 Rock density determination 62
6.5 Groyne calculations 63
6.5.1 Porosity and layer thicknesses 63
6.6 Redesign of the groyne at St. Konstantin using rock from Marciana 64
6.7 Conclusions and Recommendations 67
7 Bathymetric Survey 69
7.1 Introduction 69
7.2 Area 69

7.3 Depth 71
7.4 Implementation measurements 71
7.5 Sailing pattern evaluation sailed course and planned coarse 72
7.6 Required accuracy 72
7.7 Equipment used 73
7.8 Horizontal positioning 73
7.9 Vertical positioning 74
7.10 Survey vessel 75
7.11 Calibration echo sounder 77
7.12 Frequency and bundelwidth of echo sounder 80
7.13 Positioning GPS and echo sounder aboard 80
7.14 Variation sea level 80
7.15 Movements of survey vessel 82
7.16 Conclusion analysis of error sources 84
7.17 Results 85
7.17.1 Remark: 86
7.17.2 Attention! 87
7.17.3 Comparison previous year 88
7.18 Conclusion bathymetric survey 92
8 Project Island in sea ***93***
8.1 Demands from the hotel owner: 94
8.1.1 Technical problems: 94
8.1.2 Technical demands: 95
9 Project white lagoon ***96***
9.1 Situation description 96
9.2 Demands from the hotel owner: 96
9.2.1 Technical problems: 96
9.2.2 Technical demands: 97
9.3 Further Information: 98
Appendices ***99***
APPENDIX I: Visual Wave measurements 11 October 2004 99
APPENDIX II: Visual Wave measurements 13 October 2004 99
APPENDIX III: Measured relative heights of the groin profile (2004) 99

APPENDIX IV: Calculations rock displacement in the groin profile (2004) _____ 99

APPENDIX V: Sieve analysis data _____ 99

APPENDIX VI: Groin calculations_____ 99

APPENDIX VII: Data and Dn-distribution of small rocks at Marciana Quarry_____ 99

APPENDIX VIII: Data and Dn-distribution of large rocks at Marciana Quarry _____ 99

List of figures

FIGURE 2.1: LOCATION OF THE BREAKWATER OF THE SUNNY DAY MARINA 12
FIGURE 2.2: CONFIGURATION TETRA POD 13
FIGURE 2.3: WAVE TRANSMISSION BY OVERTOPPING OF HORIZONTALE COMPOSITE BREAKWATERS, ARMOURED WITH TETRAPODS (TANIMOTO, TAKASHI AND KIMURA 1987). 19
FIGURE 2.4: BROKEN TETRAPOD 21
FIGURE 2.5: GRAPHIC RESULTS FOR HS WITH HUDSON/VAN DER MEER/KASAWA 23
FIGURE 2.6: LEFT: PARAPET-STRUCTURE WITH CAP AND TETRA PODS IN FRONT RIGHT: BROKEN IN-SITU CONCRETE CAP 24
FIGURE 3.1: BEACHLINE MEASUREMENTS OF 2003 AND 2004 25
FIGURE 3.2: EXACT LOCATION OF REFERENCE POINT 1 27
FIGURE 3.3: EXACT LOCATION OF REFERENCE POINT 3, THE WALL (2003 PICTURES) 27
FIGURE 3.4: PROOF OF MISTAKES IN LAST YEARS NUMBERS 28
FIGURE 3.5: BEACH PROFILE NEAR HOTEL SIRIUS (L=0M) 29
FIGURE 3.6: BEACH PROFILE AT L=25 M 29
FIGURE 3.7: BEACH PROFILE AT L=50 M 30
FIGURE 3.8: BEACH PROFILE AT L=75 M 30
FIGURE 3.9: BEACH PROFILE AT L = 100 M 31
FIGURE 3.10: BEACH PROFILE AT L=125 M 31
FIGURE 3.11: MEASURING USING HORIZON AND POLES 32
FIGURE 3.12: 3D MODEL OF BEACH 36
FIGURE 3.13: TOP VIEW OF BEACH 37
FIGURE 3.14: OVERVIEW OF SAMPLING LOCATIONS AT SIRIUS BEACH 38
FIGURE 3.15: THE BEACH AT THE BEGINNING OF THE WEEK; CALM SEA, FINE WEATHER 38
FIGURE 3.16: SIRIUS BEACH AT THE END OF THE WEEK, AFTER THE STORM 40
FIGURE 4.1: WAVE HEIGHT OBSERVATIONS WITH AN ALTERNATIVE SCALE 43
FIGURE 4.2: VISUAL OBSERVATIONS 13 OCTOBER AND THEORETICAL RAYLEIGH DISTRIBUTION 44
FIGURE 4.3: VISUAL OBSERVATIONS 11 OCTOBER AND THEORETICAL RAYLEIGH DISTRIBUTION 44
FIGURE 4.4: WAVES 13 OCTOBER 45
FIGURE 4.5: DEPTH PROFILE JETTY 47
FIGURE 4.6: HS-DISTANCE 48
FIGURE 4.7: PHI-DISTANCE 48
FIGURE 4.8: WAVE HEIGHT IN TIME ACCORDING TO PRESSURE MEASUREMENT 50
FIGURE 4.9: PRESSURE MEASUREMENTS AND THEORETICAL RAYLEIGH DISTRIBUTION 50
FIGURE 5.1: TOP VIEW OF GROIN 52
FIGURE 5.2: GROIN PROFILES 54
FIGURE 6.1: MACHINES AT WORK AT MARCIANA QUARRY 58
FIGURE 6.2. THE PIT AT MARCIANA QUARRY 58
FIGURE 6.3: SINI VIR QUARRY 58
FIGURE 6.4: ROCK IS CONVERTED INTO SAND AT SINI VIR 58
FIGURE 6.5: SOME OF THE SMALL ROCKS 60

FIGURE 6.6: THE LARGE ROCKS 61
FIGURE 6.7: BRAVE STUDENTS ON THE GROYNE.....64
FIGURE 6.8: SCENERY AT SINI VIR QUARRY 65
FIGURE 7.1: ARTIFICIAL ISLAND.....70
FIGURE 7.2: AREA TO BE SURVEYED 71
FIGURE 7.3: HANDHELD GARMIN GPS AS USED IN BULGARIA 74
FIGURE 7.4: ACCURACY OF GPS 74
FIGURE 7.5: THE SETUP OF THE GARMIN FISHFINDER 100 AND ITS DISPLAY OPTIONS 75
FIGURE 7.6: SURVEY VESSEL WITH CAPTAIN 76
FIGURE 7.7: INFLUENCE OF TEMPERATURE AND SALINITY ON THE PROPAGATION SPEED OF SOUND IN WATER 78
FIGURE 7.8: WIND SETUP CALCULATED WITH CRESS 81
FIGURE 7.9 SIX DEGREES OF FREEDOM OF A SHIP.....82
FIGURE 7.10: SAILING PATTERN OF THE SURVEY VESSEL. THE BEACH IS ON THE LEFT SIDE WITH THE SIRIUS HOTEL IN THE NORTH AND THE MARINE IN THE SOUTH. 86
FIGURE 7.11: DEPTH CONTOUR MAP 2004.....87
FIGURE 7.12 RELIEF OF UNDERWATER SEA SLOPE (MODELING OF THE RELIEF OF UNDERWATER COASTAL SLOPE (VALCHINOV & PAVLOV) 88
FIGURE 7.13: DEPTH CONTOUR MAP 2003.....89
FIGURE 7.14: SAILING TRACK 2003.....89
FIGURE 7.15: SAILING TRACK 2004.....90
FIGURE 7.16: CALIBRATION POINTS (NOTICE THEIR UTM COORDINATES ON THE RIGHT) 91
FIGURE 8.1: LOCATION OF THE ISLAND IN SEA 93
FIGURE 8.2: ARTIFICIAL ISLAND IN FRONT OF SIRIUS HOTEL. 94
FIGURE 9.1 OVERVIEW OF THE BEACH, WITH BREAKWATER.....97
FIGURE 9.2 ALGAE GROWTH ON THE SOUTH SIDE.....97
FIGURE 9.3 FROM THE BREAKWATER, WITH IN THE BACK THE HOTEL ON THE HILL.....97
FIGURE 9.4 FROM THE BREAKWATER 97

List of tables

TABLE 2.1: TETRA POD DIMENSIONS AND WEIGHT 14
TABLE 2.2: KD-VALUES FOR TRUNK AND HEAD USING TETRAPODS 15
TABLE 2.3: CALCULATION OF THE SIGNIFICANT WAVE HEIGHT USING HUDSON 16
TABLE 2.4: CALCULATION OF THE SIGNIFICANT WAVE HEIGHT USING VAN DER MEER 17
TABLE 2.5: CALCULATION OF THE SIGNIFICANT WAVE HEIGHT USING HANZAWA 17
TABLE 2.6: CALCULATED PERCANTAGE OF BREAKAGE WITH BREAKAGE FORMULA (BURCHARTH) BASED ON SIGNIFICANT WAVE HEIGHT (VAN DER MEER) 20
TABLE 2.7: RESULTS VISUAL INSPECTION 21
TABLE 2.8: COMPARISON OF CALCULATED AND COUNTED BREAKAGE 22
TABLE 2.9: COMPARISON OF SIGNIFICANT WAVE HEIGHTS, USING HUDSON/VAN DER MEER/KASAWA 22
TABLE 3.1: VOLUME 0-25 M 33
TABLE 3.2: VOLUME 25-50 M 34
TABLE 3.3: VOLUME 50-75 M 35
TABLE 3.4: VOLUME 75-100 M 35
TABLE 3.5: VOLUME 100-125 M 36
TABLE 3.6: D50 VALUES 40
TABLE 4.1: INPUT TABLE CRESS 47
TABLE 5.1: VOLUME CHANGE 1 YEAR 55
TABLE 5.2: VOLUME CHANGE 2 YEARS 55
TABLE 6.1: MAIN CHARACTERISTICS OF FIVE LARGE ROCKS AT MARCIANA QUARRY 60
TABLE 6.2 MASS UNDER WATER, 'MOIST MASS' AND 'DRY MASS'OF STONES COLLECTED AT MARCIANA 62
TABLE 6.3: PARAMETERS FOR REGRESSION-EQUATIONS 63
TABLE 6.4: VALUES USED FOR AND RESULTS OF REGRESSION-EQUATIONS 64
TABLE 6.5: VAN DER MEER COEFFICIENTS IN CASE OF "NON-STANDARD" BLOCKINESS AND ELONGATION 66
TABLE 7.1 SOUND PROPAGATION SPEED 79
TABLE 7.2: PARAMETERS CRESS 81
TABLE 7.3 ERRORS IN HORIZONTAL POSITIONING 83
TABLE 7.4 ERRORS IN VERTICAL POSITIONING 84

1 Introduction

From 10 till 17 October a group consisting of Dutch and Bulgarian students and staff participated in a fieldwork about coastal Engineering to expose students to the problems related to data collection and interpretation of these data. The village of St-Constantin, situated next to Varna at the Black Sea in Bulgaria is the location for these investigations. In this area the tourism industry is booming; due to its lively city, good whether, and nice beaches. But as in many place in the world it also has problems related with its coast. Therefore research has to be carried out. In the past two years the same research is performed and this is used to compare with this year.

A short summary is given below of the activities and exercises performed during the fieldwork:

- Excursion to the beach of St. Constantine and surroundings.
- Start of the fieldwork. Preparation works for the bathymetric survey and the artificial island. Groyne measurement and beach line registration.
- Bathymetric survey with echo sounder and GPS, cross-sectional beach measurements, groyne measurements and visual wave height measurement.
- Excursion to expansion project of the harbor of Bourgas and visit to the trailing suction hopper dredger HAM 310.
- Measurements of wave pressure, visual wave height, groyne measurement and converting of bathymetric survey data.
- Excursion to two quarries of rock.
- Excursion to the oilfields, the landslide and the White Lagoon case.
- Tetrapod analysis on breakwater of the ‘Sunny Day Marina’ and damage calculation.

In the second chapter of this report an Analysis of the Tetra pods on breakwater of the “Sunny Day Marina is presented, where the damage is determined and different approaches are used and compared to determine the significant wave height. In the third chapter the beach measurements are described. An analysis of the development of the beach line and the beach profiles is compared with other years and a sieve analysis is carried out. Chapter four describes wave measurements for the area; these are made visually and with a pressure gauge. In chapter five, the contours of a groin in the area is measured and compared with data from other years.Chapters six contains information about the stones measurements in the quarries we visited. In chapter seven the bottom of the sea is mapped by using the echo sounding data. In chapter eight, the sediment characteristics are determined. At the village of St-Constantin a group of investigators wants to make an artificial island in the sea, requirements are presented in chapter eight. The final chapter nine relates about another project, the expansion of hotel White lagoon.

2 Analysis of the Tetra pods on breakwater of the "Sunny Day Marina"

The breakwater of the "Sunny Day" complex located in Varna, Bulgaria is analyzed in this chapter. The breakwater at this site is composed as a caisson type breakwater with Tetra pods in front of the caisson. The breakwater was built in 1984, and has been exposed to storm waves for a large number of years. Visual inspection shows that the quality of the concrete of the Tetra pods is below standard and there are quite some Tetra pods damaged. Whether this is a serious problem, in addition to other issues, will be discussed in this chapter.

Figure 2.1: Location of the breakwater of the Sunny Day Marina

2.1 Tetra pod Measurement

By measuring the size of the legs of the Tetra pods of "Sunny Day", the volume of the Tetra pods can be determined. Subsequently this volume can be converted to the mass. The following relations are given by the Shore Protection Manual 1984.

$$V = 0.280 \cdot H^3$$
$$H = 2.096 \cdot C$$

Where, C The length of one leg

H The overall height

V The volume of the Tetra pod

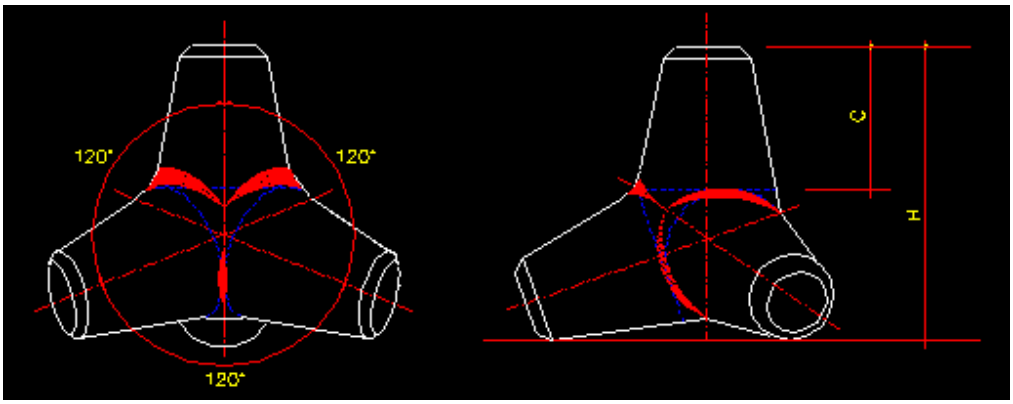

Figure 2.2: Configuration Tetra pod

The mass can be computed by using the following equation:

$$M = V \cdot \rho$$

Where, ρ Mass density [kg/m3]

The specific density of the concrete is based on a low quality concrete (more or less B25) and of course no reinforcement. Therefore a value of 2400 kg/m3 seems the most appropriate. In the table below the dimensions and the individual weight of the different Tetra pods are illustrated.

C [m]	H [m]	V [m3]	M [kg]
1,10	2,31	3,43	8236
1,15	2,41	3,92	9411
1,20	2,52	4,46	10693
1,22	2,56	4,68	11236
1,25	2,62	5,04	12086
1,30	2,72	5,66	13595

Table 2.1: Tetra pod dimensions and weight

From the table above, the different classes of Tetra pods, in terms of dimensions and weight, can be made up. Somewhat strange seems the leg-length of 1.22 meters. The value has been checked several times during the measurement; therefore a measurement error is excluded. There also seemed to be no fraction disappearing due to breakage. The odd value is probably due to the not complete filling of the concrete in the Tetra pod-mould during the casting process (poor construction).

Overall it can be concluded that Tetra pods were used with five (!) different dimensions, ranging from 8.2 to 13.6 metric tons. This seems a lot because it means that at least five different moulds had to be used, keeping in mind that a Tetra pod needs a complex mould.

The reason why different sizes are used is because at the head of the breakwater the Tetra pods have a less stable configuration, compared to the trunk. Therefore larger Tetra pods are needed at the head. Another explanation is that a Tetra pod located at a greater depth e.g. further offshore, is exposed to higher waves and therefore needs a larger mass to remain stable. The trunk of the breakwater was located at the greatest depth and consequently needs the biggest mass (13.6 tons). The other dimensions all belong to Tetra pods located at the trunk. However a breakwater of a length of about 100 meters and consisting of five different dimensions of Tetra pods is strange. Maybe Tetra pods were manufactured at different locations, or some were spares from other projects.

2.2 Calculation of the design wave

The design wave can be calculated, since the mass/equivalent cube length is now known. The formulas of Hudson, Van der Meer and Hanzawa are used.

2.2.1 Hudson:

$$H = \left[\frac{M_{50} * K_D \cot \alpha}{\rho_s} \right]^{\frac{1}{3}} \left(\frac{\rho_s}{\rho_w} - 1 \right) \text{ or } H = (K_d \cot \alpha)^{1/3} \cdot \Delta \cdot D_{n50}$$

Where,

	H	Characteristic wave height (Hs or H1/10)
	ρ_s	Mass density of concrete
	ρ_w	Mass density of water
	K_d	Stability coefficient
	M_{50}	Medium mass, in this case the weight of the Tetra pod
	D_{n50}	Equivalent cube length, $D_n = 0.65 \cdot H$
	Δ	$(\rho_s / \rho_w)-1$

Since the H1/10, the average of the highest 10 % of all waves was only briefly recommended since 1984, the significant wave height was most likely used when designing the breakwater (the breakwater was build in 1984, so probably designed before the year 1984).

Kd values	Breaking waves	Non breaking waves
Trunk	7	8
Head	5	6

Table 2.2: Kd-values for trunk and head using Tetrapods

The significant wave height, the average of the highest one third of all waves, can be calculated using the Hudson formula, see Table 2.3.

Location	Wave	H [m]	K_d	Cot a	Hs [m]
Trunk	Breaking	2,31	7	1,5	4,6
Trunk	Non breaking	2,31	8	1,5	4,8
Trunk	Breaking	2,41	7	1,5	4,8
Trunk	Non breaking	2,41	8	1,5	5,0
Trunk	Breaking	2,52	7	1,5	5,0
Trunk	Non breaking	2,52	8	1,5	5,3
Trunk	Breaking	2,62	7	1,5	5,2
Trunk	Non breaking	2,62	8	1,5	5,5
Head	Breaking	2,72	5	1,5	4,8
Head	Non breaking	2,72	6	1,5	5,1

Table 2.3: Calculation of the significant wave height using Hudson

2.2.2 Van der Meer:

$$H_s = \left(3.75 \cdot \left(\frac{N_{od}^{0.5}}{N_z^{0.25}} \right) + 0.85 \right) \cdot \Delta \cdot D_n \cdot s_{om}^{-0.2}$$

Where, Hs Significant wave height in front of the breakwater.

Dn length of cube with the same volume as tetra pods.

$$D_n = 0.65 \cdot H$$

Nod Number of units displaced out of the armour layer within a strip width of one cube length D_n (N_d=0.5).

N_z Number of waves (N_z=3000)

s_{om} Wave steepness, $s_{om} = H_s / L_{om}$

ξ = 3.0 gives the most severe attack on the slope. This is the transition zone between surging and plunging breakers. With this value the wave steepness has been calculated.

$$\xi = \frac{\tan\alpha}{\sqrt{\frac{H_s}{L_0}}}$$

This gives a wave steepness (H_s/L_0) of approximately 0.05

Location	Wave	H [m]	H_s [m]
Trunk	Breaking	2,31	4,6
Trunk	Breaking	2,41	4,8
Trunk	Breaking	2,52	5,0
Trunk	Breaking	2,62	5,2
Head	Breaking	2,72	5,4

Table 2.4: Calculation of the significant wave height using Van der Meer

2.2.3 Hanzawa:

$$H_s = \left(2.32 \cdot \left(\frac{N_{od}}{N_z^{0.5}} \right)^{0.2} + 1.33 \right) \cdot \Delta \cdot D_n$$

Where, D_n length of cube with the same volume as tetra pods. $D_n = 0.65 \cdot H$

The number of units displaced out of the armour layer within a strip width of one cube length is chosen as 0.5. The number of waves was given a value of 3000.

Location	H [m]	Hs [m]
Trunk	2,31	4,7
Trunk	2,41	4,9
Trunk	2,52	5,1
Trunk	2,62	5,3
Head	2,72	5,5

Table 2.5: Calculation of the significant wave height using Hanzawa

2.3 Maximum depth-limited wave

Due to breaking of the waves on a shallow foreshore a maximum wave height exists. A simple relation can be used for preliminary design:

$$H_s \approx 0.5 \cdot h$$

When assuming a water depth of about 9 meters in front of the breakwater and an additional wave-setup of 0.5 meters (there are no tidal fluctuations) a maximum depth-limited wave exists of 4.75 meters. When comparing this value to the calculated significant wave heights, it can be concluded that this maximum depth limited wave height is a good estimation.

2.4 Wave transmission

The significant wave height derived from the Van der Meer approach is used to calculate the wave transmission (Tanimoto, Takashi and Kimura, 1987). This is done for the head of the breakwater.

$$b_e = \frac{1}{2}\left(b_0 + b_b\right) = 7.55m$$

Where, b_0 Crest width, 2.50 m

b_b Base width, 12.6 m

R_c Crest height above sea level, 2.0 m

H_s is 5.4 m

$T_{1/3}$ is chosen 10 seconds

$$L_0 = \frac{gT^2}{2\pi} = \frac{9,81 \cdot 10^2}{2\pi} = 156.1m$$

$$\frac{h}{L_0} = \frac{9}{156.1} = 0.058$$ so it can be calculated (using a table) that L1/3 = $$\frac{h}{0.1143} = 78.7m$$

$$\frac{b_e}{L_{1/3}} = 0.096 \qquad \frac{R_c}{H_s} = 0.37$$

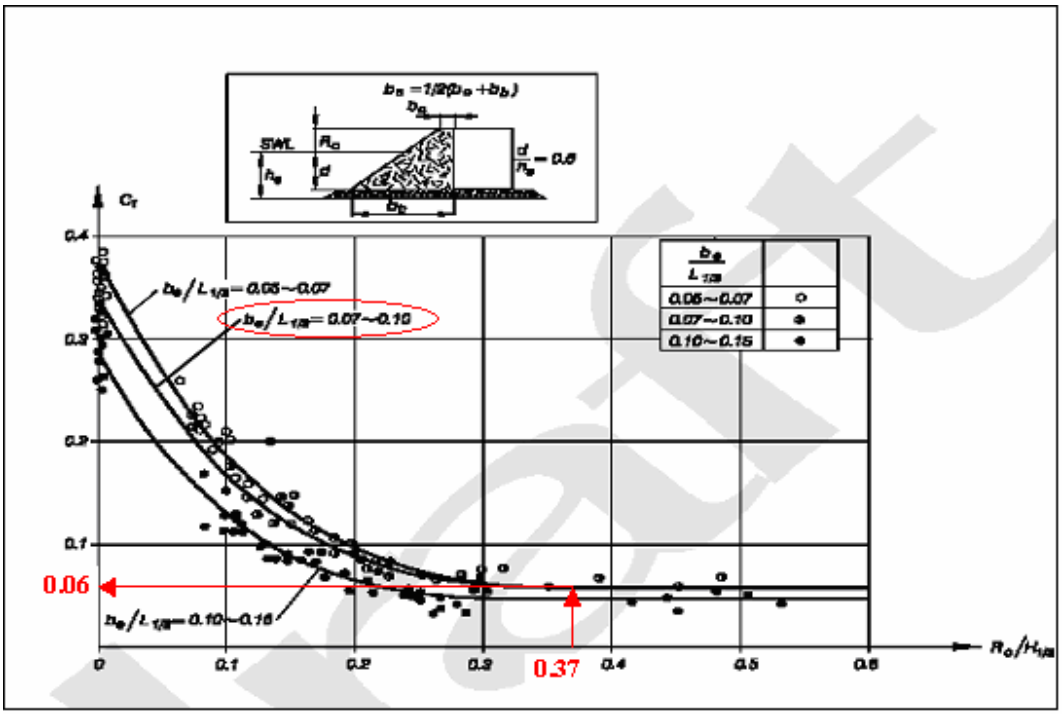

Figure 2.3: Wave transmission by overtopping of horizontale composite breakwaters, armoured with Tetrapods (Tanimoto, Takashi and Kimura 1987).

The waveheight at the leeside of the breakwater can be calculated:

$$H_T = C_T \cdot H_i$$

Where, H_T Transmitted wave height

C_T Transmission coefficiënt

H_i Incident waveheight, e.g. the significant waveheight

The transmitted wave height is $0.06 \cdot 5.4 = 0.32m$. The transmitted waveheight for the breakwater section with the parapet structure is lower than this value.

2.5 Calculation expected breakage

For the calculation of the expected breakage, the breakage formula for Tetra pods (Burcharth) is used.

$$B = C_0 * M^{C1} * f_T^{C2} * H_s^{C3}$$

Where, B relative breakage

M Armor unit mass in ton, $2.5 \leq M \leq 50$

f_T Concrete static tensile strength in MPa, $2 \leq fT \leq 4$

H_s Significant wave height in meters

C_0, C_1, C_2, C_3 Fitted parameters

The significant wave heights are based on the Van der Meer formula.

Location	M [ton]	C_0	C_1	C_2	C_3	f_T [Mpa]	H_s [m]	B [%]
Trunk	8,2	0,00393	-0,79	-2,73	3,84	2	4,6	3,9
Trunk	9,4	0,00393	-0,79	-2,73	3,84	2	4,8	4,2
Trunk	10,7	0,00393	-0,79	-2,73	3,84	2	5,0	4,4
Trunk	12,1	0,00393	-0,79	-2,73	3,84	2	5,2	4,6
Head	13,6	0,00393	-0,79	-2,73	3,84	2	5,4	4,9

Table 2.6: Calculated percantage of breakage with Breakage Formula (Burcharth) based on significant wave height (Van der Meer)

This indicates that a expected breakage of 4 to 5 % will occur, by using the breakage formula.

2.6 Counted number of broken Tetrapods

During visual inspection at the breakwater of the “Sunny Day Complex” the following broken Tetra pods were counted. The percentage of breakage is 2.9 %. The number of Tetra pods counted concerns the breakwater cross-section which was visible. This means the Tetra pods below the water level was not accounted for. However these are also not exposed to high wave forces. Unfortunately no distinction was made between breakage and the location of the head and the trunk of the breakwater.

Tetrapods		
No.Counted	No. Broken	% Broken
275	8	2,9

Table 2.7: Results visual inspection

Figure 2.4: Broken Tetrapod

2.7 General Analysis & Conclusions

During visual inspection of the breakwater at the “Sunny Beach Complex” it was clear that the quality of the concrete of the Tetra pods was very low. There was clear evidence of broken

Tetra pods due to bad construction. For example a Tetra pod was broken in two parts at the longest intersection; this was clearly due to the fact that the mould was filled with concrete on two different days. The result was a bad connection and low tensile strength. The example already mentioned before of the Tetra pod with smaller legs is also an good example of poor construction. However it must be mentioned that the actual percentage of broken Tetra pods is relative low. An over dimensioning of the Tetra pods is accounted for this, therefore the poor quality of the concrete did not lead to serious damage.

Location	B [%]
Trunk	3,9
Trunk	4,2
Trunk	4,4
Trunk	4,6
Head	4,9

Location	Counted B [%]
All	2,9

Table 2.8: Comparison of calculated and counted breakage

			Hudson	Van der Meer	Kasawa
#	Location	Wave	H_s [m]	H_s [m]	H_s [m]
1	Trunk	Breaking	4,6	4,6	4,7
2	Trunk	Non breaking	4,8		
3	Trunk	Breaking	4,8	4,8	4,9
4	Trunk	Non breaking	5,0		
5	Trunk	Breaking	5,0	5,0	5,1
6	Trunk	Non breaking	5,3		
7	Trunk	Breaking	5,2	5,2	5,3
8	Trunk	Non breaking	5,5		
9	Head	Breaking	4,8	5,4	5,5
10	Head	Non breaking	5,1		

Table 2.9: Comparison of Significant wave heights, using Hudson/Van der Meer/Kasawa

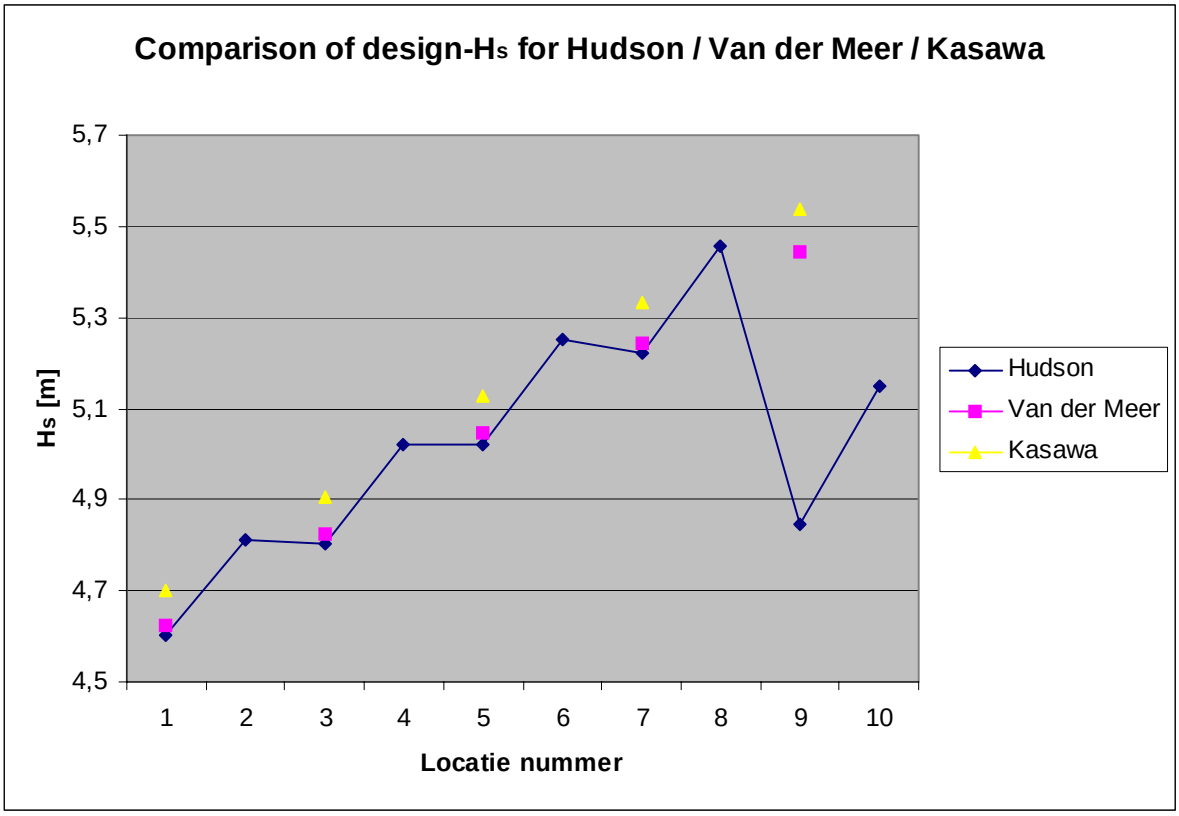

Figure 2.5: Graphic results for Hs with Hudson/Van der Meer/Kasawa

The numbers on the x-axis coincide with the numbers in the table above; where one until eight indicates the trunk and numbers nine and ten are related to the head of the breakwater.

Clearly is illustrated in the graph that the difference in significant wave height between the three formulas is in most cases not much. Also must be mentioned that the values above indicate the significant wave height in relation to a already dimensioned armour unit, e.g. a low significant wave height, means a conservative approach. The most conservative approach is Hudson and the least conservative is Hanzawa.

The formula of Van der Meer contributes the most parameters, with respect to the Hudson formula, which does not take into account the wave steepness, porosity, damage and number of waves. Hanzawa does include the number of waves and the damage but it doesn't include the wave steepness. Hudson however does contain a "dustbin-factor" in which the accepted degree of damage and wave (non) breaking is implicitly included. Hudson also makes a distinction between the head and the trunk section of the breakwater. This result can be clearly seen at number nine, which indicates the head section. The design wave height is for

the Hudson approach significantly lower. Overall it can be concluded that the Van der Meer approach obtains the most relevant parameters and is the most appropriate solution.

2.8 Additional: The Parapet Structure

In the Northern section of the breakwater a parapet-structure is situated, which consists of prefabricated elements. Over the precast elements a cap has been made with in-situ concrete and reinforcement in longitudinal direction. At some places the in-situ concrete is broken (see also the pictures below).

Figure 2.6: Left: Parapet-structure with cap and Tetra pods in front Right: Broken in-situ concrete cap

Because of the bad attachment between the interface of the precast parapet-structure and the in-situ cap, the waves could penetrate the surface (through present cracks and there was also no reinforcement through the interface of the parapet and the in-situ cap). Because of the high pressures during wave loading the waves could subsequently penetrate the structure. This caused finally the failure of the cap. It must be stressed that the failure of this cap means no failure of the breakwater. The cap was only of esthetic essence.

3 Beach measurements

3.1 Beach line

During two days investigations have been made to mark the line between sea and land. This was done using a so-called Global Positioning System (GPS) device. This device collects data from satellites and stores it in his memory. Afterwards this data can be put on a computer and plotted using a spreadsheet program (like excel). Also the data from last year is available and so these numbers can be compared to see the changes in the beach line.

It should be noted that not all data from the GPS device is used. During the measurements the machine was turned on while walking to the beach and back. These numbers have not been used because they are irrelevant to this comparison. Also the irrelevant numbers from last year were erased. The results are plotted in Figure 3.1.

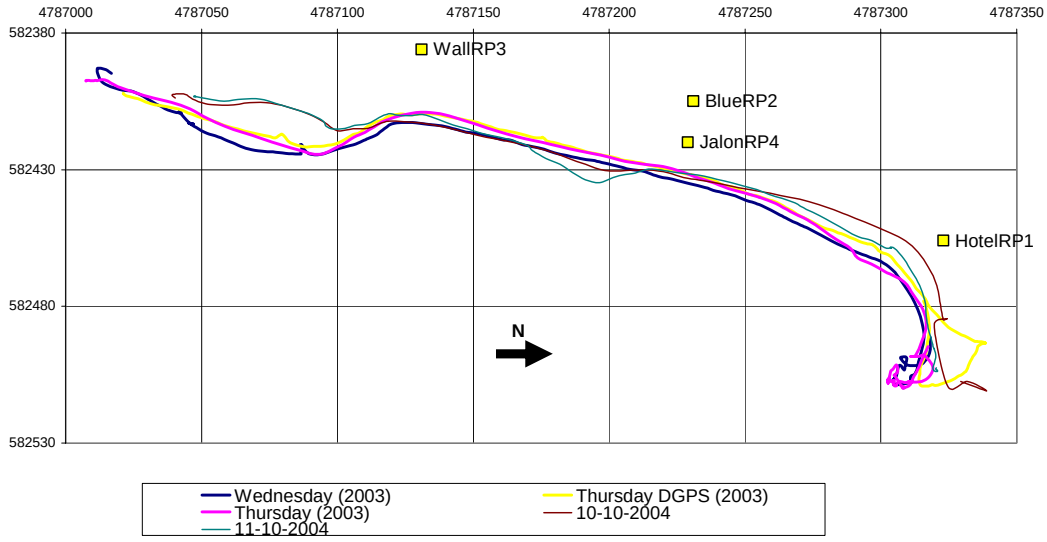

Figure 3.1: Beachline measurements of 2003 and 2004

One can easily see that at the left of the graph (and therefore also left side of the beach) a lot of sand has disappeared. In the middle some accretion has occurred and also at the right some erosion is visible.

3.2 Comparison between two measuring systems

In the exercise it is mentioned that the measurements should be taken with two different systems, being GPS and DGPS. Although only one system is used (GPS) it is possible to say something about the accuracies of both systems. With GPS the accuracy is in the order of meters, compared to DGPS with accuracy in the order of centimeters or millimeters. This kind of accuracy seems unreasonably high, because when measuring beaches it simply is not needed. For example, when the water level rises a little bit, the beach line will retreat far more, resulting in a far less accuracy. Therefore the measurements that were taken using the GPS are accurate enough.

3.3 Beach profiles

Not only is the beach line a good indication of the erosion and accretion taking place. Also the beach profile has to be considered. Therefore also 5 beach profiles have been measured. At first the location of the baseline has to be decided. It is advisable to take a straight line between two points which won't move. This is because in the future one could want to redo these measurements to compare the results. For making accurate measurements it is also advisable the line can be checked over and over again during those measurements, so one can verify his location is still on the baseline. Therefore these reference points should also be in a visibility line, meaning while walking on this line, both reference points should be visible.

This is exactly what was done last year and this year the same baseline was used. The baseline is the virtual line between the hotel at the north side of the beach (Sirius hotel), which acted as reference point 1 (see Figure 3.2) and a wall on the other side of the beach, called reference point 3 (Figure 3.3). The hotel is easily recognizable when standing on the beach.

Figure 3.2: Exact location of Reference Point 1

Just below the end of the arrow is a concrete flat, where the bar for the reference point was placed. Note that this flat concrete area is just at the downside of concrete staircase.

To recognize the other Reference Point, pictures where used from the group who visited Varna (or Bapha) in 2003. This point is located just near the staircase made of stone. This staircase is going up in a circling way.

Figure 3.3: Exact location of Reference Point 3, the wall (2003 pictures)

Now the baseline is located the measurements can be done. Also because one wants to compare the numbers these locations should be the same as the ones that were used before. Last year the measurements were done every 25 meters starting at the hotel. This year the same locations were used.

It should be noted that comparing the numbers of 2004 with 2003 was quite difficult. When making the first graphs containing the results from both years (randomly starting at 50 meters away from the hotel) the result was that the beach had risen, as can be seen below.

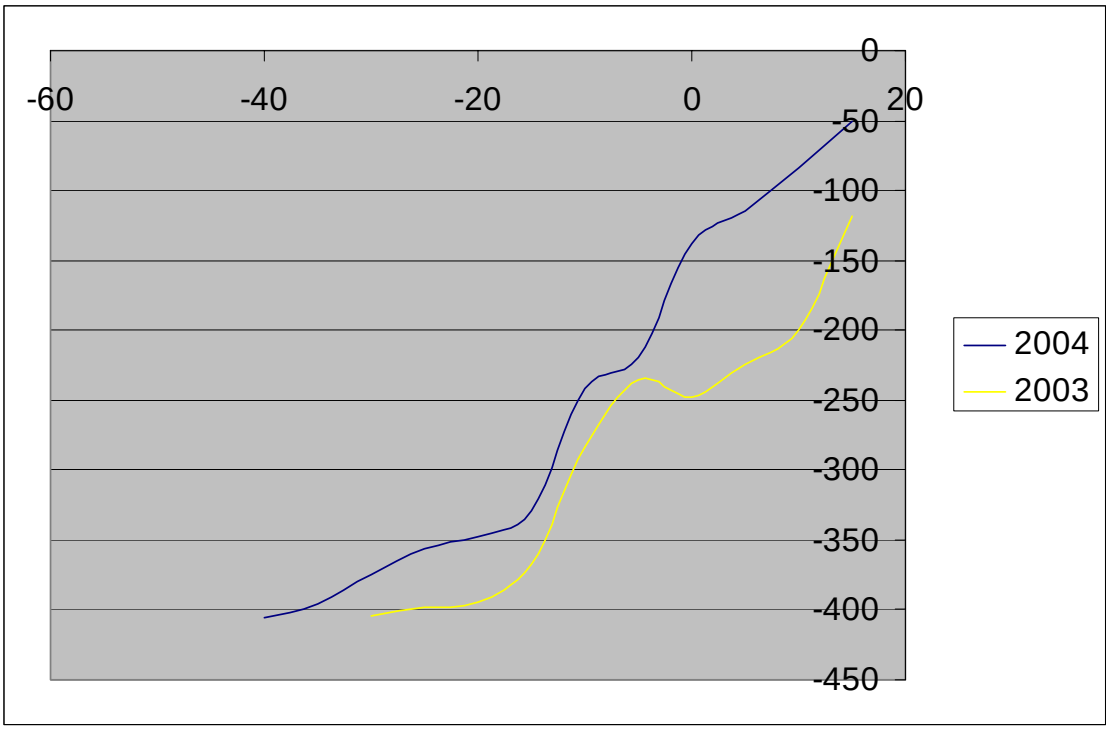

Figure 3.4: Proof of mistakes in last years numbers

This is a strange result since there is no information about any suppletion or whatsoever. Therefore the results from last year where examined carefully and the conclusion was, some mistakes were made in the formulas. The formulas were linked incorrectly to the reference level resulting in height differences of even meters in some cases.

Added to this, the sheet contained a number of reference levels. In some cases, after thorough examination, one can assume the wrong reference level is used, in some cases it is really difficult to decide which reference level should be used. Therefore comparing the results of 2004 with 2003 is difficult and probably not without errors. Although the numbers of 2004 should be correct, the difference with 2003 is unknown due to the mistakes that have been made last year.

Nevertheless all effort has been put in the graphs to make them as accurate as possible.

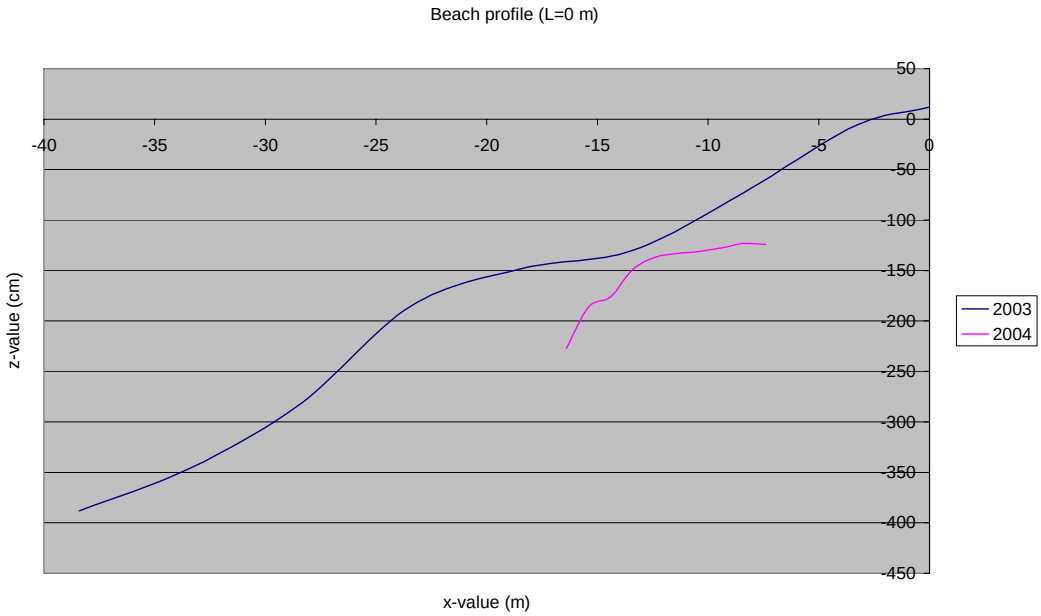

Figure 3.5: Beach profile near hotel Sirius (L=0m)

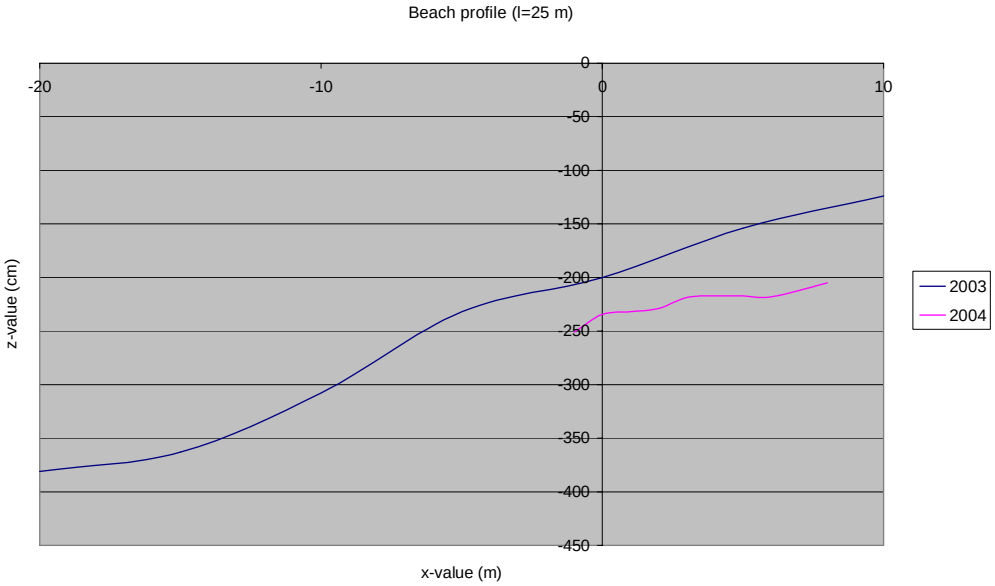

Figure 3.6: Beach profile at L=25 m

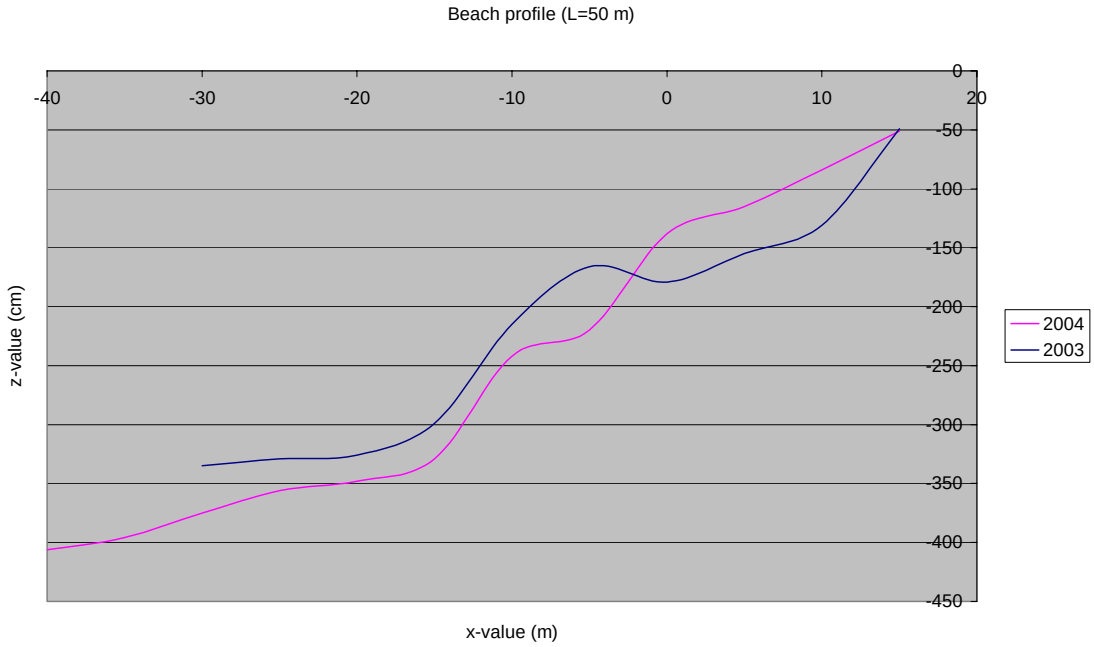

Figure 3.7: Beach profile at L=50 m

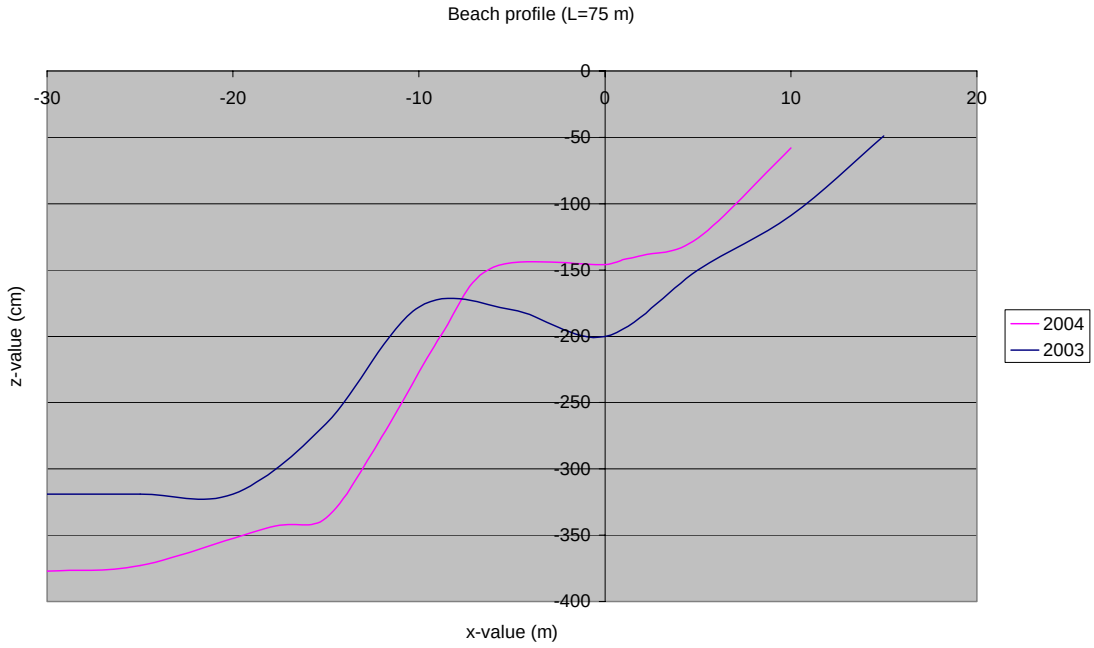

Figure 3.8: Beach profile at L=75 m

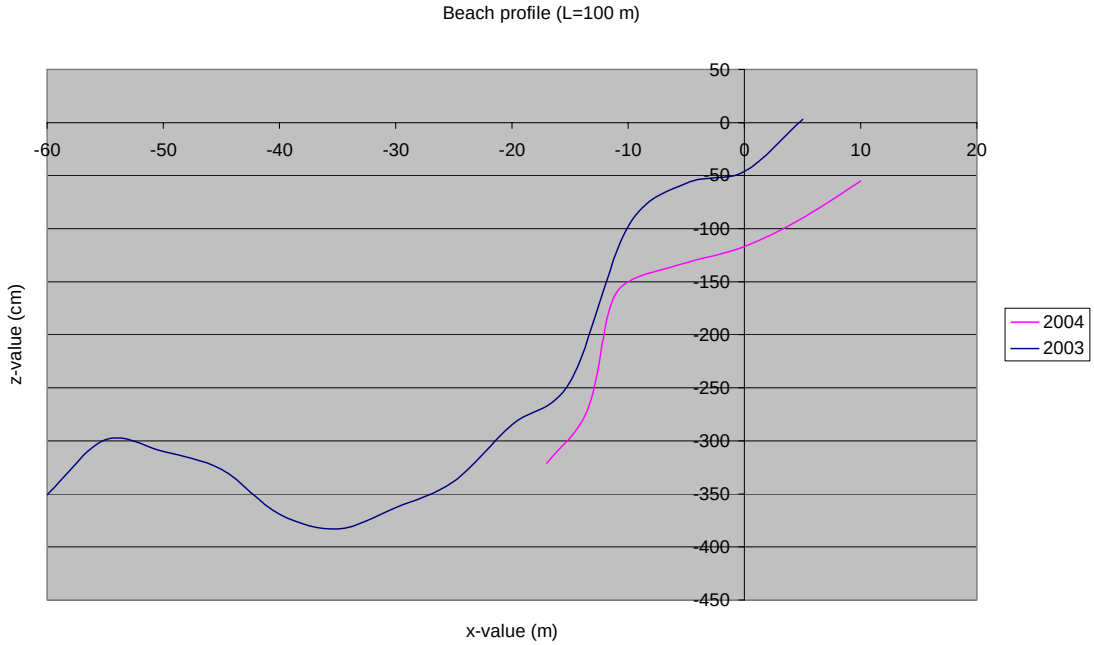

Figure 3.9: Beach profile at L = 100 m

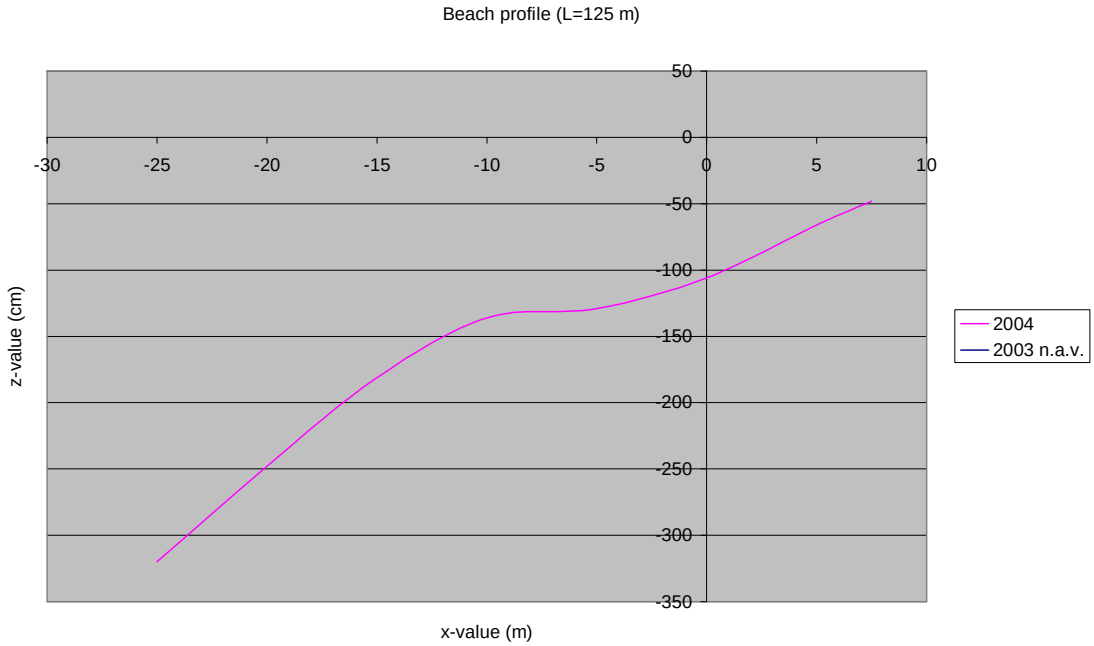

Figure 3.10: Beach profile at L=125 m

3.4 Comparison between two measuring systems

In the case of the beach profiles also two measuring systems can be used. Only one was used by our teams and therefore comparison between the systems is difficult. Using a theodolite (like was done by our teams) maybe is over accurate. The results have accuracies in the order of millimeters (although they were noted in centimeters). This seems too high, because the level of the beach changes every minute a few centimeters, for example by wind, water or people walking over it. The accuracies that can be achieved using only visual instruments (as demonstrated in Figure 3.11) can be assumed to be in the order of 5 to 10 centimeters. Note that this is only an assumption; this measuring system was not used. To make a good conclusion about this, one should have comparable numbers. For now, one can say that the measurements that were done are at least accurate enough. About being over accurate nothing wise can be said.

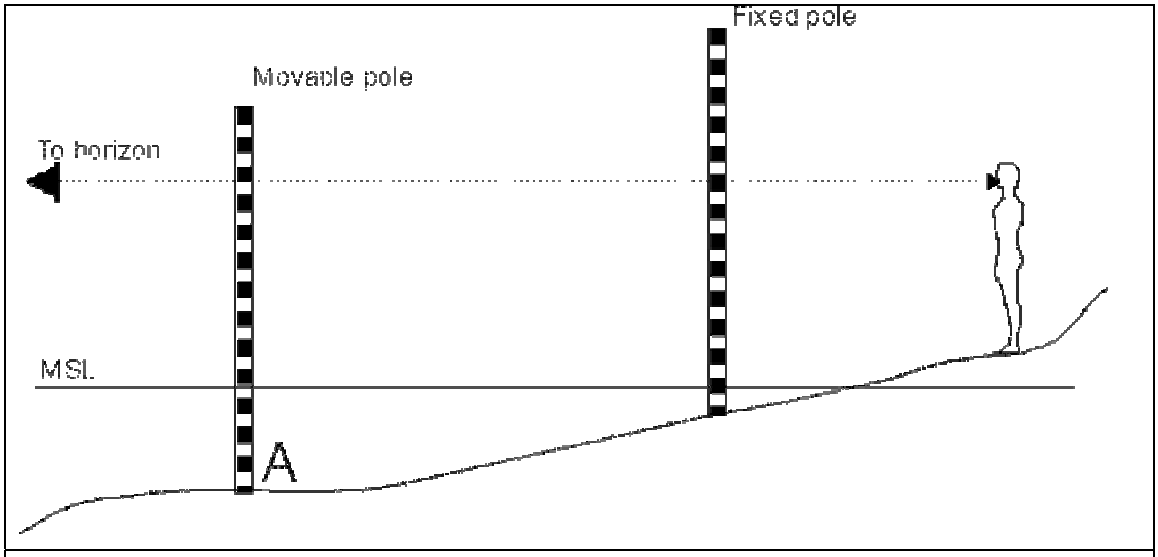

Figure 3.11: Measuring using horizon and poles

3.5 Volume Calculation

Last year (2003) the volume of the beach was calculated over the area where beach measurements were done. In 2004 not the same area was measured, but only approximately half of it. This makes it impossible to compare the results between the two years. If the results from 2003 were separated in smaller areas those areas could have been compared. Another thing is that the total volume of the beach from last year was about 1.7 * 106 m3. A simple

calculation by hand shows that this can not be correct. The area that was considered was about 200 m * 140 m = 28000 m2 (very roughly). This means the average depth that was taken into account last year would be around 1.7 * 106 m3 / 28000 m2 = 60,7 m. This does not sound reasonable.

Now the results from this year are presented in areas of every 25 meters, starting from the Sirius hotel. It should be noted that for every part the volume of sand was taken that was in the observed area to a depth of 5 m below the reference point. This point was taken because it is far below the water level (which was approximately near 2 m below the reference point). Therefore it can be assumed that also in next years the same area can be taken into account. The fact that in all results the fill volume is zero, shows that nowhere the measurements were below -5 m.

The results are shown in tables (Table 3.1 - Table 3.5) below:

VOLUME COMPUTATIONS 0-25 m	
UPPER SURFACE	
Grid File:	F:/STUDIE/5318/RESULTS/SURFERSRC0-25.GRD
Grid size as read:	38 cols by 50 rows
Delta X:	0.659459
Delta Y:	0.510204
X-Range:	-16.4 to 8
Y-Range:	0 to 25
Z-Range:	-2.50754 to -1.23392
CUT & FILL VOLUMES	
Positive Volume [Cut]:	1886.22
Negative Volume [Fill]:	0

Table 3.1: Volume 0-25 m

VOLUME COMPUTATIONS 25-50 m	
UPPER SURFACE	
Grid File:	F:/STUDIE/5318/RESULTS/SURFERSRC25-50.GRD
Grid size as read:	38 cols by 50 rows
Delta X:	1.48649
Delta Y:	0.510204
X-Range:	-40 to 15
Y-Range:	25 to 50
Z-Range:	-4.06 to -0.509998
CUT & FILL VOLUMES	
Positive Volume [Cut]:	3098.58
Negative Volume [Fill]:	0

Table 3.2: Volume 25-50 m

VOLUME COMPUTATIONS 50-75 m	
UPPER SURFACE	
Grid File:	F:/STUDIE/5318/RESULTS/SURFERSRC50-75.GRD
Grid size as read:	38 cols by 50 rows
Delta X:	1.48649
Delta Y:	0.510204
X-Range:	-40 to 15
Y-Range:	50 to 75
Z-Range:	-4.06788 to -0.461522

CUT & FILL VOLUMES	
Positive Volume [Cut]:	3380.78
Negative Volume [Fill]:	0

Table 3.3: Volume 50-75 m

VOLUME COMPUTATIONS 75-100 m	
UPPER SURFACE	
Grid File:	F:/STUDIE/5318/RESULTS/SURFERSRC75-100.GRD
Grid size as read:	38 cols by 50 rows
Delta X:	1.08108
Delta Y:	0.510204
X-Range:	-30 to 10
Y-Range:	75 to 100
Z-Range:	-3.78981 to -0.550004
CUT & FILL VOLUMES	
Positive Volume [Cut]:	2761.64
Negative Volume [Fill]:	0

Table 3.4: Volume 75-100 m

VOLUME COMPUTATIONS 100-125 m	
UPPER SURFACE	
Grid File:	F:/STUDIE/5318/RESULTS/SURFERSRC100-125.GRD
Grid size as read:	38 cols by 50 rows
Delta X:	0.945946

Delta Y:	0.510204
X-Range:	-25 to 10
Y-Range:	100 to 125
Z-Range:	-3.38777 to -0.433485
CUT & FILL VOLUMES	
Positive Volume [Cut]:	2903.86
Negative Volume [Fill]:	0

Table 3.5: Volume 100-125 m

To get some insight in how the beach looked at the moment of measuring a 3D model is shown in Figure 3.12 and Figure 3.13

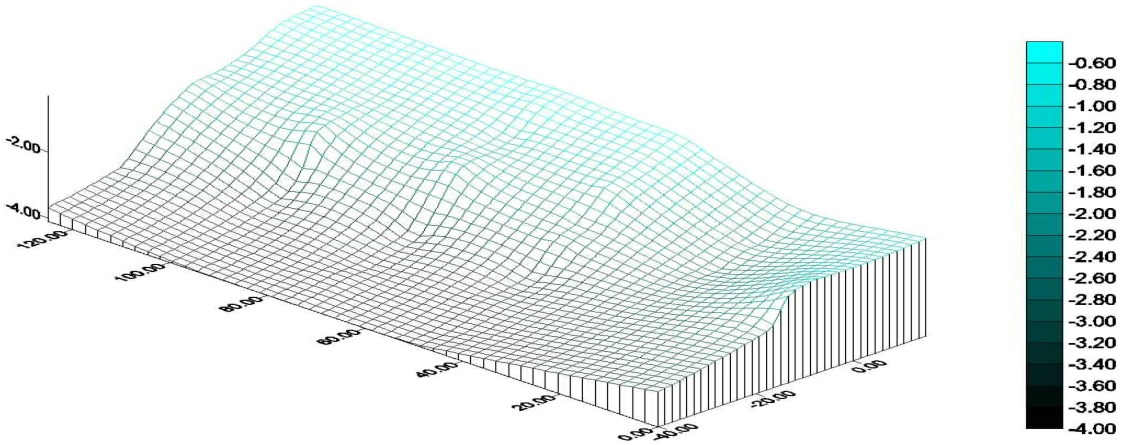

Figure 3.12: 3D model of beach

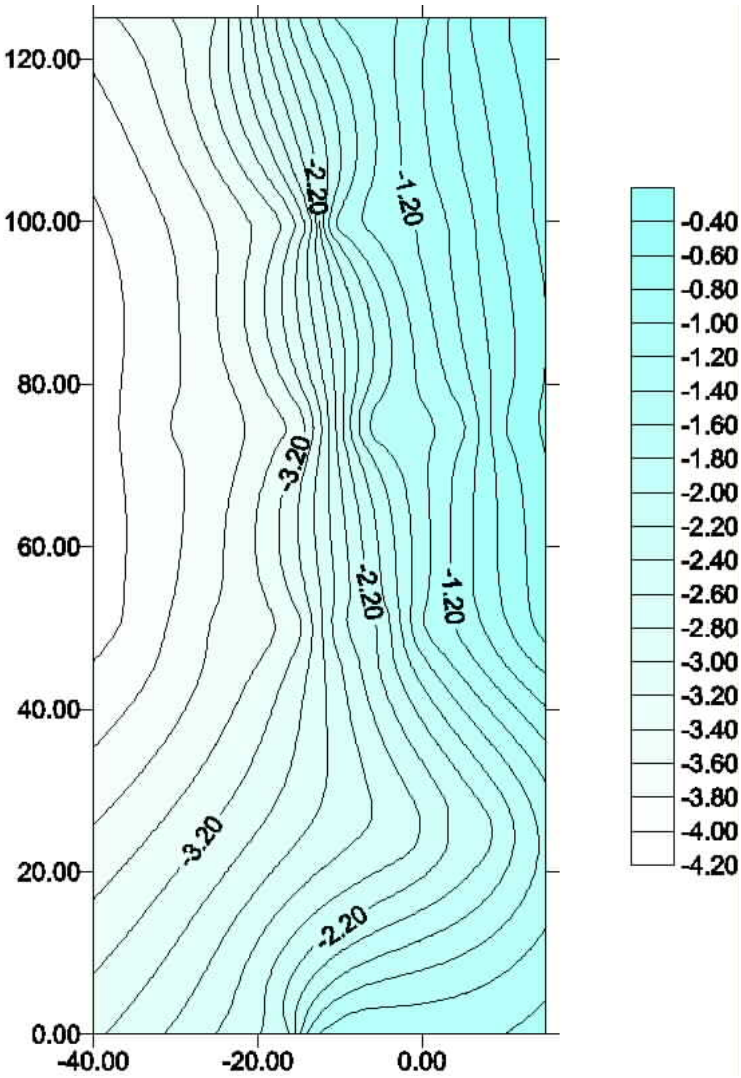

Figure 3.13: Top view of beach

It is also possible to calculate the total volume of the beach with the grid files of all the areas combined. This would not be correct to do, because the areas have not been measured over the same width of the beach. The program will fill in the blanks and suggest there is sand where it is probably not. This calculation would be less accurate than the ones presented above.

3.6 Report on the sampling of beach sand on Sirius Beach and sieve analysis at TU Delft

To carry out morphological computations valid for the breaker zone in front of Hotel Sirius, the type of beach sand on the spot needs to be known. The most accurate way to determine the type of sand is to carry out sieve analysis on samples collected at the research location.

3.6.1 Sampling

On Monday October 11th samples of the sand of Sirius Beach were taken. Samples were taken just below mean sea level (MSL). We call the waterline at the moment the samples were collected (calm weather, low waves) the MSL as in the tide in the Black Sea is virtually non-existent, so this is assumed to be the waterline under normal circumstances (see 10 in the picture below), and further in the same cross-section of the dry beach: a few meters from the waterline (5), in the middle of the beach (7) and in front of the yellow building at the upper boundary of the beach. Other samples were taken (on the dry beach) in front of Hotel Sirius (12), at the north end of the beach, and in front of the wall (8) at the southern limit of the beach.

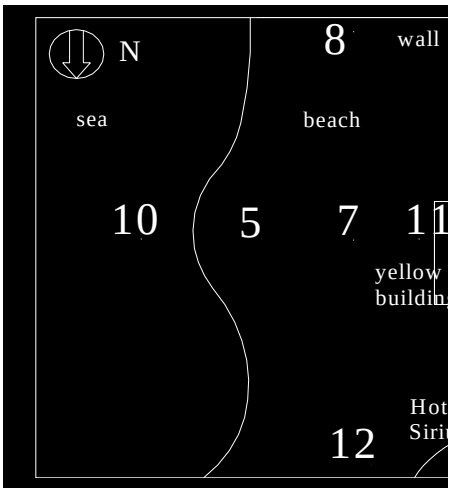

Figure 3.14: Overview of sampling locations at Sirius Beach

Figure 3.15: The beach at the beginning of the week; calm sea, fine weather

We chose these locations to get a good overview of the spread in the gradation of the sand and the spread of the median grain size of the sand particles over the beach.

The samples were taken a few decimetres below the surface to eliminate the chance that only fine particles transported by the wind were collected, whereas we were mainly interested in sediment-transport by wave motion.

The samples were numbered with the available plastic number tags. That is the reason why the samples have such a remarkable number sequence.

The sand was brought to Delft, where the sieve analysis was carried out in the Hydraulic Laboratory of the Faculty of Civil Engineering and Geosciences.

3.6.2 Sieve analysis

Every sample was examined by executing sieve analysis on the sand. Sieves with the following mesh sizes were used:

106 µm, 150 µm, 180 µm, 212 µm, 300 µm, 355 µm, 425 µm, 600 µm

The sieves were weighed first, then the samples were sieved and finally the fractions remaining on each sieve were weighed.

Using the acquired information several curves can be drawn. The most usual way to plot results from sieve analysis is plotting them on a log-normal scale. In this graph the horizontal axis represents the mesh sizes in an order of increasing mesh sizes, and the vertical axis shows the exceedence of the mesh sizes (in cumulative percentages). For well graded sand this results in an S-shaped curve. Reading the graph starting at the 50% value on the vertical axis shows a value on the horizontal axis which we call D50. This value represents the grain size which is exceeded by 50% of the sample. For well graded samples, with a rather straight line between D15 en D85, D50 is practically the same as the median grain size (Dm). D50/Dm is a key value in many important morphological equations and thereby an indispensable quantity in morphological computations.

Another way to plot data from sieve analysis is using a log-gauss scale. For well-graded samples (resulting in S-curves on a log-normal scale) this should result in a more or less straight line. If not, this could be a sign that key information (for instance the sand fraction from of the sieves) has been lost, or that the sand has a remarkable gradation.

Graphs on log-normal scale are given in appendix Graphs on log-gauss scale are represented in appendix shows the D50 of each sample.

D50 of each sample

Sample	5	12	8	11	7	10
D50 (μm)	365	405	410	390	395	320

Table 3.6: D50 values

3.6.3 Conclusions from D50 values

The order of D50-values corresponds to the order expected, taking into account the sampling location. The samples on the higher parts of the beach show the largest D50. Most notably sample 12 and 8, taken at the upper limits of the beach at the north and south sides of the beach respectively. Sand deposited here is only deposited during storms, when also larger grains are moved to other places, as the shoreline hardly ever moves under normal circumstances. So when it is deposited in such places it takes rough circumstances again to move them back. Smaller grains are more likely to be part of the dynamic profile, so it was to be expected and has actually appeared that the samples taken closer to the shoreline (5) and at MSL (10) have a smaller D50. Sample 10 shows the smallest D50, being taken on the shoreline, where small grains, which are in suspension in the breaker zone, settle.

Later in the week, when the weather deteriorated, the sea got rougher and the shoreline receded. The locations with the largest median grain size still weren't threatened by the progressing sea, though.

Figure 3.16: Sirius Beach at the end of the week, after the storm

3.6.4 Recommendations

For four out of six samples the mass of the fraction with a grain size larger than 600 μm exceeded 30% of the total mass sample, whereas the sieves with small mesh sizes hardly collected any sand at all. Next years group should replace at least one, maybe two, of the sieves with small mesh sizes by sieves with larger mesh sizes to obtain more accurate and reliable results.

Also a sample at some place in the surf zone should be considered. Here, the sample should show a larger D50. This smaller value would be caused by the effect of the orbital movements of water particles near the seabed, which causes the smaller sediment particles to be in suspension constantly. This, in turn, results in a larger D50.

4 Wave Measurements

4.1 Introduction

On 11 and 13 October, visual observations were made of the occurring waves with the use of a theodolite. In total 200 wave heights and wave periods were observed near the jetty north of the Dolphin hotel and afterwards analyzed.

On the 13th of October also a measurement with a pressure meter was executed though on a different site in the Sunny Day Marina due to storm conditions. Here wave periods were also visually determined.

By using Cress, wave transformation is determined. Data of the measurements can be found in Appendices I and II.

4.2 Approach: Visual observations

The first visual observations were made by the use of a theodolite and a rod. The rod was attached to the end of the jetty and the theodolite was placed in a straight line, and upper and lower limits of the waves were observed for hundred or more waves. During the observation of the hundred waves, the average wave period was determined by dividing the total observation time by the number of observed waves.

Due to storm conditions the second observation was made using a new scale, based upon the structure of the jetty. The total distance between two parallel horizontal steel bars was considered to be 5. By calibrating this new scale later on with the use of a photograph, wave heights in metric units were determined (see Figure 4.1).

Figure 4.1: Wave height observations with an alternative scale

4.3 Approach: Pressure measurements

The pressure measurements were made using a pressure meter and a laptop with a simple computer program. The computer program stored the pressure data every 0.1s in a text file that was used later on to transform measured pressure into wave heights by using linear wave theory. The average wave period was determined in the same way as the visual observations, by observing in total 100 waves.

4.4 Results

4.4.1 Visual observations

After observing wave heights, the significant wave height was determined by taking the average height of the 33 highest observed waves. After that, the probability of every occurring wave height was determined as the number of waves with that wave height divided by the total number of waves. By adding up the probability of the wave heights, a cumulative distribution function of the wave height is found.

The Rayleigh distribution function is defined as

$$P(H < H) = 1 - e^{(-2H/Hs)^2}$$

The observed data can be compared to this theoretical distribution function by plotting them into the same graph, see Figure 4.2 and Figure 4.3.

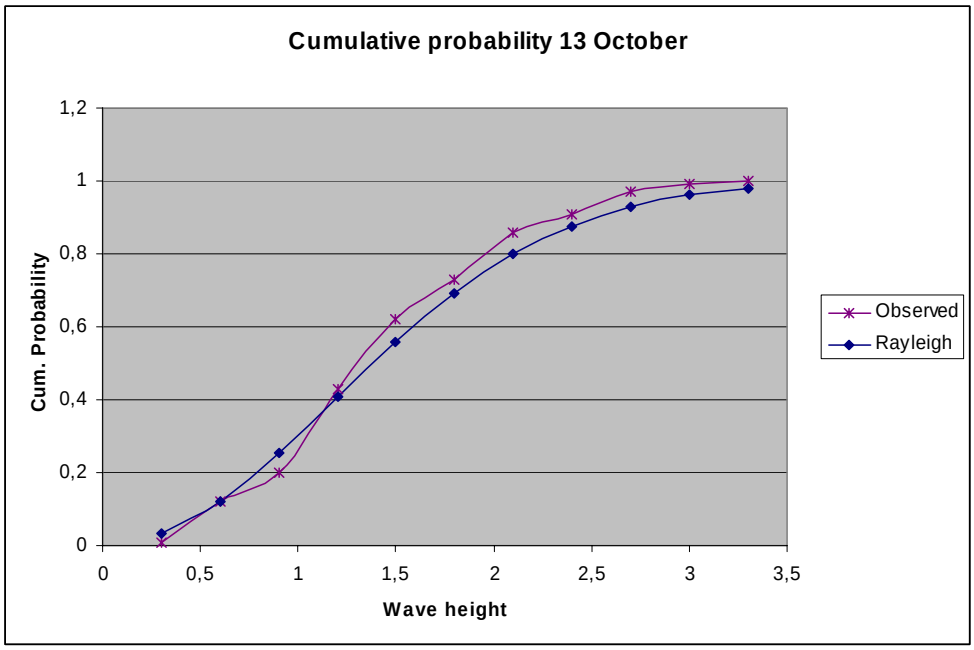

Figure 4.2: Visual observations 13 October and theoretical Rayleigh distribution

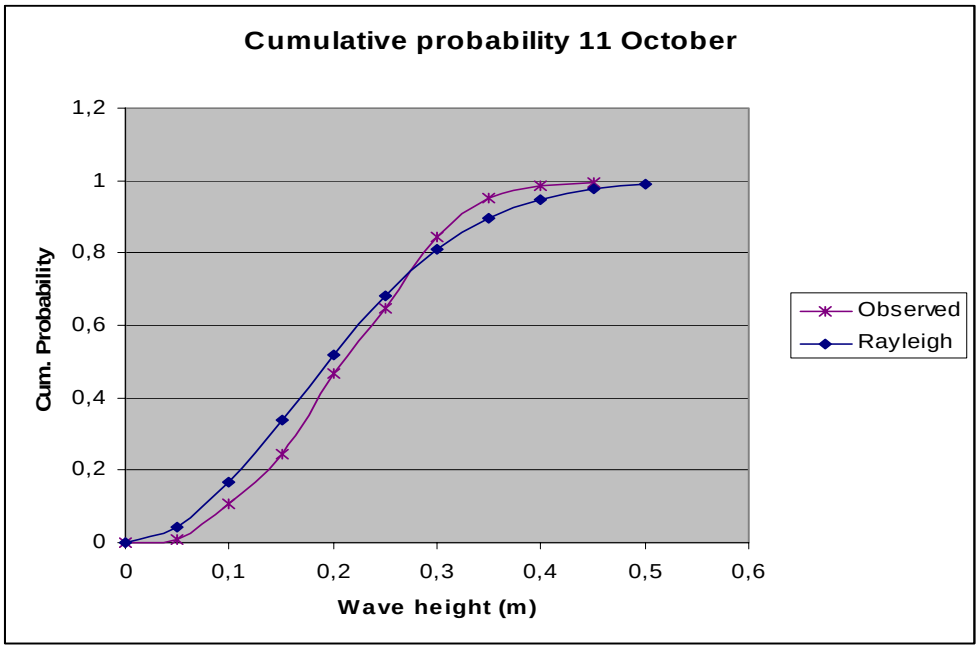

Figure 4.3: Visual observations 11 October and theoretical Rayleigh distribution

Although the observed and theoretical graphs show clear similarity, a difference can be noticed. There are less high waves observed in practice than theoretically expected. This is possibly due to the fact that the waves are not observed in deep water but in shallow water; therefore the higher waves are already influenced by breaking. Also, inaccuracy in the observations has to be taken into account.

4.5 Analysis of the observations with CRESS

4.5.1 Refraction

In our observations the waves approached the shore at an angle of 10 degrees near the jetty. Due to the shallower water near the jetty refraction occurs and the approach angle at deep water is estimated at 20 degrees.

4.5.2 Shoaling and breaking

The waves observed on that day were relatively high because of the strong wind. Approaching the shallower water near the jetty, shoaling occurred and breaking, depending on the wave height. Due to the shoaling the deep water wave kept on rising until the end of the jetty and then broke. After breaking the wave height reduced towards the shoreline. Smaller waves broke around beacon-distance.

Figure 4.4: Waves 13 October

These observations will now be compared using calculations with Cress (IHE version).

The calculation of wave energy decay of coastal hydraulics is used for this matter, to compare the observed shoaling and refraction with the theoretical values.

4.6 Cress calculation

First the input values are calculated:

A shallow water wave height $H_s = H_1 =$ 2.35 m was observed at a depth h = 2.85 m.
The observed wave period T_m was 6.84 s. $T_p = T_m / 0.8 =$ 8.55 s.

Then the following equations are used:

H1 = H0*Ks*Kr

$$K_s = \frac{1}{\frac{1+2kh}{\sinh(2kh)}\tanh(kh)}$$

with $k = 2\pi / L$

$$L_0 = \frac{gT^2}{2\pi} = 114.0m \rightarrow h/L_0 = 0.025 \rightarrow L = 44.0m \rightarrow K_s = 1.168$$

$$K_r = \sqrt{\frac{\cos\theta_0}{\cos\theta_1}} = \sqrt{\frac{\cos 20°}{\cos 10°}} = 0.977$$

H_0 = 2.35 m / (1.168 * 0.977) = 2.1 m. This is the deep water wave height.

The deep water approach angle was estimated at 20°, no current velocities (Black Sea), a density of 1018 kg/m^3, a friction coefficient of 0.01 and a wind speed of 10 m/s give the following input table:

H_0	2.1 m	ρ	1018 kg/m^3
T_p	8.55 s	F_w	0.01
θ_0	20°	V_w	10 m/s
u	0 m/s	Eta	0 m
nu	0°	Dx	10

Table 4.1: Input table Cress

Depth profile near the jetty (from hydrographical map and echo-sounder)

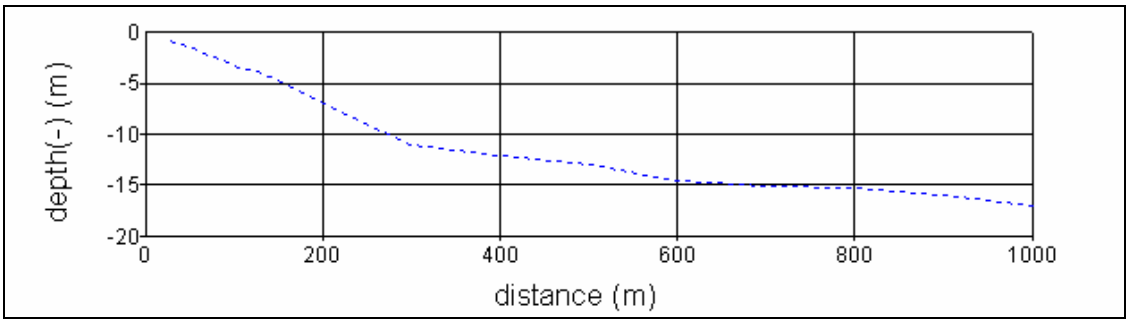

Figure 4.5: Depth profile jetty

Running Cress gives the following results:

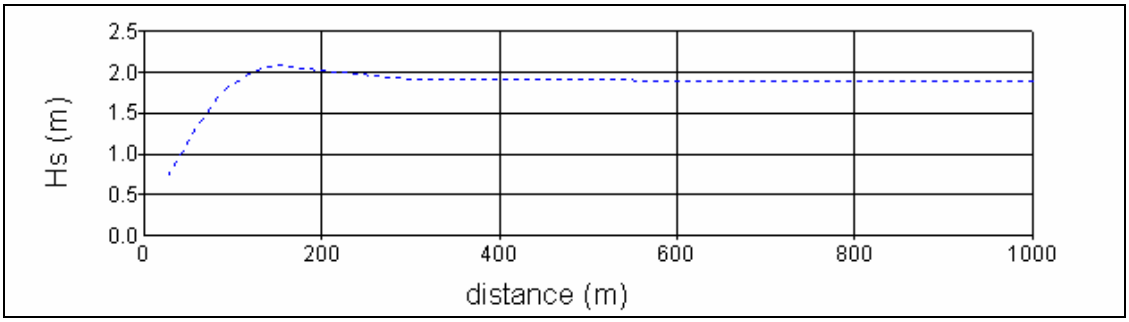

Figure 4.6: Hs-distance

This graph shows that the waves start growing at around 300 m distance from the shoreline due to shoaling. They break at a distance of about 160 m from the shore. The broken waves then decrease in height gradually towards the shoreline. This is as observed, the bigger waves break at the end of the jetty, the smaller ones around the location of the beacon and towards the shoreline they decrease gradually.

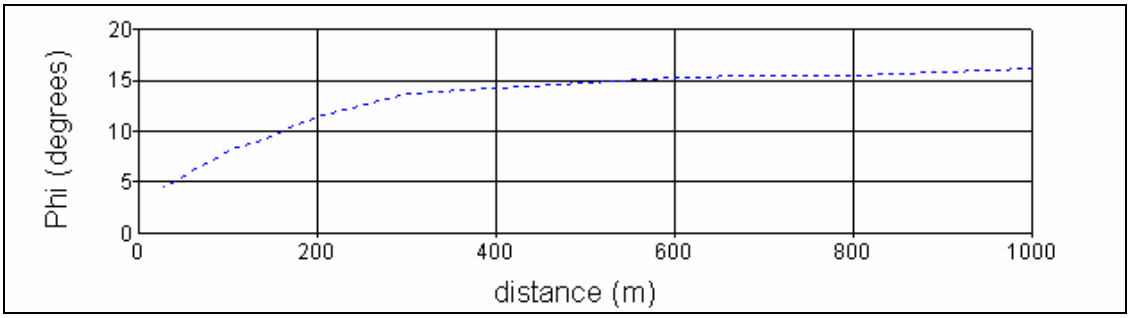

Figure 4.7: Phi-distance

Resulting from this graph is an approach angle of about 5-10 degrees around the beacon, starting with a deep water wave approach angle of 20 degrees. This was observed as well. This means the refraction is as expected.

4.7 Pressure measurements

With the pressure and the depth in the marina, one can calculate the wave heights.

We have taken a 1030 seconds time record, divided in 0.1 second per measurement. This results in 10,000 measurement points.

The wave period is calculated by counting the number of times that the waves in the graph passes the mean pressure from peak to through. This number is divided by the total time of the record. The wave period thus calculated is 8.4s.

The water depth (h) in the marina is 3.5m and the position of the instrument (z) is 1,36 m under the mean water surface.

Wave length is calculated with formula for transitional water, and is 48m.

$$L = \frac{gT^2}{2\pi}\tanh\left(\frac{2\pi}{L}h\right)$$

The wave height [a] can be determined, using linear wave theory in transitional water depth with formula:

$$p = -\rho g z + \rho g a \frac{\cosh k(h+z)}{\cosh kh}\cos kx \sin \omega t$$

a simplified formula is used (assuming θ=0 and x=0, parallel waves at the wall):

$$a = \frac{p + \rho g z}{\rho g}\frac{\cosh kh}{\cosh k(h+z)}$$

In which:	a	wave height	[m]
	p	pressure measured by gauge	[kPa]
	ρ	density water	[kg/m^3]
	T	period	[s]
	L	Wavelength	[m]
	k	wave number	[m^{-1}]
	h	water depth in marina	[m]
	z	position of the pressure measurement (negative from the water surface	[m]
	ω	wave celerity	[s-1]

The result is presented in Figure 4.8.

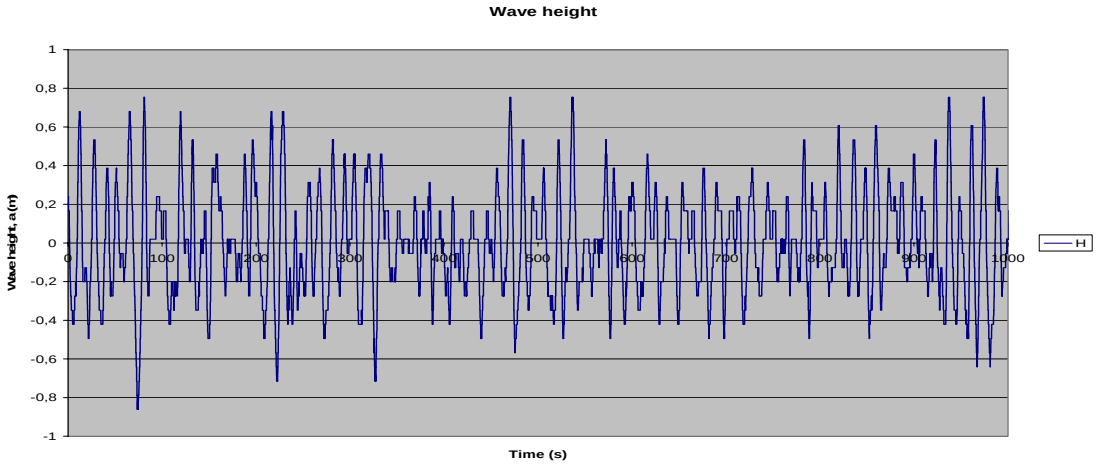

Figure 4.8: Wave height in time according to pressure measurement

To determine H_s, the wave heights are measured by hand. By estimating the wave height for the first 500s, one gets 34 waves, with the significant wave height of 1,13 m. To compare the measurements to see whether they are Rayleigh distributed the same method is used as in the visual measurements. The result is presented in Figure 4.9.

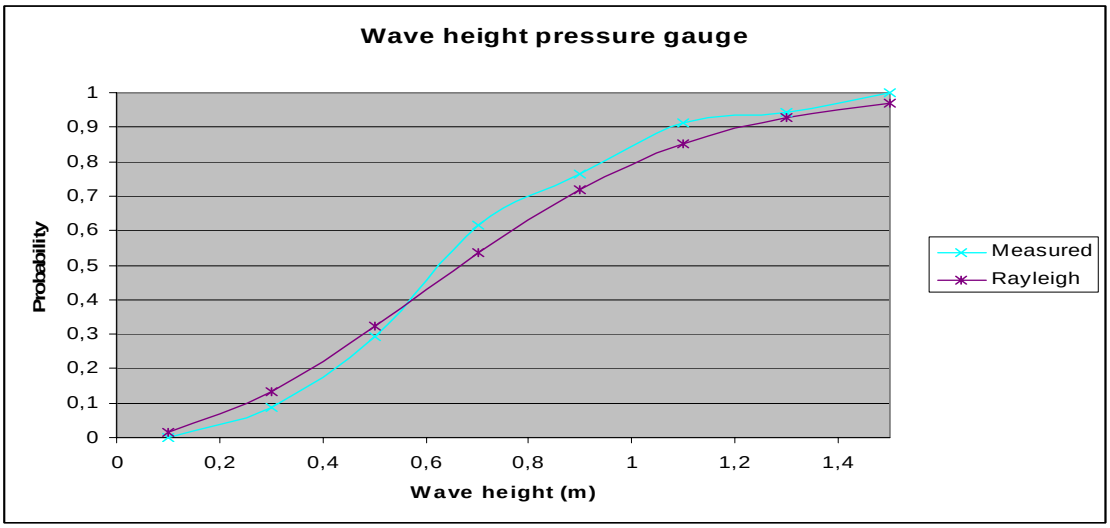

Figure 4.9: Pressure measurements and theoretical Rayleigh distribution

Although the observed and theoretical graphs again show clear similarity, the same difference can be noticed as in the visual observations; there are less high waves observed in practice than theoretical. This again is possibly due to the fact that the waves are not observed in deep water but in shallow water; therefore the higher waves are already influenced by breaking. This is a similar result as observed in the visual observations. There could also be influence of the standing waves in the marina.

Pressure reading is fairly accurate because it registers a Rayleigh distributed wave height. And errors made by inaccuracy of measurements are minimized by the use of hard and software.

5 Profile measurements of a groin

5.1 Introduction

A groin is a structure, which is built to trap littoral drift of the shore. The structure is designed to fulfill its task for many years. The assignment of this exercise is to do measurement of the groin profile. By comparing the results with the results of 2002 and 2003 the changes can be observed and indicates damage of the groin quiet well.

The resulting damage can be compared with the theoretical damage that is calculated using the method “van der Meer” suggests (not sufficient data to calculate in this exercise).

5.1.1 Van der Meer

Although van der Meer is not applied in this exercise, the calculation method is briefly explained (“introduction bank, bed and shore protection”, Schiereck 2001).

$$\frac{H_{sc}}{\Delta d_{n50}} = 6.2\,P^{0.18}\left(\frac{S}{\sqrt{N}}\right)^{0.2}\xi^{-0.5} \qquad \text{(plunging breakers)}$$

$$\frac{H_{sc}}{\Delta d_{n50}} = 1.0\,P^{-0.13}\left(\frac{S}{\sqrt{N}}\right)^{0.2}\xi^{P}\sqrt{\cot\alpha} \qquad \text{(surging breakers)}$$

$$\xi = \frac{\tan\alpha}{\sqrt{H/L_0}}$$

P is a measure for the structure’s permeability.

S is a measure for the damage

N is the number of waves

ξ is the Irribarren number

$$\xi_{\text{transition}} = \left[6.2\,P^{0.31}\sqrt{\tan\alpha}\right]^{\left(\frac{1}{P+0.5}\right)}$$

The expression for plunging breakers is used when ξ< ξtransition.

The expression for surging breakers is used when ξ> ξtransition.

5.2 Location of measurements

To make a good comparison of the groin profile, the same cross-sections are measured as the groups took last two years. The coordinate system is explained in Figure 5.1 and by the group of two year ago (with red paint the starting point is indicated on the groin):

At the end of the breakwater we searched for a fixed point that was easy to recognize and would not move or disappear in future. We chose for the right side of the breakwater and outlet channel (see photograph and drawing) seen from the shoreline on. As a starting point for the measurements we ignored the bended piece of the breakwater. We noticed that in the last horizontal concrete plate (the one before the slope, as indicated on the drawing) a little corner was missing (see detail drawing). We took this corner as a reference point of the line we stipulated along the breakwater (x = 0, x-axis along the breakwater). The starting point of the line is set 1,5 m perpendicular to this corner. Every 5 meters we marked a point, and we decided to measure a cross-profile every 10 meters perpendicular to this line, starting at L = 5 m (see drawing), ending at L = 55 m.

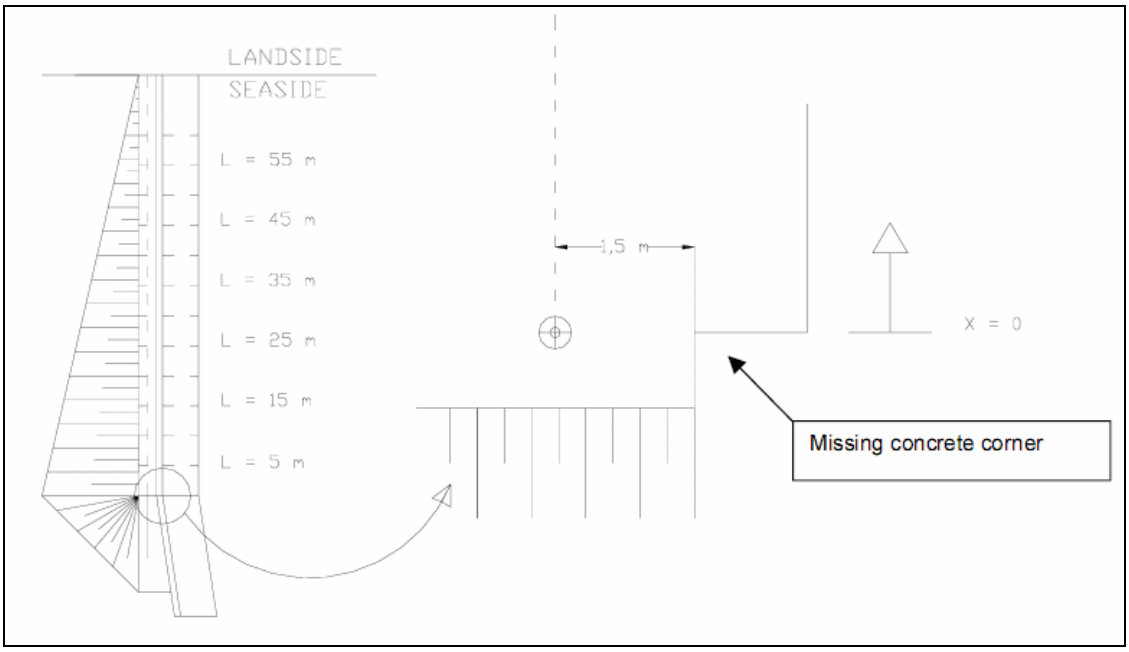

Figure 5.1: Top view of groin

5.3 Method used to measure profiles

The measurements were done by different teams all using the same equipment. After the x-axis (positive in southern direction) and the y-axis (positive in landwards direction) were determined measuring could start (the last group painted red points every 10 meters on the groin). On the five cross-sections perpendicular to the x-axis the relative height is measured. The measured points on the cross-sections were all close to each other (approximately one meter) but on the crest of the groin the surface was a flat and almost horizontal concrete plate and here the profile was not included. The measuring on the non horizontal parts of the groin should have been done every 0.5 meter on the x-axis, but this year also other x-values were used. This results in an inconsistency when the results were compared.

The relative heights of the points were measured using a theodolite. The theodolite was placed on a stable location from where every part of the groin could be seen. The relative height could be read from a rod fixed on a hemisphere (relative height is the height compared to the height of the point the theodolite is at). The assumption is made that the concrete deck of the groin is stable and can be used as a reference height. The measured heights are corrected in such a way that the coordinates in the y-axis are constant for all years.

A hemisphere is used to level out the influence of individual blocks. According to instructions the size of the hemisphere should be approximately $d_{hemisphere}$ = ½* d50. Only two hemispheres are available for the measurements (diameter of 0,25 meter and 0,75 meter). Both are not the right size but a diameter of 0,75 was used last year. Because the measurements are done to compare them with earlier results the hemisphere with a diameter of 0,75 meter is used.

5.4 Results of the measured profiles

The goal of the measurements is to estimate the changes in volume of the groin and the displacements of rocks on the groin. Using the theodolite a good impression of the aspects involved in groin charting can also be experienced.

5.5 Displacement of rocks

A first estimate of the rock displacement is to compare results of measurements done in different years. The relative heights of the different years are plotted for all cross-sections. In 2002 and 2004 students measured 6 different profiles. In 2003, two cross-sections were not included and thus not shown in the graphs.

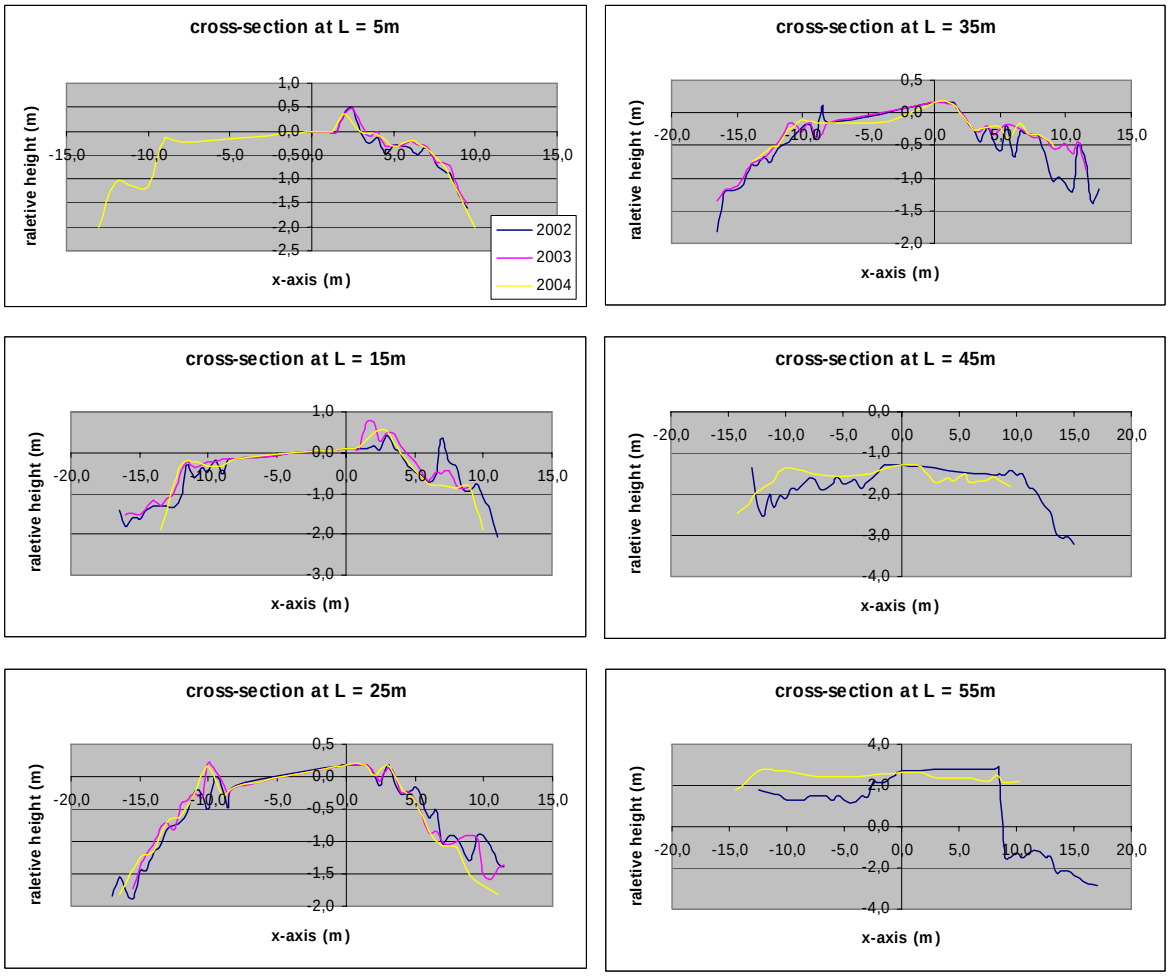

Figure 5.2: Groin profiles

In cross-section L=5m difference can be seen in the 2002 and 2003 profiles. In 2002 a small hemisphere is used and differences are not leveled out as much as in the later years. The 2004 profile is almost the same as the year before and differences can be explained by the larger grid in 2004.

In cross-section L=15m the differences in profiles are larger. A part of the northern side (around x = -15m) material seem to have been disappeared. Also the big bump at the southern part (x = 7.0m) has disappeared. The bump should have been measured in 2004 if it was there, but if the cross-section was not measured at the right place (e.g. at L=16m) could still have been there. Noticing this difference further investigation at this place is recommended.

In cross-section L=25m the differences are small. The 2002 profile is less leveled due to the hemisphere. The differences near the water surface are more remarkable. At L= 10m rocks of 50 centimeter have been disappeared since last year. Further investigation is recommended for this side of the cross-section.

In cross-section L= 35m the different profiles fit strikingly well apart from the differences due to the different hemispheres.

Cross-sections at L= 45m and L= 55m are not measured in 2003. The two profiles hardly fit for both years and don't really look like groins. The use of these figures is subject of discussion.

5.6 Change of total volume

The measured heights on the cross-sections were interpolated on a grid of 0,5 meter. The area of these 0,5 meter strokes were calculated and added for every cross-section. Because the lower boundary is fixed on the sea bed it is not accessible for measurements another must be determined. The water level is variable and can also not be chosen as boundary. The profiles used for the calculations are the widest possible that are measured every year.

The calculated value is the volume of the groin per running meter. In the tables the difference in volume is indicated. For the first four sections a comparison is made for the three following years, for the two sections close to the beach the profiles of 2002 and 2004 are compared but no importance should be attached to the results of these years.

The changes in volume involve the total of the cross-sections and thus allow movement of material. Rocks can move down from the top without changing total volume!

Volume change compared to year before		
L	2003	2004
5	0,7	-0,3
15	1,8	-1,6
25	0,3	-1,5
35	1,2	0,5

Table 5.1: Volume change 1 year

Volume change compared to two years before	
L	2004
45	3,1
55	32,3

Table 5.2: Volume change 2 years

(L = 5, only the southern part of the groin was measured).

5.7 Remarks

A few remarks are made on the results and the interpretation of it below, most of the remarks are mentioned through the text in this chapter.

5.7.1 Accuracy

Height measurements are accurate on the millimeter, the horizontal distances of the cross-section less than a few centimeters thus the height accuracy is not useful. Especially the accuracy in the volume calculations is lower. The values are interpolated from the measured values (sometimes two coordinates are one meter apart) and accuracy of the height can be less than decimeters.

5.7.2 Differences of water level

Two different groups made the measurements on two separate days of 2004. The first day the whether was very good with hardly any wind, the second day the weather was worse with more wind. The difference in water level can be explained by the weather change. The brim of the groin was also less accessible, resulting in differences of water level at L= 35, L=45 and L= 55 meter.

6 Quarry Exercise

6.1 Introduction

In the quarry the properties of a given heap of rocks have been determined. Of each block of stone the Dn50, elongation and blockiness are required.

From a representative number of stones the weight and dimensions have been derived at the quarry. The variation in blockiness and elongation of this sample also has to be determined.

For each block the Dn is determined from the weight, after which data are plotted on a log-gauss scale. Then it is easy to determine the Dn50.

6.2 The Quarries

The quarry exercise was done on Thursday October 13th. We visited two quarries run by Eskana SA. Eskana is a company, with a stock exchange quotation at the Bulgarian Stock Exchange (BSE) in Sofia, which runs six quarries in eastern Bulgaria. We visited the company's largest quarries, Marciana and Sini Vir.

After an early leave from our hotel we arrived at Marciana quarry, where we were received very hospitably with drinks and cakes. After a lunch, offered by Eskana, at a drink water storage reservoir, we went to Sini Vir quarry. Both quarries serve different purposes.

Marciana is a quarry with a deep pit from which crushed stone is mined. Crushed, well graded stone is produced for road foundations and asphalt applications, limestone, mineral concrete and chalk. Marciana is an opencast pit with application of borings. The produced fractions are 5/30 mm, 25/60 mm, 60/150 mm, 0/75 mm and some micronised products from 20 µm to 300µm.

Figure 6.1: Machines at work at Marciana quarry

Figure 6.2. The pit at Marciana quarry

The stones at Sini Vir quarry are mined in a similar way as at Marciana. Here, rocks two types of stone are found: yellow and grey rock. The quality of produced stones varies significantly: the yellow stone is the softer type and the grey stones the harder. Eskada attempts to keep them separated by blasting the rock in a sophisticated way. The produced fractions are 5/15 mm, 5/25 mm, 25/60 mm. Stones from the Sini Vir quarry are mainly used for asphalt coverings, railway ballast and concrete.

Figure 6.3: Sini Vir quarry

Figure 6.4: Rock is converted into sand at Sini Vir

6.3 Measurements

6.3.1 Small rocks

At Marciana quarry two experiments were carried out. One experiment meant to collect a number of rocks that could be carried by one person. We decided after measuring 23 rocks that this would be satisfying. The weight of these rocks roughly ranged from 15 kg to 50 kg. We also measured the three axial lengths of each rock, the longest axial length being l and the shortest axial length being d.

With these data we were able to calculate the Elongation of each rock. Besides the dimensions, the weight is of use to determine the Blockiness, because calculate the blockiness the volume is required. As the volume of the rocks wasn't determined at the quarry, the density of the rock was needed. As expounded later on in this section the density of the rock at Marciana appeared to be 2350 kg/m^3.

The elongation and the blockiness are determined using the guidelines from the CUR 154 manual.

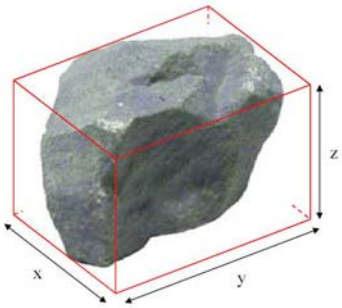

Elongation is defined as:

$$l/d = \frac{longest\ axial\ length(x)}{shortest\ axial\ length(z)}$$

Blockiness is defined as:

$$BLx = \frac{Volume\ of\ the\ rock\ block}{X \bullet Y \bullet Z} \bullet 100\%$$

A table containing the dimensions, mass, elongation, blockiness and other values derived from these data, such as Dn (using $D_n = \sqrt[3]{\frac{m}{\rho_s}}$) is added as appendix VI.

Graphs showing the Dn-distribution of the small rocks on both a log-normal and a log-gauss scale have been added in the same annex.

The Dn50 of the small rocks, read from the log-gauss graph, has a value of 0.212 m.

The graphs show a poor gradation of the rocks. Seemingly we have been quite picky in collecting the rocks. A large number of arbitrarily chosen rocks would have shown an S-curve on a log-normal scale and straight line on a log-gauss scale.

Figure 6.5: Some of the small rocks

6.3.2 Large rocks

The other experiment comprised of the determination of the dimensions and the estimation of the blockiness of some larger rocks (far too heavy to carry).

The dimensions, elongation, estimated blockiness, volume, mass and Dn of five large rocks is compiled in Table 6.1.

	x (m)	y (m)	z (m)	l/d	BLx (est.)	Volume (m^3)	Mass (kg)	Dn (m)
1	3.6	1.32	1.31	2.75	70%	4.36	10240	1.63
2	1.8	1.9	1.4	1.36	60%	2.87	6751	1.42
3	2.44	1.44	1.7	1.69	55%	3.29	7720	1.49
4	2.65	1.2	1.35	2.21	85%	3.65	8575	1.54
5	1.4	1.2	0.75	1.87	75%	0.95	2221	0.98
mean	2.38	1.41	1.30	1.83	69%	2.71	6359	1.36

Table 6.1: Main characteristics of five large rocks at Marciana quarry

A graph containing the Dn-distribution on a log-normal scale is added as Appendix VII.

We think the data set is too small to give any sensible comment on the shape of this curve.

Dn50 is determined by simply taking the median value, which is 1.49 m, from Table 6.1.

Note:

Determination of the elongation and blockiness of these large rocks is somewhat subjective. We let several people record the dimensions of the large rocks, which wasn't always easy, because we could hardly move the stones.

To make the blockiness more reliable we let several persons estimate the blockiness of the larger rocks. Additionally, from the smaller rocks we had already derived a quite accurate blockiness, which we could use as a comparison.

The large rocks we chose were rather blocky. We argued that, by doing this, we would make a smaller estimation error than if we had chosen more spherical rocks. Therefore all large rocks have a high estimated blockiness, with an average of 69%. The small rocks which were chosen arbitrarily, in this context meaning independent of their shape, had an average blockiness of 54.8% (Appendix V). We think, bearing in mind our observations, this difference of 14% is an acceptable result.

Figure 6.6: the large rocks

6.4 Rock density determination

To determine the density of rock, two stones were collected at Marciana and brought to Delft. In the Hydraulic Laboratory at the Faculty of Civil Engineering and Geosciences, following the procedure from NEN 5186, the mass under water, 'moist mass' and 'dry mass' of each stone had to be determined.

$$\rho_r = \frac{m_3 * \rho_w}{m_2 - m_1}$$, with m1 = mass under water; m2 = 'moist mass'; m3 = 'dry mass';

ρr = density of the rock; ρw = density of water

The resulting values for both stones and the mean value are put in order in Table 6.2.

Stone	Mass under water (m1)	'Moist mass' (m2)	'Dry mass' (m3)	Density ρr
1	46.9 g	78.01 g	76.01 g	2261 kg/m^3
2	49.7 g	84.88 g	79.55 g	2443 kg/m^3
mean	48.3 g	81.45 g	77.78 g	2352 kg/m^3

Table 6.2 Mass under water, 'moist mass' and 'dry mass'of stones collected at Marciana

The two stones we collected show quite a big difference in density. This surprises us, because the stones were collected at the same location. Last years' group however calculated almost exactly the same average density, so we think a density of 2350 kg/m^3 (the rounded value) is a plausible result.

A problem we encountered determining the mass under water was that the value changed very quickly, because the porous dry stones gained mass by absorbing water. We recorded the mass as soon as possible after submerging the stones, but still we didn't know if the stones had the same saturation rate at that moment.

When we determined the 'moist mass' we were quite sure the stones were virtually completely saturated, as they had been submerged for more than three days.

6.5 Groyne calculations

6.5.1 Porosity and layer thicknesses

Now we have some knowledge about the properties of the rock from Marciana we can calculate the porosity and layer thickness of a construction made from these stones.

The elongation and blockiness values are important to determine the porosity of placed blocks in hydraulic structures. For our calculations we used the elongation and blockiness of the small rocks we examined at Marciana. The reasons for this choice is that these stones had the same order of magnitude as stones usually encountered in hydraulic structures and the results are more accurate than those derived from the large rocks.

The regression-equations from tests have as a general format:

Parameter = A + B·BLcm + C·(l/d)m + D σ(BLc)

BLcm = mean value of blockiness

(l/d)m = mean value of elongation

σ(BLc) = standard deviation of blockiness

The slope op the groyne at St. Konstantin is estimated at 1:3. For this slope the coefficients are:

Parameter	A	B	C	D
Singe layer porosity nv	43.46	-0.2233	3.789	-0.4233
Layer thickness kt	1.1038	-0.0025	-0.1541	-0.0003
Double layer porosity nv	36.20	-0.2240	3.613	0.1942

Table 6.3: Parameters for regression-equations

The results for all parameters are shown in Table 6.3 BLcm, (l/d)m and σ(BLc) are calculated using values from Appendix V.

Mean value of blockiness BLcm (%)	54.8
Mean value of elongation (l/d)m	1.77
Standard deviation of blockiness σ(BLc)	20.2
Singe layer porosity nv (%)	29.4
Layer thickness kt (m)	0.69
Double layer porosity nv (%)	34.2

Table 6.4: Values used for and results of regression-equations

Figure 6.7: Brave students on the groyne

6.6 Redesign of the groyne at St. Konstantin using rock from Marciana

The groyne in St. Konstantin has been designed with Hudson. If the stone density of the stones used in the present groyne is known, the design wave height and period for this groyne can be calculated.

Due to the fact that we didn't bring a stone from the groyne in St. Konstantin to The Netherlands, the density of these stones had to be estimated. We were told that the density of the rock used in Bulgaria is slightly lower than the most popular rock used for hydraulic engineering purposes worldwide, so we assumed a density of 2600 kg/m3 and a Dn50 of 1 m.

This density and Dn50 have been used to recalculate the design wave height.

Hudson-formula, rewritten:

$$H_S = \sqrt[3]{\frac{M \cdot K_D \cdot \Delta^3 \cdot \cot\alpha}{\rho_S}}$$, with $$\Delta = \frac{\rho_S - \rho_W}{\rho_W} = \frac{2600 - 1000}{1000} = 1.6$$

.

$$H_S = \sqrt[3]{\frac{2600 \cdot 3.5 \cdot 1.6^3 \cdot 3}{2600}}$$ = 3.50 m, with KD = 3.5 (rough angular quarry stone, 2 layers, breaking wave)

Now this wave height is used to calculate the necessary Dn50 if stones from the Marciana quarry are used. For this the Van der Meer equations have been used, which are:

$$\frac{H_s}{\Delta D_{n50}} = 6.2 P^{0.18} \left(\frac{S_d}{\sqrt{N}} \right)^{0.2} \xi^{-0.5}$$

$$\frac{H_s}{\Delta D_{n50}} = 1.0 P^{-0.13} \left(\frac{S_d}{\sqrt{N}} \right)^{0.2} \xi^{P} \sqrt{\cot\alpha}$$

Figure 6.8: Scenery at Sini Vir quarry

The two coefficients have to be changed in case of “non-standard” blockiness and elongation, according to Stewart:

BLc-range	l/d range	Armour Porosity (%)	Placement method	"6.2"	"1.0"
40%-50%	1.3 - 3.0	38.7	standard	7.09	-
40%-50%	1.3 - 3.0	36.1	dense	6.68	1.67
50%-60%	1.3 - 3.0	37.1	standard	6.44	1.51
50%-60%	1.3 - 3.0	35.2	dense	7.12	2.08
60%-70%	1.3 - 3.0	35.5	standard	7.71	2.63
60%-70%	1.3 - 3.0	34.4	dense	10.85	-
50%-60%	1.0 - 2.0	36.1	standard	8.50	1.45
50%-60%	1.0 - 2.0	34.6	dense	8.80	-

Table 6.5: Van der Meer coefficients in case of “non-standard” blockiness and elongation

As we use the values of the smaller rocks, which have a mean value of elongation of 1.77 and a mean value of blockiness of 54.8%, choosing a standard placement method, the coefficients to be used are 6.44 and 1.51.

Additionally, some values of quantities in the Van der Meer equations have to be assumed.

Assumptions:

Permeability P = 0.1

Number of waves N =7500

Damage level S = 10

$$\xi_{transition} = [6.2 \cdot P^{0.31}\sqrt{\tan\alpha}]^{(\frac{1}{P+0.5})} = [6.2 \cdot 0.1^{0.31}\sqrt{1/3}]^{(\frac{1}{0.1+0.5})} = 2.55$$

In the next equation an assumption has been made for the wave period and wavelength. With a period of 8 seconds we obtain a wavelength (L0) of about 100 meter.

$$\xi = \frac{\tan\alpha}{\sqrt{H_S}/L_0} = 1.78$$

1.78 < 2.55, so we need the Van der Meer equation for plunging breakers:

$$\frac{H_S}{\Delta \cdot D_{n50}} = 6.44 \cdot P^{0,18}\left(\frac{S_d}{\sqrt{N}}\right)^{0,2} \xi^{-0,5} = 6.44 \cdot 0,1^{0,18}\left(\frac{10}{\sqrt{7500}}\right)^{0,2} \cdot 1.78^{-0,5} = 2.07$$

$$\Delta = \frac{\rho_S - \rho_W}{\rho_W} = \frac{2350 - 1000}{1000} = 1.35$$

$$D_{n50} = \frac{H_S}{2.07 \cdot \Delta} = 1.25m$$

This shows a Dn50 of 1.25 m is needed when using stones from Marciana quarry.

This value is 25% higher than the assumed Dn50 for the stones used in St. Konstantin. Using $D_n = \sqrt[3]{\frac{m}{\rho_s}}$ results in a mass of approximately 4.6 tons per stone.

6.7 Conclusions and Recommendations

Due to the fact the density of the stones in the quarry is much less in accordance to the density of stones normally used for groynes, it is hard to say we if we can use the stones from the quarry. By using the Van der Meer equation we made a few assumptions like the wave period and wave length. Also the angle of the slope of the groin is an assumption. In this way the result of the calculations to obtain the required Dn50 is not very accurate or reliable.

Although the calculated Dn50 of 1.25 m isn't an unrealistic value for stones used in hydraulic structures, we don't think the rock at Marciana quarry is suitable for hydraulic engineering purposes. We think so, because the stone broke easily and remains of the stones were left on hands that picked up stones, causing 'white' hands. This means the rock is easily eroded; a quality that is not appreciated at all in hydraulic engineering.

The stones measured at the quarry should be chosen arbitrarily and not because someone likes its shape or colour. Picking the stones like this will produce more reliable results concerning elongation and especially blockiness.

It is recommended to make sure the stones used to determine the density of the rock at the quarries are examined under equal circumstances. To make sure the stones are really dry when the ‘dry mass’ is determined the stones can be dried in an oven first. After determining the ‘dry mass’ the stones should be submerged to determine the mass under water. The mass should be read immediately after submerging the stone. Only then the stones will have absorbed a minimum quantity of water. Next, the stones should stay in the water for a few days, after which the ‘moist mass’ can be determined. We expect the density of the stones won’t show such a big difference as in our experiment if they are treated in a perfectly equal way. Not too much attention should be paid to accuracy in this type of calculations, however.

7 Bathymetric Survey

7.1 Introduction

In continuation of the survey executed in the year 2003 a bathymetric survey is carried out because the area in front of the measured beach has to be surveyed to a somewhat greater depth. This survey is necessary because more information is needed about the change of the coastline and beach width between the St. Elias marina and hotel Sirius in St. Constantine.

This year additional information about the water profiles is also needed to design an artificial island offshore. A hotel will be built on this island. The island will be connected to the shore to expand the beach. This is because a lot of hotels have been build in St Constantine but there is a shortage of beach to give enough space for the guests.

Changes offshore beneath the water level influence the change of the coastline. The water depths are measured using a Fishfinder in combination with a GPS. The Fishfinder is attached on the boat and can measure the depth. The GPS is used to determine the position of the boat in the horizontal plane.

Therefore the purpose of this survey is to get some insight in the morphology of this beach as a basis for further coastal protection works. The bathymetric survey was thus carried out to obtain data concerning the depth that would be required to design an artificial island in front of the coast.

Of all the students three groups were formed. These groups had to carry out a survey in order to be able to design this artificial island offshore. Therefore we had to determine the following aspects before starting the measurements. First the area to be surveyed will be determined and a sailing track will be made. Then the implementation of the measurements will be discussed. After that the required accuracy will be discussed and the equipment used during the measurements. Subsequently the results of the bathymetric survey will be given and an evaluation will be made. The results of this year will be compared with the results of the previous years as well. Finally a conclusion will be given.

7.2 Area

For calculations of beach stability, for the design of the coastal protection in front of the Sirius and for the design of the artificial island it is necessary to have some kind of depth information. Therefore a survey vessel is used to measure the underwater slope.

First the area to be surveyed has to be determined. The artificial island will be constructed in front of the beach halfway the Sirius hotel and the St Elias marina, see Figure 7.1. The original plan worked out by the three groups consisted of three boat runs.

Figure 7.1: Artificial island

The first two groups would measure broadly respectively area one and two. The third group would measure the area where the island will be located more accurately. The area of the survey can be seen in Figure 7.2. The scale mentioned in the figure is not correct.

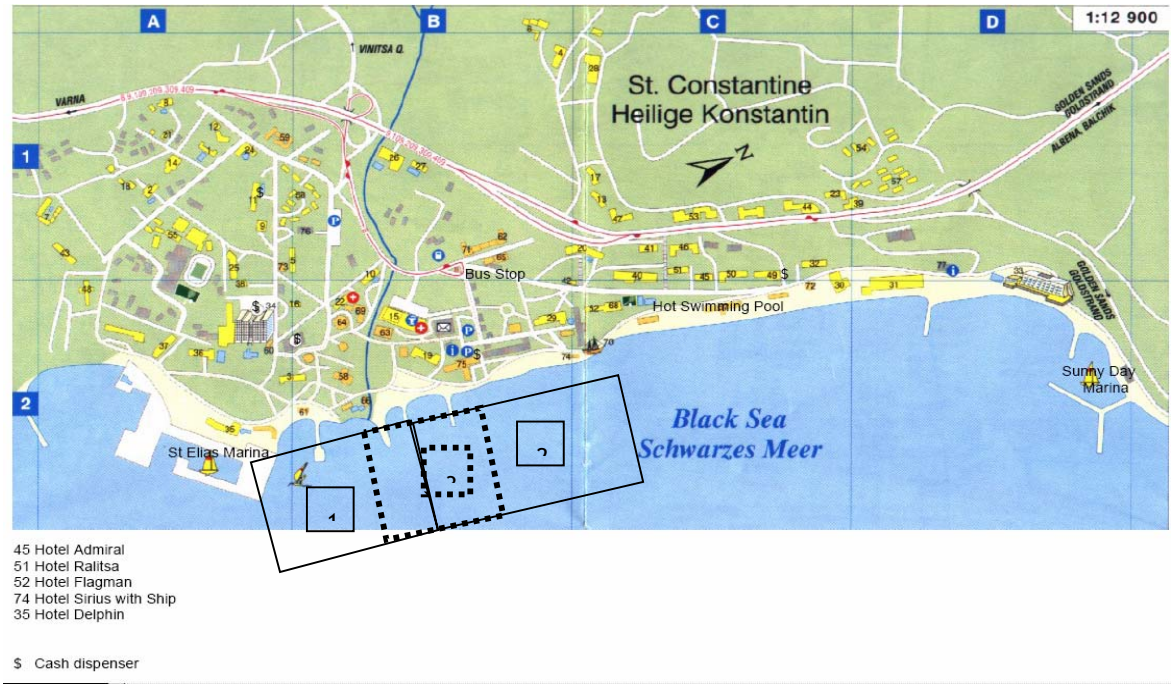

Figure 7.2: Area to be surveyed

7.3 Depth

Beyond a certain depth the building of an artificial island is not feasible. So depths in excess of 20m are not interesting for this survey and therefore not measured. In 2003 the bathymetric survey was carried out emphasizing the quantification of the sediment volume changes. Therefore the seaward limit of the measured area was that of the closure depth. The closure depth is often the outer edge of the transport zone corresponding to the highest wave that may occur. The measured area in 2003 was up to a depth of MSL -11m. This was also done in 2004. Yet, this year a single run with the boat was made to a depth of MSL-16m in order to obtain more insight in the bottom relief in the specific area where the island would be made.

7.4 Implementation measurements

As mentioned before the measurements are accomplished with a small boat and a fish finder and GPS system. In order to get a reliable bathymetry along the whole beach, the vessel has to sail in straight lines somewhat perpendicular to the coastline. The position of the vessel is

linked to the measurement of the fish finder. Consequently the water depth at an exact position is known.

The GPS was used to determine the right track during sailing. In the beginning of the first trip it was difficult to control that we really sailed the planned track as we only saw the position on the GPS, but not the already sailed route. After examining the instrument we got a dotted line representing the route we already sailed. Then it was possible to instruct the skipper about the track.

Because of the relatively high waves we could not sail in the surf zone. This means there is a lack of data between the measurements from the beach profile into the sea and the measurements from the fish finder. Therefore the beach survey and the bathymetric survey cannot be connected very precisely.

7.5 Sailing pattern evaluation sailed course and planned coarse

Because of the available time of only one hour per group we had to adapt our sailing route. The weather was getting worse so only two boat runs could be made. Therefore we decided that both groups would measure the whole area but they would sail different tracks so a finer grid would be created.

7.6 Required accuracy

The question that arises when considering this survey is: “How accurate would you want your measurements to be, to be able to give a reliable representation of the bottom, for the purpose of making a preliminary design of an artificial island of the coast of St. Constantine?”

It is clear that measurements of accuracy in order of millimeters would be impossible to achieve considering the survey equipment, students knowledge and available time.

On the other hand, measurements with accuracies in the order of hundreds or even tens of meters would be useless considering the area to be surveyed (approximately 1 km2) and its relative small depth. (max. 16m)

So the answer with respect to the desired accuracy must lie between these to extremes.

Considering this, the following desired order of accuracies is given:

Horizontal positioning : in order of meters (3-4m)

Vertical positioning: in order of decimeters (10-30cm)

7.7 Equipment used

Accuracy is limited and depends among other things on the available instruments, proper execution and local conditions at time of measuring. Before presenting the available instruments for the bathymetric measurement in 2004 a brief look at the equipment used in 2003 is given.

In 2003 a DGPS in combination with an echo sounder were used and the following was concluded: 'When analyzing the accuracies of the different instruments, it's clearly that these are not adapted to each other. The DGPS is very accurate on one hand, but it turns out to be the vessel and the way it's navigated to be of much more influence on the results. Next to that the influence of the calibration of the echo sounder is relatively high.'1

This year it was decided to use a handheld GARMIN GPS linked to a GARMIN Fishfinder 100. The reasons for this were that the accurate measuring capabilities of a DGPS system (owned by the Bulgarians) where to high for this kind of survey. Also, the setting up of the DGPS required too much time and would have to be done by the Bulgarians contributing little to the learning experience of the students. The handheld GPS and Fishfinder would be quicker and easier to set up and able to be used by the students with no great drawbacks concerning accuracy.

7.8 Horizontal positioning

In 2004 the instrument used to determine horizontal positioning was a GARMIN handled GPS (see Figure 7.3). This GPS was Egnos/Waas enabled increasing its accuracy. The accuracy of the handheld GPS can be seen in Figure 7.4.

[1] Report 2003

Figure 7.3: Handheld Garmin GPS as used in Bulgaria

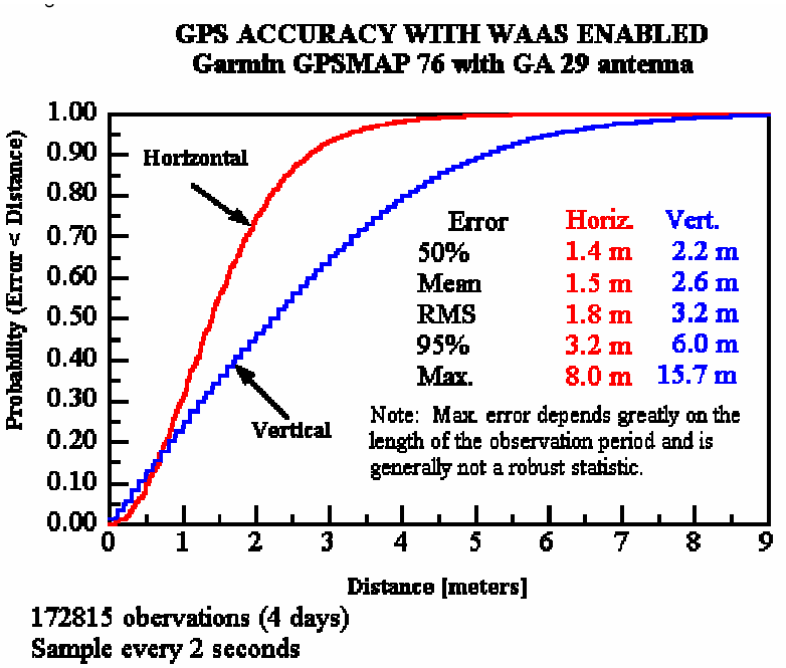

Figure 7.4: Accuracy of GPS

7.9 Vertical positioning

The depth information was measured by a GARMIN Fishfinder 100 Figure 7.5. An echo sounder originally conceived for aiding fishermen in finding fish, this echo sounder proved also suitable to perform depth measurements. However, the specific accuracy is not known (not mentioned in the manual) but the following rule of thumb concerning accuracy of depth measurement by echo sounders can be followed2:

Depth until 30m: 0.20m +0.6% d

Depth between 30m-60m: 0.15m + 0.7%d

[2]VOUB-cursus deel 8 en 9 van VBKO t.b.v. het keuzevak Baggertechniek. Juli 1999. blz.71

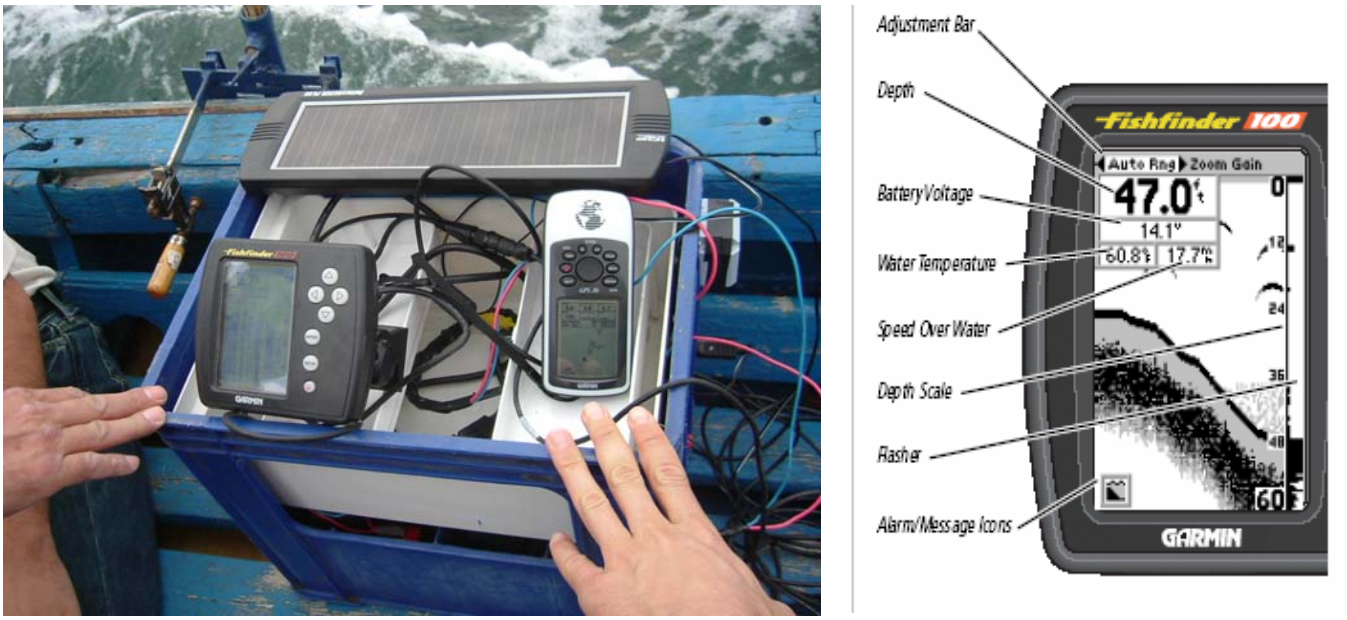

Figure 7.5: The setup of the GARMIN Fishfinder 100 and its display options

The echo sounder was linked to the GPS and at a fixed time interval of 5 seconds the GPS would store the X,Y coordinates and the Z coordinate provided by the Fishfinder, thus producing a series of points recording the sailed route and it's concerning depth.

7.10 Survey vessel

A local fisherman provided us with a small boat Figure 7.6 on which the echo sounder and transducer could be installed.

The transducer and GPS were installed halfway the boat on port-side and the transducer was mounted vertically at a depth of MSL-0.23m in the water.

Figure 7.6: Survey vessel with captain

The data produced by the GPS and Fishfinder has to be interpreted by different software programs to generate sailing routes and contour maps. The following programs besides Excel where used:

- Ozzie mapping
- Golden Software Surfer 7
- Analysis of error sources

A number of factors beside the accuracy of the equipment that can produce measuring errors are mentioned here

- Variations in water temperature
- Variations in water density
- Frequency and bundelwidth properties of echo sounder
- Positioning GPS and Echo sounder aboard
- Movements of survey vessel
- Variation sea level

To determine if these errors are significant and which have to be taken into account when determining the total accuracies of the survey each of the factors are treated below and the order of error is presented and compared in a table.

7.11 Calibration echo sounder

Before starting the measurements the echo sound has to be calibrated. In principle the echo sounder measures the time expired between de transmitting of the sound pulse and the receiving of the first reflected signal (echo). The sound wave has completed in this time a distance of two times the distance from transducer to bottom.

By multiplying the halfway time with the sound propagation speed v of the sound wave then the distance from the transducer to the bottom is known. The water depth is determined by adding up the distance from the transducer to the surface of the water.

This means the correct depth of the transducer into the water has to be known.

The propagation speed v depends on the density and conductivity capability of the medium in which the sound wave is propagating. In this case the medium is water. Therefore the best possible value for the propagation speed of sound in water has to be determined.

The propagation speed of sound in water depends on:

- (Variations in) water temperature
- (Variations in) water density

This propagation speed v can be calculated according to the following formula:3

$$v = 1449.2 + 4.6t - 0.055t^2 + 0.00029t^3 + (1.34 - 0.01t).(s - 35) + 0.016d$$

In which:

v = propagation speed of sound (m/s)

t = temperature (C)

s = salinity (promille)

d = water depth (m)

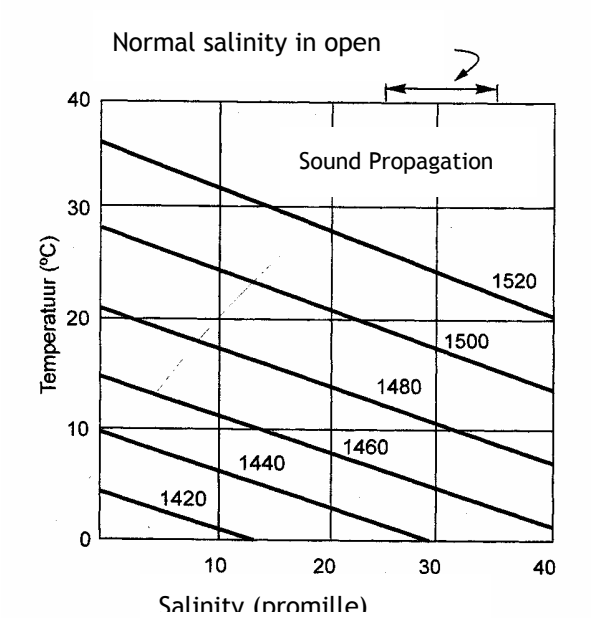

Figure 7.7: Influence of temperature and salinity on the propagation speed of sound in water

[3] VOUB-cursus deel 8 en 9 van VBKO t.b.v. het keuzevak Baggertechniek. Juli 1999. blz.70

From the

Figure 7.7 it can be seen that temperature and salinity have a large influence on the propagation speed of sound in water. The saltier the water the larger the sound propagation speed is.

The temperature could be read from the Fishfinder which read: 17.8 ºC. The assumption is made that the fishfinder does not adapt the propagations speed of sound to the change in temperature. The fishfinder is able to measure a temperature range from about -15°C to 70°C. Assumed is that the fishfinder is adjusted to a temperature range of 10 to 25 °C.

The density of the water was measured with another instrument and was found to be: 1018 kg/m3 at MSL-0.23cm. Therefore the salinity of the Black Sea is 18‰.

The Fishfinder 100 has the possibility to switch from a 'freshwater' to a 'saltwater' mode. It is not possible to set a determined salinity that is why this can give an inaccuracy. Furthermore it is not known at which density the Fishfinder is set when switched to either mode. Assumed is that the Fishfinder will measure with a salinity of about the average salinity in the oceans of 25 ‰.

Now it is possible to calculate the range in the sound propagating speed.

	Temperature (C)	Salinity (‰)	Sound propagating speed (m/s)
	18	25	1495
	10	25	1470
	25	25	1515
Circumstance this year	18	18	1485
	10	18	1465
	25	18	1495

Table 7.1 Sound propagation speed

The exact circumstances during our measurements have been a temperature of 18º C and a salinity of 18 ‰. This results in a sound propagating speed of 1485 m/s. According to Table 7.1 and

Figure 7.7 the sound propagating speed differs 20 below or 30 above these value. This results in an inaccuracy in the results caused by an inaccurate tuning of the sound propagating speed of maximum 20 cm.

In most of the circumstances the Fishfinder will measure with a sound propagation speed that is too high because the salinity in the Black Sea is definitely lower than a normal sea salinity value. This results in a measured depth that is larger than the real depth.

The Fishfinder 100 was calibrated in the harbor with the help of a lead and rope providing a depth in the harbor of MSL-3.5 m.

7.12 Frequency and bundelwidth of echo sounder

The frequency and bundelwidth at which the echo sounder is set are important aspects that influence the accuracy of the instrument. Unfortunately little is known about the settings of the Fishfinder but in general the following can be assumed:

Introduced error: 10-20 cm[4]

7.13 Positioning GPS and echo sounder aboard

Unlike last year the echo sounder transducer and the GPS where located on the same spot aboard this not introducing inaccuracies with respect to horizontal positioning.

Introduced error: none

7.14 Variation sea level

[4] VOUB-cursus deel 8 en 9 van VBKO t.b.v. het keuzevak Baggertechniek. Juli 1999. blz.96

In the Black Sea no tidal variation occurs. However some water movements occur because of the wind setup.

The increase of the water level is caused by the fetch, water depth, wind speed and angle wind direction. The wind setup is determined using cress, see Figure 7.8. Different values for the parameters are used.

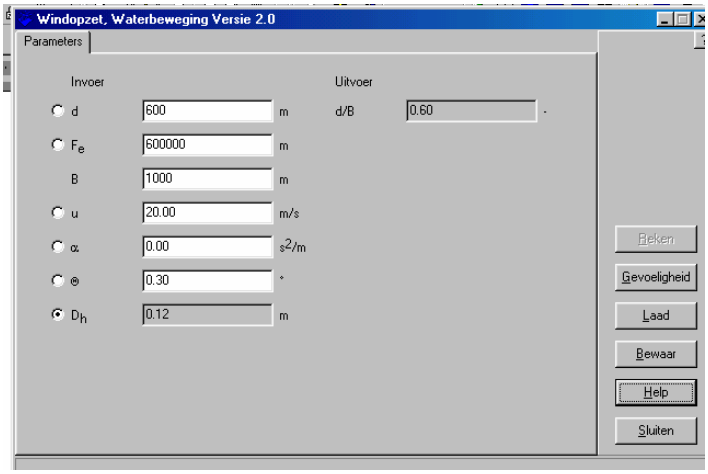

Figure 7.8: Wind setup calculated with Cress

Because the Black Sea is a very deep sea the wind setup has not a large influence on the water level variation. This is shown in table x.

Parameters								
Water depth [m]	600	300	900	600	600	600	600	600
Fetch [m]	600000	600000	600000	600000	300000	900000	600000	600000
Width foreland [m]	1000	1000	100	2000	2000	2000	2000	2000
Wind speed [m/s]	20	20	20	20	20	20	10	15
Wind setup [m]	0.12	0.24	0.08	0.12	0.06	0.18	0.03	0.07

Table 7.2: Parameters Cress

Concluding, the wind setup is in the order of 20 cm.

7.15 Movements of survey vessel

A much more significant source of inaccuracy is introduced by the movement of the survey vessel.

Two causes of measurement error can be discerned:

- inaccuracy introduced by movements induced by waves:
- inaccuracy introduced by the effect of the velocity of the vessel

The first cause is especially important on relative small survey vessel, which was the case in Bulgaria. The degrees of freedom are presented in Fig. XX

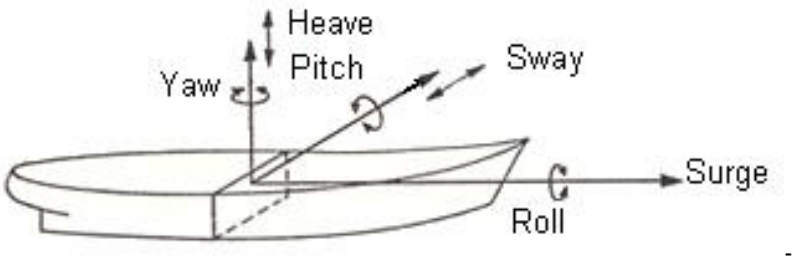

Figure 7.9 six degrees of freedom of a ship

The roll and pitch of a vessel can cause that narrow echo sounder bundle to measure the distance to the bottom which is not perpendicularly under the ship but located further from the ship. Depending on the depth and the degree of rotation the introduced inaccuracy could be very significant! During the measurement in 2004 the maximum measured depth was 16m. When sailing near the breaker zone and later because of weather conditions the roll and pitch introduced by sailing where considerable. (One of the students even got nauseous on board). Thus in an attempt to quantify this affect the following is assumed:

Max depth: 16m

Max rotation due to roll/pitch: 10 degrees

Measure distance: 16.25m

Error: 0.25m

Of course also the effect of heave can have influence on the measured depth. A very rough estimate of the effect of heave on the ship is about 0.5 m.

All these effects can be avoided by the correct mounting of the transducer and only measuring during favorable (calm conditions).

Because this concerns a small vessel sailing at low speeds in open sea squat is not significant. Also because of the low velocities the Doppler Effect can be neglected.

Introduced error by movements of survey vessel:

Cause	Error (m)	Remarks
GPS accuracy	3.2m	95 % by Egnos enabled GPS
Positioning GPS and Echo sound aboard	none	
Largest error	3.2m	

Table 7.3 Errors in horizontal positioning

Cause	Error (m)	Remarks
Fishfinder accuracy	0.21	Rule of thumb: Depth till 30m: 0.20m +0.6% d with maximum depth 16m
Variations in water temperature Variations in water density	0.20	It is unknown at which temperature and density the fishfinder measures. Differences in temperature and density influence the sound propagation speed.
Frequency and bundelwidth properties of echo sounder	0.1-0.2 m	

Movements survey vessel	0.25 m	
Variation sea level	0.20 m	Calculated with Cress: because the Black Sea is very deep the wind setup is small
Largest error	0.25m	

Table 7.4 Errors in vertical positioning

7.16 Conclusion analysis of error sources

From Table 7.3 and Table 7.4 the most significant measurement errors can be seen. These are within accuracy boundaries we defined when setting up the survey.

7.17 Results

In this paragraph the results of the bathymetric survey in 2004 are presented. In Figure 7.9 the sailing pattern of the survey vessel is shown. The measurements started in the St Elias marina in the lower left corner of the figure. From this marina the vessel sailed northwards to the Sirius hotel after which various tracks perpendicular to the beach have been measured. The second run was made in the same way and the vessel sailed in between the sailing pattern of the first run.

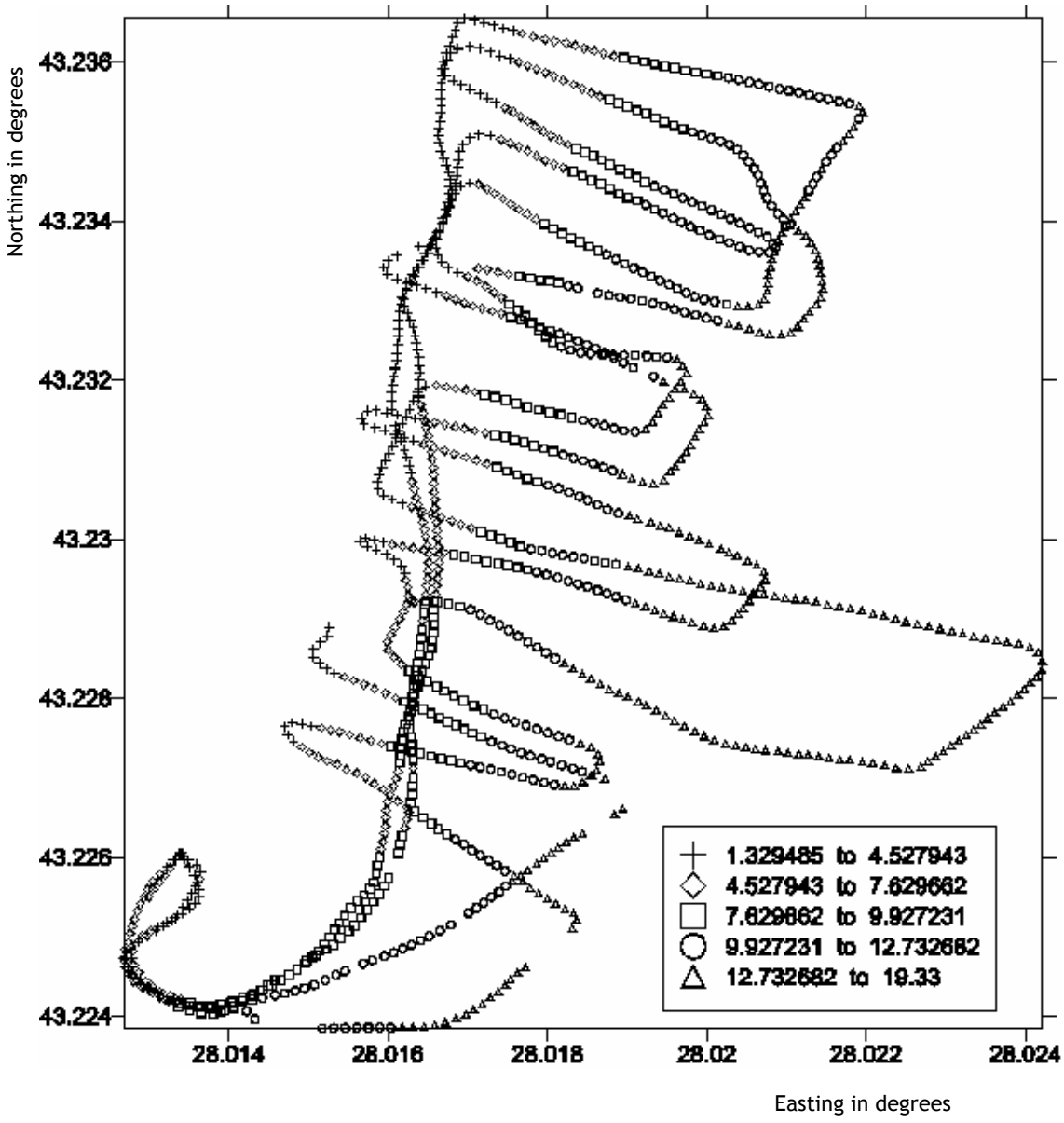

Figure 7.10: Sailing pattern of the survey vessel. The beach is on the left side with the Sirius hotel in the north and the marine in the south.

7.17.1Remark:

When downloading the data, the GPS was set on the 'degrees' mode and not in UTM, consequently all the output coordinates were in degrees instead of UTM.

When using programs such as Surfer these programs don't take this into account, plotting a slightly distorted image. With programs such as Coordinate Calculator 4.0 (www.rdnap.nl) these coordinates can be transformed into UTM coordinates, the problem was that it was not possible to import a database in the program, due to the missing of the Dbutil extension. However, when looking at the size of the considered area the introduced distortion is very small and can be neglected.

Figure 7.11 shows the bathymetry representing the results of the depth measurements with the survey vessel. The beach is situated on the left in the figure. The Sirius hotel is in the north and the marine in the south. The lightest blue colors represent the shallow water and the beach. This is in the left part of the figure. The depth increases gradually to the right of the figure. This year the depth was measured until 11 meter. One single run with the vessels was made until a depth of 16 meter. Before generating a contour map all the depth values had to be corrected with the value of the depth of the transducer MSL-0.23m.

7.17.2Attention!

When interpreting depth contour maps generated with programs such as Surfer the following must be considered:

The program interpolates the values generated from the GPS and Fishfinder by the so called Kriging-methode. This means that on the contour map, only the areas where the sailing routes are relatively parallel and close to each other are interpolated correctly and thus giving a good representation of the depth.

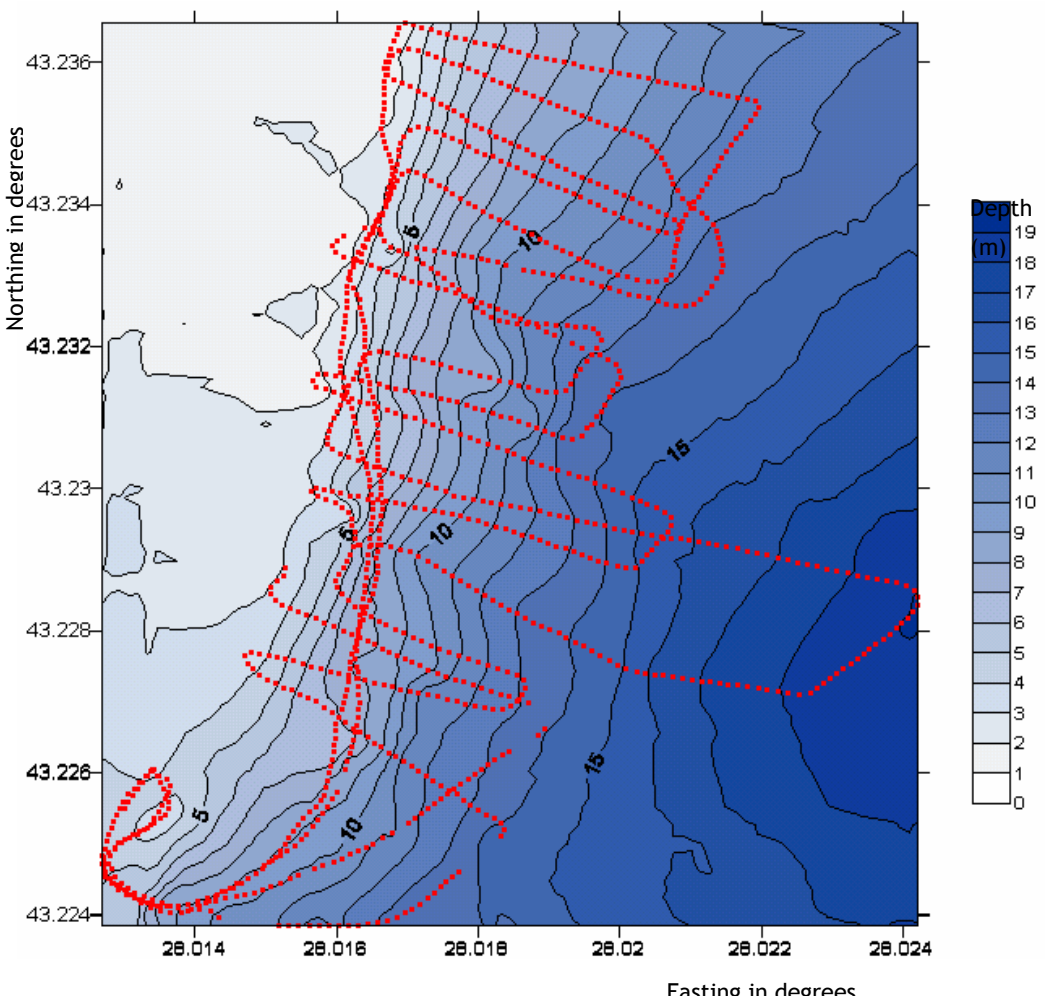

Figure 7.11: Depth contour map 2004

7.17.3Comparison previous year

In 2003 the following figure was generated by the University of Sofia.

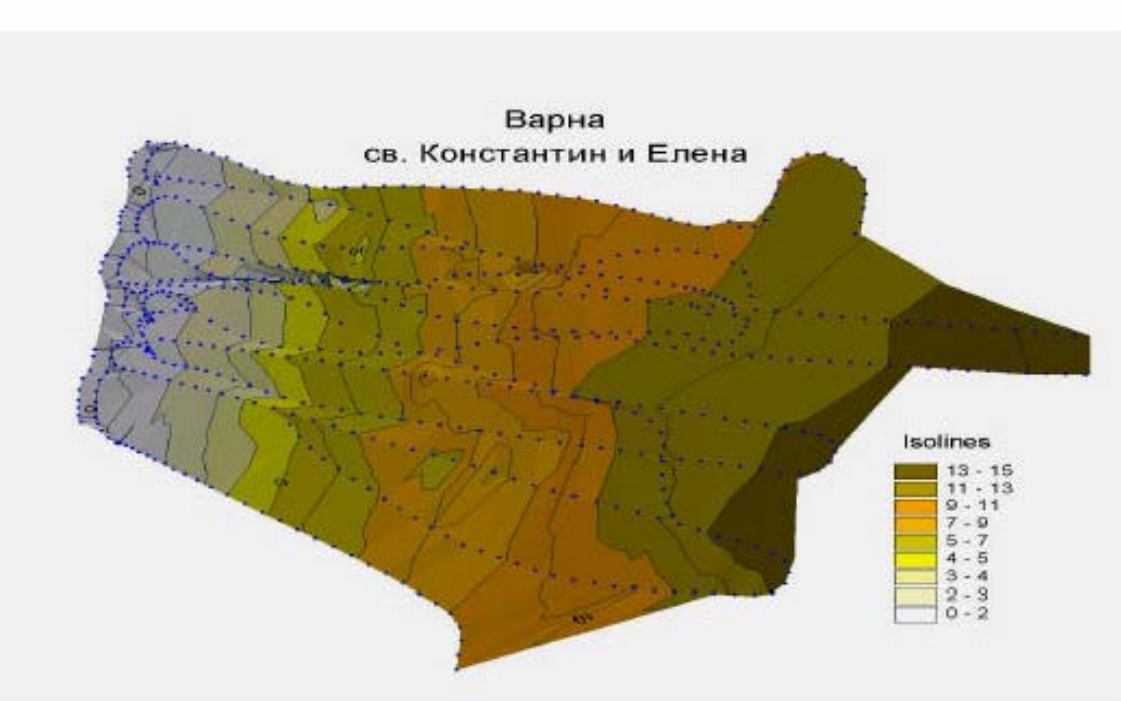

Figure 7.12 Relief of underwater sea slope (Modeling of the relief of underwater coastal slope (Valchinov & Pavlov)

According to Figure 7.12 it seems that there are ridges present in the underwater slope. Though when trying to verify this with measurements done in 2004, these ridges could not be found. When analyzing the figure one notices that the ridges coincide exactly with the runs (to and from the coast) of the survey vessel. This is peculiar. It seems that the ridges where introduced by the execution of the survey and its interpretation. Possible explanation for the observed ridges in could be:

- The transducer was not mounted vertically on ship. This means that the echo sounder does not measure the bottom perpendicular under the survey vessel, introducing measurement differences between sailing from and to the beach.
- Position echo sounder and antenna on the survey vessel where not the same.
- The clock of the echo sounder and DGPS where not synchronized.

Figure 7.13 and Figure 7.14 where generated by the Dutch students in 2003.

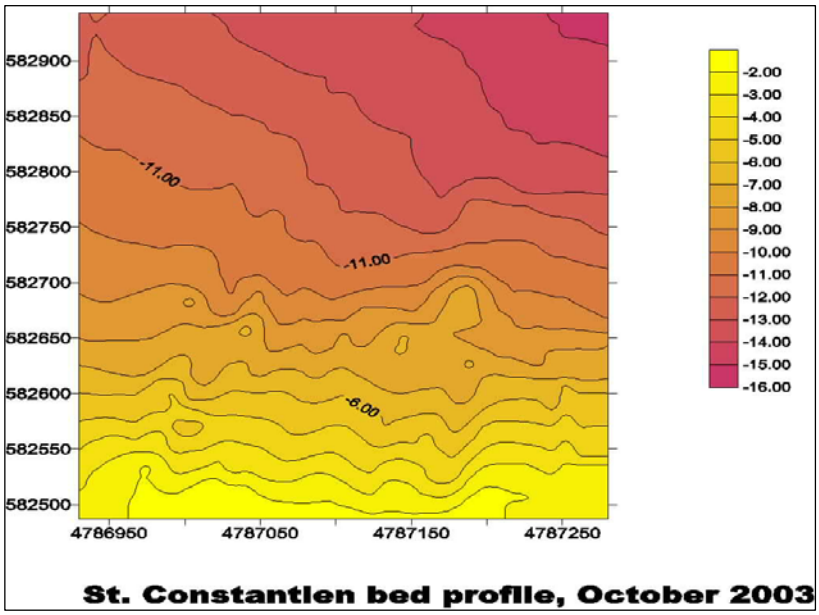

Figure 7.13: Depth contour map 2003

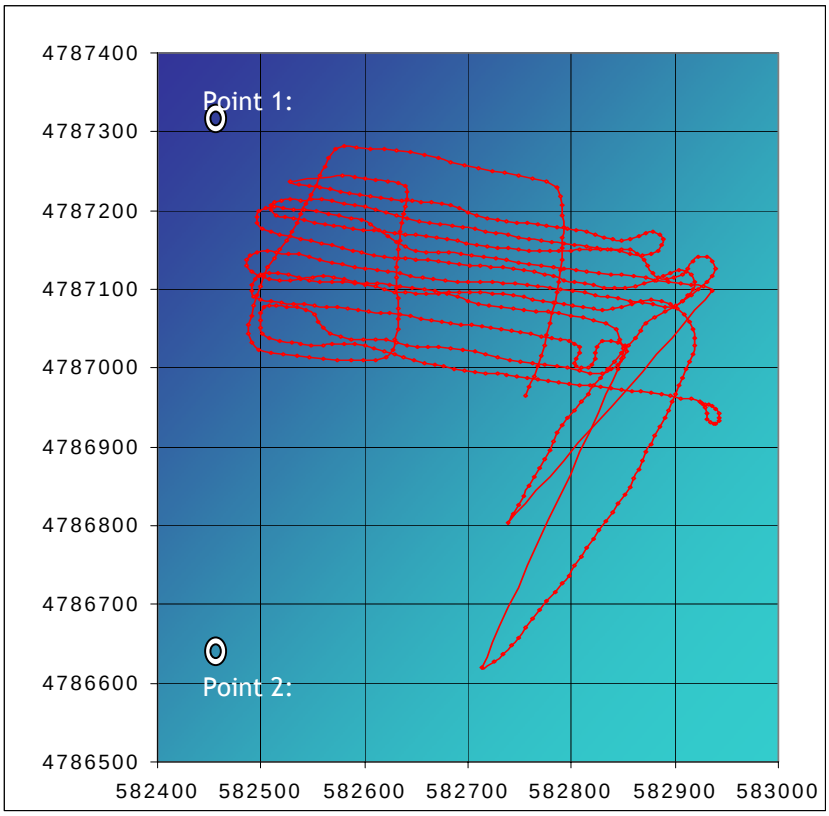

Figure 7.14: Sailing track 2003

Figure 7.15 shows the sailing track of the survey vessel in 2004. It is clear that this year the whole area between hotel Sirius and the St Elias marine has been surveyed. The gaps in the sailing track are a result of a discontinuity in the measurements. At one point during the measurement the battery of the GPS had to be replaced. This can be seen as an interruption in the plotted track.

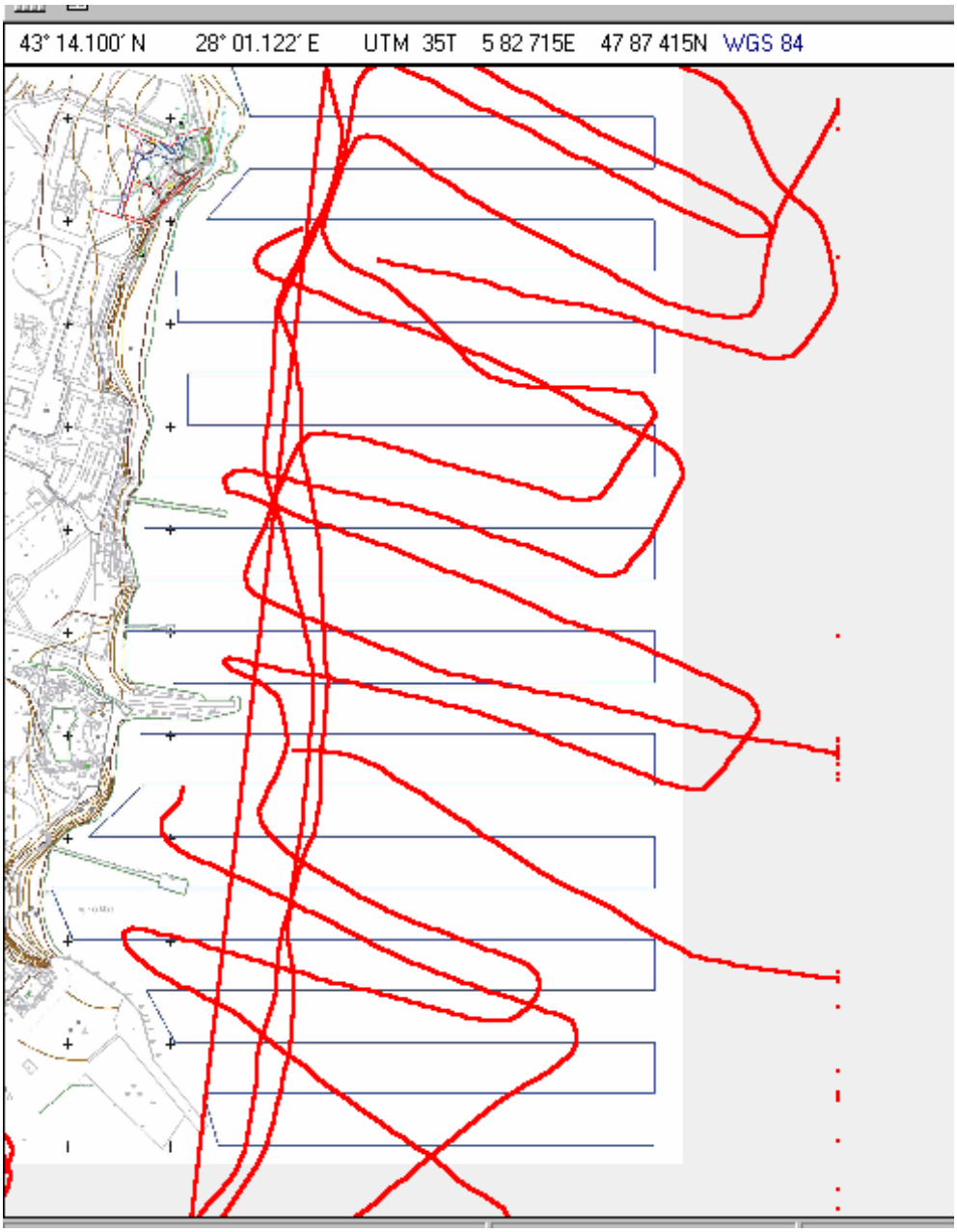

Figure 7.15: Sailing track 2004

This year we used two calibration points to make plots of the bathymetry. These points are shown inFigure 7.16 Point 1 is in front of the Sirius hotel and point 2 is on the end of the jetty.

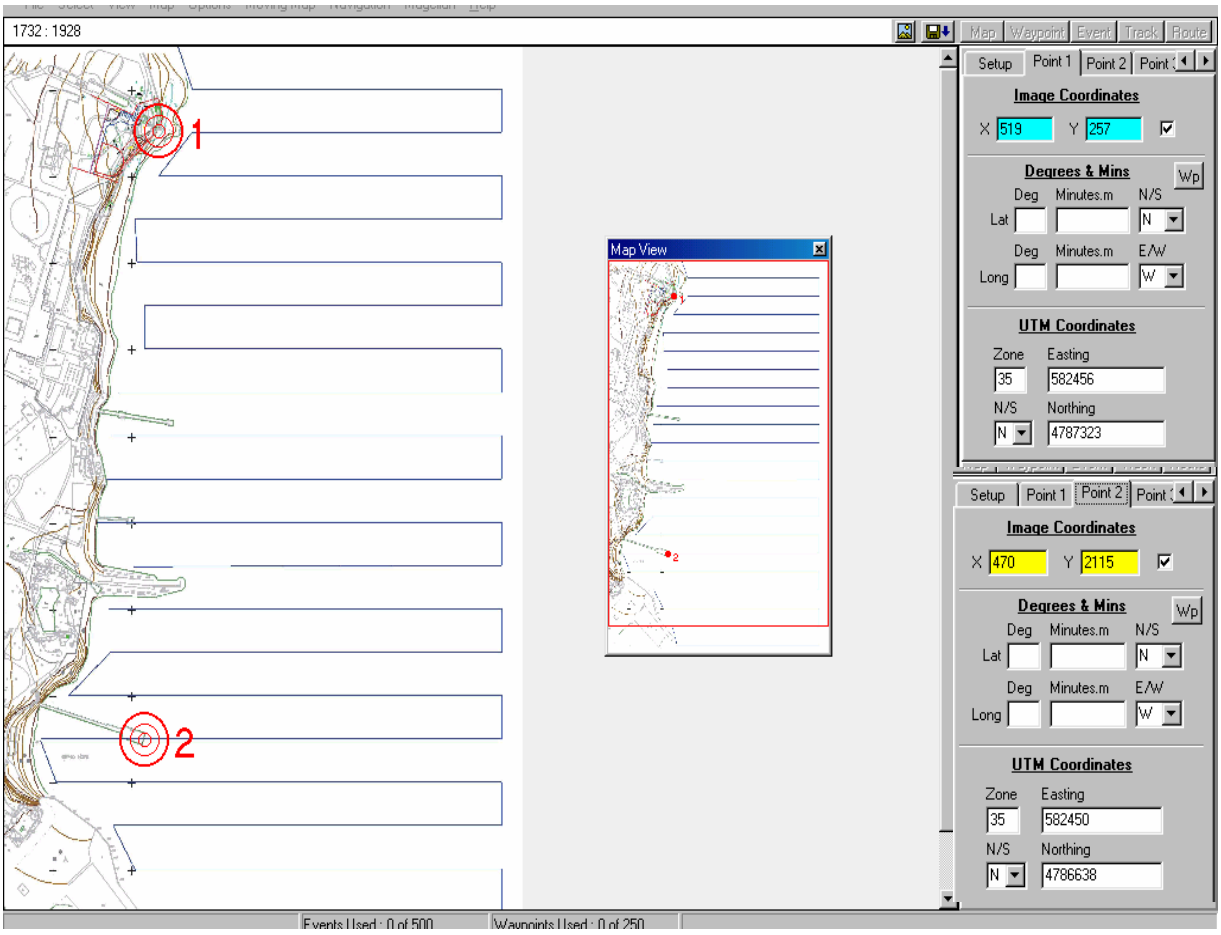

Figure 7.16: Calibration points (notice their UTM coordinates on the right)

In comparison with 2003 this year we measured a larger area. Last year measurements were made from the Sirius hotel to the first jetty but this year we surveyed an almost twice as large region. A consequence is that last year the sailing track is denser. This difference is clear by comparing Figure 7.14 and Figure 7.15 Therefore the measurements in the region from the Sirius hotel to the first jetty of last year will be more accurate.

The results of 2003 are shown in Figure 7.13. In this figure also some ridges are present in the underwater slope. In the report of the previous year it was stated that the echo sounder and the DGPS were not on the same position on the survey vessel. Last year the handhold GPS was handled in the fore and the echo sounder was attached to the vessels hull in the middle. This introduces a distance between these devices. The difference in height between the measured

and actual depth is then added or subtracted depending on the navigation direction of the vessel. This means that the direction of the vessel influences the water depth. So these ridges in the figure have no morphological meaning. This would be quite strange as we can expect there is no long shore current creating sand ripples.

In the results of this year no significant ridges are present in the underwater slope.

An important reason for this could be that this year the Fishfinder and GPS system were on the same position on the survey vessel. This means no distances were introduced between the devices.

The data of the bathymetric maps from 2003 and 2004 are hard to compare qualitatively. This is because a different area was measured and another measuring method was used with different instruments and configuration of the echo sounder and DGPS system on the vessel.

7.18 Conclusion bathymetric survey

This year, the area were the bathymetry was carried out was between the marina and the Sirius hotel. A Garmin handheld GPS, a Fishfinder 100 echo sounder and a fishing boat were used. The accuracy of the measurement is treated. The most significant error in horizontal positioning is 3.2m and 0.25m in vertical positioning. The results of last year's bathymetry are presented and compared with this years result.

It is difficult to compare the results. This year we measured a larger area but, less accurately then last year. Depending on the area of interest on the map the reader must consult one of the depth contour maps.

8 Project Island in sea

By a hotel owner in St. Constantine, Bulgaria the idea arose of creating an artificial island in the sea with a hotel on the island. The location of this artificial island is shown in the figure below.

Figure 8.1: Location of the island in sea

The hotel owner has this idea to meet demands in a growing tourist industry. By creating an artificial island with a hotel on top, an exclusive location for a hotel is realized and part of the island can be used as an attractive beach. The beach in front of Sirius is partly artificial since it has been expanded after the construction of the hotel. In front of the hotel already exists a breakwater, this was constructed due to coastline regression. Additionally, the hotel owner is also the owner of a quarry; therefore he wants to use sand from his quarry for beach nourishment. Dimensions of the island are given in the figure below. A total volume of sand will be necessary in the order of 700.000 m^3.

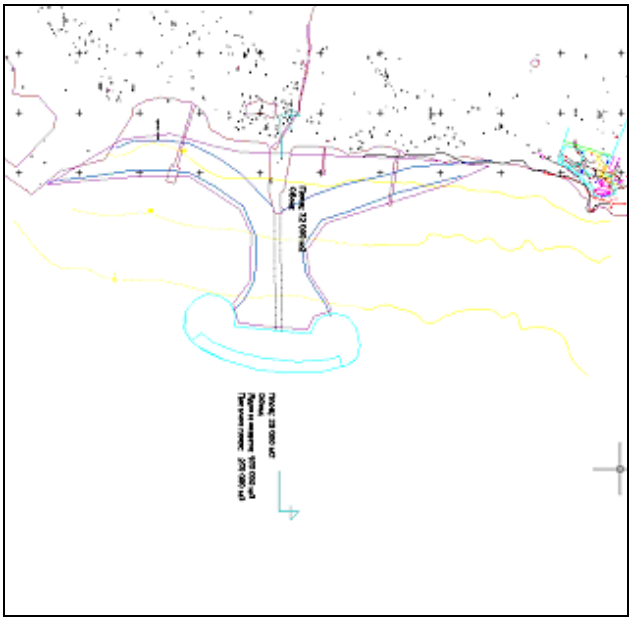

Figure 8.2: Artificial Island in front of Sirius Hotel.

8.1 Demands from the hotel owner:

- Construction of an artificial island
- Hotel on top of the island
- Large beach surface
- Use of sand and probably rock from his quarry as construction materials

8.1.1 Technical problems:

- The island will be exposed to waves and currents, it will be necessary to design and construct shore protections on the island.
- Is the sand (d50, Δ) from the quarry suitable for beach nourishment in front of Hotel Serius.
- The construction of a large island will have a morphological impact on the surrounding beaches. How is this minimalised and what will be the impact on the coastline.

8.1.2 Technical demands:

- The wave and storm conditions conditions need to be known. In this way the design wave can be computed. However wave data is probaly scarce or not available at all. Fortunately by using Argoss wave measurements can be obtained, monitoredby satellites. Otherwise estimates would be derived from windspeed calculation, fetch lenght, depht etc.
- For the design of the island, to make sediment tranpsort computations and to monitor morphological changes a bathymetric survey of the area should be made. The island will be located to a depht of about 13-15 meters. In the direct location of the island a bathymetric survey to a depht of about 20 meters will be necessary. Some distance away from the island a bathymeric survey to a depht of approximately 12 meters will do. Als to the probably large impact of the island asks for survy wich consists from St. Elias Marina to the breakwater of the Golden Sands Beach (see site map above).
- Sediment samples from the quarry and at the beach site, where the artificial island is planned, have to be taken in order to asses whether the sand can be used for beach nourishment.

9 Project white lagoon

9.1 Situation description

The project is situated in Sini Vir, at the Black Sea about 50 km North from Varna, Bulgarya. Tourism is increasing in this region. A hotel owner has some problems and some ambition with his hotel to expand. Therefore he wants to hire a group of specialists to make suggestions to fulfill these demands. A group of students was a suggestion. The hotel owner is willing to invest app. 1000 man hours in this investigation. And he has app. 100,000 euro available for the execution.

9.2 Demands from the hotel owner:

- The hotel owner of the White lagoon wants to expand his activities in his hotel. Therefore he wants to double the amount of rooms to accommodate 1200 tourists before the summer of 2005. He wants a new building, and needs advice for the location of that building.
- The hotel owner has problems with its beach. The beach is very unattractive because it has a lot of algae growth.
- Also he wants a larger beach surface for his tourists.

9.2.1 Technical problems:

- The owner has open ground around his present hotel. But is not certain of the quality of this ground and fears a landslide from the overleaping hill. This is fairly common in the region since it is clay ground.
- The beach and water quality is threatened by algae growth. This might be due to the dumping of water from a hot water sulfur spring through a pipeline app. 50m into the sea. Problems with water circulation are also seen.
- A very big offshore breakwater lies in front of the beach (build app 30 years ago), but no indications of the functionality of the breakwater is found. No indications for longshore sediment transport are seen.

- The beach has to be expanded but sediment sources are scarce in the neighborhood.

Figure 9.1 Overview of the beach, with breakwater

Figure 9.2 Algae growth on the south side

Figure 9.3 From the breakwater, with in the back the hotel on the hill

Figure 9.4 From the breakwater

9.2.2 Technical demands:

- Wave measurements in front of the breakwater. This is necessary as boundary condition to determine the sediment transport capacities and the water circulation. Wave statistics of the region (i.e. Varna) should be available.
- Wind measurements in the bay, wind can attribute to sediment transportation and water circulation. Data required on wind. (Local airfield might be a source)
- Current measurements in the bay. To measure circulation, measurements should be made in summer, when tourists use the beach. Tidal difference is very low in the black sea.

- Sediment transport calculations to determine the sediment transport capacities are important for the nourishment.
- Investigation after bathymetry, important for the sediment computations and the nourishment, important for possible extension of the pipeline.
- Water quality measurements. Samples to determine salinity, oxygen.
- Investigation of possible borrow-sites for sand.

And:

- Knowledge of German language is required

9.3 Further Information:

Contact:

- Boyan
- Manager of the hotel

Appendices

APPENDIX I: Visual Wave measurements 11 October 2004

APPENDIX II: Visual Wave measurements 13 October 2004

APPENDIX III: Measured relative heights of the groin profile (2004)

APPENDIX IV: Calculations rock displacement in the groin profile (2004)

APPENDIX V: Sieve analysis data

APPENDIX VI: Groin calculations

APPENDIX VII: Data and Dn-distribution of small rocks at Marciana Quarry

APPENDIX VIII: Data and Dn-distribution of large rocks at Marciana Quarry

APPENDIX I: Visual Wave measurements 11 October 2004

wave height (cm)							
30	25	25	50	15	15	35	35
20	5	35	30	20	25	25	20
25	20	20	30	25	20	20	15
10	45	25	25	30	15	20	25
25	30	35	35	20	40	25	30
35	30	20	20	15	40	15	25
15	30	10	40	25	15	20	30
20	25	30	30	15	25	20	30
25	15	35	40	20	20	25	15
15	25	25	30	30	30	20	30
35	20	35	30	10	20	15	35
30	35	35	15	25	15	30	15
30	10	10	20	30	15	20	10
20	10	20	30	10	30	20	
30	20	35	35	10	15	25	
15	10	10	25	30	20	25	
10	10	10	15	30	20	30	
25	25	20	25	25	30	20	
30	20	35	15	10	20	25	
20	25	30	15	35	20	25	
15	15	40	20	20	15	30	
10	40	35	20	10	20	20	
35	30	30	20	15	25	30	
45	5	35	25	30	25	25	
30	10	35	20	30	20	20	

APPENDIX II: Visual Wave measurements 13 October 2004

HEIGHT *(different scale)*	**Real Height** *(meters)*	**HEIGHT** *(different scale)*	**Real Height** *(meters)*
1	0,3	5	1,5
2	0,6	5	1,5
2	0,6	5	1,5
2	0,6	5	1,5
2	0,6	5	1,5
2	0,6	5	1,5
2	0,6	5	1,5
2	0,6	5	1,5
2	0,6	5	1,5
2	0,6	5	1,5
2	0,6	5	1,5
2	0,6	5	1,5
2	0,6	5	1,5
2	0,6	5	1,5
3	0,9	6	1,8
3	0,9	6	1,8
3	0,9	6	1,8
3	0,9	6	1,8
3	0,9	6	1,8
3	0,9	6	1,8
3	0,9	6	1,8
3	0,9	6	1,8
4	1,2	6	1,8
4	1,2	6	1,8
4	1,2	6	1,8
4	1,2	7	2,1
4	1,2	7	2,1
4	1,2	7	2,1
4	1,2	7	2,1
4	1,2	7	2,1
4	1,2	7	2,1
4	1,2	7	2,1
4	1,2	7	2,1
4	1,2	7	2,1
4	1,2	7	2,1
4	1,2	7	2,1
4	1,2	7	2,1
4	1,2	7	2,1
4	1,2	8	2,4
4	1,2	8	2,4
4	1,2	8	2,4
4	1,2	8	2,4
4	1,2	8	2,4
4	1,2	9	2,7
4	1,2	9	2,7
5	1,5	9	2,7
5	1,5	9	2,7
5	1,5	9	2,7
5	1,5	9	2,7
5	1,5	10	3
5	1,5	10	3
5	1,5	11	3,3

APPENDIX III: Measured relative heights of the groin profile (2004)

L = 5		L = 15		L = 25		L = 35		L = 45		L = 55	
x	z	x	z	x	z	x	z	x	z	x	z
-13	-2	-13,5	-2	-16,5	-2	-13,8	-0,65	-14,2	-0,91	-14,5	-0,595
-12	-1,074	-12	-0,401	-15	-1,43	-13,3	-0,58	-13,2	-0,72	-14	-0,47
-11	-1,134	-11	-0,341	-14	-1,345	-12,3	-0,43	-12,7	-0,47	-12,8	0,16
-10	-1,154	-10	-0,441	-13	-0,89	-11,8	-0,41	-12,2	-0,36	-12	0,38
-9	-0,134	-9	-0,431	-12	-0,76	-11,2	-0,18	-11,7	-0,26	-11,5	0,4
-8	-0,224	-8	-0,271	-11	-0,43	-10,7	-0,12	-11,2	-0,16	-11	0,3
0	0	0	0	-10	-0,025	-10,2	-0,02	-10,7	0,08	-10	0,28
1,3	-0,004	1	0,01	-9	-0,48	-9,65	-0,04	-9,6	0,2	-7,5	0,04
2	0,361	2	0,394	-8,15	-0,33	-8,1	-0,06	-7	-0,01	-3,7	0,04
3	-0,004	3	0,414	0	0	-7,1	-0,06	-3,5	-0,01	0	0,275
4	-0,089	4	-0,106	1,45	-0,005	-3,5	-0,04	0	0,26	1,4	0,26
5	-0,319	5	-0,551	2	-0,16	0	0,26	1,4	0,26	2,05	0,16
6	-0,209	6	-0,871	3	0	1,4	0,24	2	0,1	3,05	-0,04
7	-0,359	7	-0,901	4	-0,35	2,5	-0,04	3	-0,17	4,6	-0,025
8	-0,679	8	-0,971	5	-0,575	3	-0,17	4	-0,06	5,8	-0,06
9	-1,304	9	-0,951	6	-1,025	4,05	-0,12	4,5	-0,15	7,3	-0,17
10	-2	10	-2	7	-1,255	5,1	-0,13	5,6	0,05	7,7	-0,19
				8	-1,275	5,6	-0,3	6	-0,19	8,3	0,12
				9	-1,71	6,5	-0,07	7,6	-0,11	8,8	-0,23
				11	-2	7,1	-0,22	8	-0,04	10,3	-0,21
						7,6	-0,24	9,5	-0,27		
						8	-0,25				
						8,7	-0,34				
						9,1	-0,43				

z-values related to reference height

APPENDIX IV: Calculations rock displacement in the groin profile (2004)

The graphs of the groin profiles are based on the following values (values are corrected in a way that relative height of x=0 is equal over the years for every profile):

Correction values (used to equal the basepoints of the cross-section, fill in yellow blocks)

L = 5

2002		2003		2004	
XX	0,0	XX	0,0	XX	0,0
x	z	x	z	x	z
0,0	0,0	0,0	0,0	-13,0	-2,0
0,5	0,0	0,5	0,0	-12,0	-1,1
1,0	0,0	1,0	0,0	-11,0	-1,1
1,5	0,0	1,5	0,0	-10,0	-1,2
2,0	0,4	2,0	0,4	-9,0	-0,1
2,5	0,5	2,5	0,5	-8,0	-0,2
3,0	0,0	3,0	0,2	0,0	0,0
3,5	-0,3	3,5	-0,1	1,3	0,0
4,0	-0,1	4,0	0,0	2,0	0,4
4,5	-0,5	4,5	-0,3	3,0	0,0
5,0	-0,3	5,0	-0,3	4,0	-0,1
5,5	-0,3	5,5	-0,3	5,0	-0,3
6,0	-0,4	6,0	-0,2	6,0	-0,2
6,5	-0,5	6,5	-0,3	7,0	-0,4
7,0	-0,4	7,0	-0,3	8,0	-0,7
7,5	-0,7	7,5	-0,6	9,0	-1,3
8,0	-0,8	8,0	-0,7	10,0	-2,0
8,5	-0,9	8,5	-0,8		
9,0	-1,3	9,0	-1,2		
9,5	-1,6	9,5	-1,5		

L = 15

2002		2003		2004	
XX	0,0	XX	0,0	XX	-0,1
x	z	x	z	x	z
-16,5	-1,4	-16,0	-1,5	-13,5	-1,9
-16,0	-1,8	-15,5	-1,5	-12,0	-0,3
-15,5	-1,6	-15,0	-1,5	-11,0	-0,2
-15,0	-1,6	-14,5	-1,4	-10,0	-0,3
-14,5	-1,4	-14,0	-1,2	-9,0	-0,3
-14,0	-1,3	-13,5	-1,3	-8,0	-0,2
-13,5	-1,3	-13,0	-1,1	0,0	0,1
-13,0	-1,3	-12,5	-1,0	1,0	0,1
-12,5	-1,3	-12,0	-0,4	2,0	0,5
-12,0	-1,0	-11,5	-0,2	3,0	0,5
-11,5	-0,3	-11,0	-0,4	4,0	0,0
-11,0	-0,6	-10,5	-0,3	5,0	-0,4
-10,5	-0,4	-10,0	-0,2	6,0	-0,8
-10,0	-0,5	-9,5	-0,2	7,0	-0,8
-9,5	-0,2	-9,0	-0,2	8,0	-0,9
-9,0	-0,5	-8,5	-0,2	9,0	-0,8
-8,5	-0,2	-8,0	-0,2	10,0	-1,9
-8,0	-0,2	0,0	0,1		
0,0	0,1	0,5	0,1		
0,5	0,1	1,0	0,1		
1,0	0,1	1,5	0,7		
1,5	0,1	2,0	0,8		
2,0	0,2	2,5	0,3		
2,5	0,1	3,0	0,5		
3,0	0,4	3,5	0,5		
3,5	0,1	4,0	0,2		
4,0	0,0	4,5	-0,1		
4,5	-0,3	5,0	-0,2		
5,0	-0,5	5,5	-0,5		
5,5	-0,6	6,0	-0,7		
6,0	-0,7	6,5	-0,5		
6,5	-0,6	7,0	-0,5		
7,0	0,3	7,5	-0,4		
7,5	-0,2	8,0	-0,8		
8,0	-0,3	8,5	-0,9		
8,5	-0,9	9,0	-0,8		
9,0	-1,0				
9,5	-0,8				
10,0	-1,1				
10,5	-1,4				
11,0	-2,1				

L = 25

2002		2003		2004	
XX	0,0	XX	0,0	XX	-0,2
x	z	x	z	x	z
-17,0	-1,8	-15,5	-1,7	-16,5	-1,8
-16,5	-1,6	-15,0	-1,4	-15,0	-1,3
-16,0	-1,7	-14,5	-1,2	-14,0	-1,2
-15,5	-1,9	-14,0	-1,1	-13,0	-0,7
-15,0	-1,5	-13,5	-0,8	-12,0	-0,6
-14,5	-1,5	-13,0	-0,7	-11,0	-0,3
-14,0	-1,2	-12,5	-0,8	-10,0	0,2
-13,5	-1,1	-12,0	-0,4	-9,0	-0,3
-13,0	-0,8	-11,5	-0,4	-8,2	-0,2
-12,5	-0,7	-11,0	-0,3	0,0	0,2
-12,0	-0,7	-10,5	-0,3	1,5	0,2
-11,5	-0,6	-10,0	0,2	2,0	0,0
-11,0	-0,2	-9,5	0,1	3,0	0,2
-10,5	-0,3	-9,0	-0,1	4,0	-0,2
-10,0	-0,5	-8,5	-0,3	5,0	-0,4
-9,5	0,0	-8,0	-0,2	6,0	-0,8
-9,0	-0,2	0,0	0,2	7,0	-1,1
-8,5	-0,5	0,5	0,2	8,0	-1,1
-8,0	-0,1	1,0	0,2	9,0	-1,5
0,0	0,2	1,5	0,2	11,0	-1,8
0,5	0,2	2,0	0,0		
1,0	0,2	2,5	-0,1		
1,5	0,2	3,0	0,1		
2,0	0,0	3,5	0,0		
2,5	-0,1	4,0	-0,2		
3,0	0,2	4,5	-0,2		
3,5	-0,1	5,0	-0,4		
4,0	-0,3	5,5	-0,6		
4,5	-0,3	6,0	-0,9		
5,0	-0,2	6,5	-0,8		
5,5	-0,3	7,0	-1,0		
6,0	-0,6	7,5	-1,0		
6,5	-0,5	8,0	-1,0		
7,0	-1,0	8,5	-0,9		
7,5	-0,9	9,0	-0,9		
8,0	-1,0	9,5	-1,0		
8,5	-1,1	10,0	-1,5		
9,0	-1,3	10,5	-1,6		
9,5	-0,9	11,0	-1,4		
10,0	-0,9	11,5	-1,4		
10,5	-1,1				
11,0	-1,3				
11,5	-1,4				

L = 35

2002		2003		2004	
XX	0,0	XX	0,1	XX	0,1
x	z	x	z	x	z
-16,5	-1,8	-16,5	-1,3	-13,8	-0,7
-16,0	-1,2	-16,0	-1,2	-13,3	-0,7
-15,5	-1,2	-15,5	-1,2	-12,3	-0,5
-15,0	-1,2	-15,0	-1,1	-11,8	-0,5
-14,5	-1,1	-14,5	-1,0	-11,2	-0,3
-14,0	-0,8	-14,0	-0,8	-10,7	-0,2
-13,5	-0,8	-13,5	-0,7	-10,2	-0,1
-13,0	-0,7	-13,0	-0,7	-9,7	-0,1
-12,5	-0,8	-12,5	-0,6	-8,1	-0,2
-12,0	-0,6	-12,0	-0,5	-7,1	-0,2
-11,5	-0,5	-11,5	-0,3	-3,5	-0,1
-11,0	-0,4	-11,0	-0,2	0,0	0,2
-10,5	-0,3	-10,5	-0,2	1,4	0,2
-10,0	-0,2	-10,0	-0,3	2,5	-0,1
-9,5	-0,2	-9,5	-0,1	3,0	-0,3
-9,0	-0,4	-9,0	-0,4	4,1	-0,2
-8,5	0,1	-8,5	-0,3	5,1	-0,2
-8,0	-0,2	-8,0	-0,2	5,6	-0,4
0,0	0,2	0,0	0,2	6,5	-0,2
0,5	0,2	0,5	0,2	7,1	-0,3
1,0	0,2	1,0	0,2	7,6	-0,3
1,5	0,2	1,5	0,2	8,0	-0,3
2,0	0,0	2,0	0,0	8,7	-0,4
2,5	-0,1	2,5	-0,1	9,1	-0,5
3,0	-0,3	3,0	-0,3		
3,5	-0,4	3,5	-0,3		
4,0	-0,2	4,0	-0,2		
4,5	-0,4	4,5	-0,3		
5,0	-0,6	5,0	-0,2		
5,5	-0,2	5,5	-0,2		
6,0	-0,7	6,0	-0,2		
6,5	-0,3	6,5	-0,3		
7,0	-0,3	7,0	-0,3		
7,5	-0,3	7,5	-0,4		
8,0	-0,4	8,0	-0,4		
8,5	-0,7	8,5	-0,4		
9,0	-1,0	9,0	-0,5		
9,5	-1,0	9,5	-0,5		
10,0	-1,1	10,0	-0,5		
10,5	-1,2	10,5	-0,6		
11,0	-0,5	11,0	-0,5		
11,5	-0,8	11,5	-0,9		
12,0	-1,4				
12,5	-1,2				

L = 45

2002		2003		2004	
XX	0,0	XX		XX	1,5
x	z	x	z	x	z
15,0	-3,2			-14,2	-2,5
14,5	-3,0			-13,2	-2,3
14,0	-3,1			-12,7	-2,0
13,5	-3,0			-12,2	-1,9
13,0	-2,4			-11,7	-1,8
12,5	-2,3			-11,2	-1,7
12,0	-2,0			-10,7	-1,5
11,5	-1,9			-9,6	-1,3
11,0	-1,8			-7,0	-1,6
10,5	-1,5			-3,5	-1,6
10,0	-1,5			0,0	-1,3
9,5	-1,4			1,4	-1,3
9,0	-1,5			2,0	-1,4
8,5	-1,5			3,0	-1,7
8,0	-1,6			4,0	-1,6
0,0	-1,3			4,5	-1,7
-0,5	-1,3			5,6	-1,5
-1,0	-1,3			6,0	-1,7
-1,5	-1,3			7,6	-1,7
-2,0	-1,5			8,0	-1,6
-2,5	-1,6			9,5	-1,8
-3,0	-1,7				
-3,5	-1,9				
-4,0	-1,6				
-4,5	-1,7				
-5,0	-1,7				
-5,5	-1,6				
-6,0	-1,8				
-6,5	-1,8				
-7,0	-1,9				
-7,5	-1,7				
-8,0	-1,6				
-8,5	-1,8				
-9,0	-1,9				
-9,5	-1,9				
-10,0	-2,1				
-10,5	-2,0				
-11,0	-2,3				
-11,5	-2,0				
-12,0	-2,5				
-12,5	-2,3				
-13,0	-1,4				

L = 55

2002		2003		2004	
XX	0,0	XX		XX	-2,4
x	z	x	z	x	z
17,0	-2,9			-14,5	1,8
16,5	-2,8			-14,0	1,9
16,0	-2,7			-12,8	2,6
15,5	-2,5			-12,0	2,8
15,0	-2,4			-11,5	2,8
14,5	-2,2			-11,0	2,7
14,0	-2,1			-10,0	2,7
13,5	-2,2			-7,5	2,4
13,0	-1,5			-3,7	2,4
12,5	-1,5			0,0	2,7
12,0	-1,2			1,4	2,7
11,5	-1,2			2,1	2,6
11,0	-1,3			3,1	2,4
10,5	-1,5			4,6	2,4
10,0	-1,3			5,8	2,3
9,5	-1,5			7,3	2,2
9,0	-1,5			7,7	2,2
8,5	2,9			8,3	2,5
8,0	2,8			8,8	2,2
0,0	2,7			10,3	2,2
-0,5	2,5				
-1,0	2,4				
-1,5	2,2				
-2,0	2,1				
-2,5	2,2				
-3,0	1,5				
-3,5	1,5				
-4,0	1,2				
-4,5	1,2				
-5,0	1,3				
-5,5	1,5				
-6,0	1,3				
-6,5	1,5				
-7,0	1,5				
-7,5	1,5				
-8,0	1,5				
-8,5	1,3				
-9,0	1,3				
-9,5	1,3				
-10,0	1,3				
-10,5	1,5				
-11,0	1,6				
-11,5	1,7				
-12,0	1,7				
-12,5	1,8				

APPENDIX V: Sieve analysis data

Sample 8					
Mesh size (mm)	Mass (g)		Percentage (%)	Cumulative (%)	$(D_m-D_n)^2$
rest	0				
0,106	0	0	0	0	0,092416
0,15	0	0	0	0	0,0676
0,18	0,1	0,001229	0,122850123	0,122850123	0,0529
0,212	2,3	0,028256	2,825552826	2,948402948	0,039204
0,3	4,8	0,058968	5,896805897	8,845208845	0,0121
0,355	9,7	0,119165	11,91646192	20,76167076	0,003025
0,425	24,8	0,304668	30,46683047	51,22850123	0,000225
0,6	39,7	0,487715	48,77149877	100	0,0361
Total	81,4	1			0,30357

Sieve analysis data sample 8

Sample 5					
Mesh size (mm)	Mass (g)		Percentage (%)	Cumulative (%)	$(D_m-D_n)^2$
rest	0				
0,106	0,1	0,001894	0,189393939	0,189393939	0,067081
0,15	0,1	0,001894	0,189393939	0,378787879	0,046225
0,18	0,1	0,001894	0,189393939	0,568181818	0,034225
0,212	3,1	0,058712	5,871212121	6,439393939	0,023409
0,3	7,2	0,136364	13,63636364	20,07575758	0,004225
0,355	13,2	0,25	25	45,07575758	0,0001
0,425	21	0,397727	39,77272727	84,84848485	0,0036
0,6	8	0,151515	15,15151515	100	0,055225
Total	52,8	1			0,23409

Sieve analysis data sample 5

Sample 12					
Mesh size (mm)	Mass (g)		Percentage (%)	Cumulative (%)	$(D_m-D_n)^2$
rest	0,2	0,003017	0,301659125	0,301659125	
0,106	0,2	0,003017	0,301659125	0,60331825	0,089401
0,15	0,1	0,001508	0,150829563	0,754147813	0,065025
0,18	0,2	0,003017	0,301659125	1,055806938	0,050625
0,212	2,5	0,037707	3,770739065	4,826546003	0,037249
0,3	3,4	0,051282	5,128205128	9,954751131	0,011025
0,355	6,2	0,093514	9,351432881	19,30618401	0,0025
0,425	22,9	0,3454	34,53996983	53,84615385	0,0004
0,6	30,6	0,461538	46,15384615	100	0,038025
Total	66,3	1			0,29425

Sieve analysis data sample 12

Sample 11					
Mesh size (mm)	Mass (g)		Percentage (%)	Cumulative (%)	$(D_m-D_n)^2$
rest	0,2	0,002516	0,251572327	0,251572327	
0,106	0	0	0	0,251572327	0,080656
0,15	0,1	0,001258	0,125786164	0,377358491	0,0576
0,18	0,1	0,001258	0,125786164	0,503144654	0,0441
0,212	2,7	0,033962	3,396226415	3,899371069	0,031684
0,3	5,8	0,072956	7,295597484	11,19496855	0,0081
0,355	12,6	0,158491	15,8490566	27,04402516	0,001225
0,425	30,4	0,38239	38,23899371	65,28301887	0,001225
0,6	27,6	0,34717	34,71698113	100	0,0441
Total	79,5	1			0,26869

Sieve analysis data sample 11

Sample 7					
Mesh size (mm)	Mass (g)		Percentage (%)	Cumulative (%)	$(D_m-D_n)^2$
rest	0	0	0	0	
0,106	0,1	0,001418	0,141843972	0,141843972	0,083521
0,15	0	0	0	0,141843972	0,060025
0,18	0,1	0,001418	0,141843972	0,283687943	0,046225
0,212	2,1	0,029787	2,978723404	3,262411348	0,033489
0,3	4,7	0,066667	6,666666667	9,929078014	0,009025
0,355	10,9	0,15461	15,46099291	25,39007092	0,0016
0,425	27,7	0,392908	39,29078014	64,68085106	0,0009
0,6	24,9	0,353191	35,31914894	100	0,042025
Total	70,5	1			0,27681

Sieve analysis data sample 7

Sample 10					
Mesh size (mm)	Mass (g)		Percentage (%)	Cumulative (%)	$(D_m-D_n)^2$
rest	0,1	0,001253	0,125313283	0,125313283	
0,106	0,1	0,001253	0,125313283	0,250626566	0,045796
0,15	0,1	0,001253	0,125313283	0,37593985	0,0289
0,18	0,4	0,005013	0,501253133	0,877192982	0,0196
0,212	9,3	0,116541	11,65413534	12,53132832	0,011664
0,3	16,2	0,203008	20,30075188	32,8320802	0,0004
0,355	23,9	0,299499	29,94987469	62,78195489	0,001225
0,425	24,5	0,307018	30,70175439	93,48370927	0,011025
0,6	5,2	0,065163	6,516290727	100	0,0784
Total	79,8	1			0,19701

Sieve analysis data sample 10

	Sample 8	Sample 5	Sample 12	Sample 11	Sample 7	Sample 10
D_{50}	0.41	0.365	0.405	0.39	0.395	0.32
σ	0,208248	0,18287	0,205026	0,195919	0,198857	0,167763

D_{50} and σ of all samples

APPENDIX VI: Groin calculations

x (m)	x (cm)	z (m)	z (cm)	y (m)	y (cm)	l/d	BLx	$(X_i-X_{gem})^2$
0.43	43	0.3	30	0.36	36	1.43333	43.98262686	116.89595
0.43	43	0.28	28	0.35	35	1.53571	47.71329611	50.143024
0.46	46	0.29	29	0.37	37	1.58621	40.64960044	200.07733
0.44	44	0.28	28	0.36	36	1.57143	44.13435264	113.6381
0.45	45	0.17	17	0.31	31	2.64706	76.2601998	460.77756
0.3	30	0.23	23	0.26	26	1.30435	96.30209445	1722.8829
0.46	46	0.2	20	0.33	33	2.3	39.5256917	233.13559
0.46	46	0.19	19	0.32	32	2.42105	42.75402892	144.97222
0.4	40	0.24	24	0.32	32	1.66667	37.46952571	300.15369
0.39	39	0.23	23	0.31	31	1.69565	39.94096083	220.62673
0.43	43	0.19	19	0.31	31	2.26316	42.84385766	142.81714
0.36	36	0.19	19	0.27	27	1.89474	56.22145724	2.0362926
0.42	42	0.14	14	0.28	28	3	58.15396067	11.286178
0.31	31	0.15	15	0.23	23	2.06667	88.32920534	1124.5785
0.15	15	0.3	30	0.22	22	0.5	85.32129809	931.88723
0.33	33	0.2	20	0.26	26	1.65	49.09983633	32.428853
0.33	33	0.17	17	0.25	25	1.94118	57.79952213	9.0303383
0.35	35	0.22	22	0.28	28	1.59091	37.10575139	312.89077
0.33	33	0.22	22	0.27	27	1.5	37.5558725	297.16924
0.31	31	0.14	14	0.22	22	2.21429	77.10203318	497.62737
0.16	16	0.25	25	0.2	20	0.64	90.69148936	1288.596
0.34	34	0.22	22	0.28	28	1.54545	33.82881199	439.55882
0.35	35	0.2	20	0.27	27	1.75	37.48733536	299.53691
						$(l/d)_m$=1.77	Blc_m=54.8 m	8952.7467

D_{n50} = 0,212 m ; ρ_r = 2350 kg/m³

Stone data of rock used for regression-equations

Slope 1:3

Parameter	**A**	**B**	**C**	**D**
Singe layer porosity n_v	43.46	-0.2233	3.789	-0.4233
Layer thickness k_t	1.1038	-0.0025	-0.1541	-0.0003
Double layer porosity n_v	36.20	-0.2240	3.613	0.1942

Parameters for regression-equations

Mean value of blockiness BLc_m (%)	54.8
Mean value of elongation $(l/d)_m$	1.77
Standard deviation of blockiness σ(BLc)	20.2
Singe layer porosity n_v (%)	29.4
Layer thickness k_t (m)	0.69
Double layer porosity n_v (%)	34.2

Values used for and results of regression-equations

APPENDIX VII: Data and D_n-distribution of small rocks at Marciana Quarry

Dn	Mass	X	Y	Z	Exceedence
[m]	[kg]	[cm]	[cm]	[cm]	
0,266	48	43	36	30	100,0 %
0,265	47,25	43	35	28	95,5 %
0,264	47,15	46	37	29	90,9 %
0,262	46	44	36	28	86,4 %
0,255	42,5	45	31	17	81,8 %
0,252	40,6	30	26	23	77,3 %
0,223	28,2	46	33	20	72,7 %
0,223	28,1	46	32	19	68,2 %
0,22	27,05	40	32	24	63,6 %
0,217	26,1	39	31	23	59,1 %
0,215	25,5	43	31	19	54,5 %
0,212	24,4	36	27	19	50,0 %
0,207	22,5	42	28	14	45,5 %
0,206	22,2	31	23	15	40,9 %
0,198	19,85	15	22	30	36,4 %
0,198	19,8	33	26	20	31,8 %
0,196	19,05	33	25	17	27,3 %
0,195	18,8	35	28	22	22,7 %
0,189	17,3	33	27	22	18,2 %
0,189	17,3	31	22	14	13,6 %
0,188	17,05	16	20	25	9,1 %
0,187	16,65	34	28	22	4,5 %
0,187	16,65	35	27	20	0,0 %

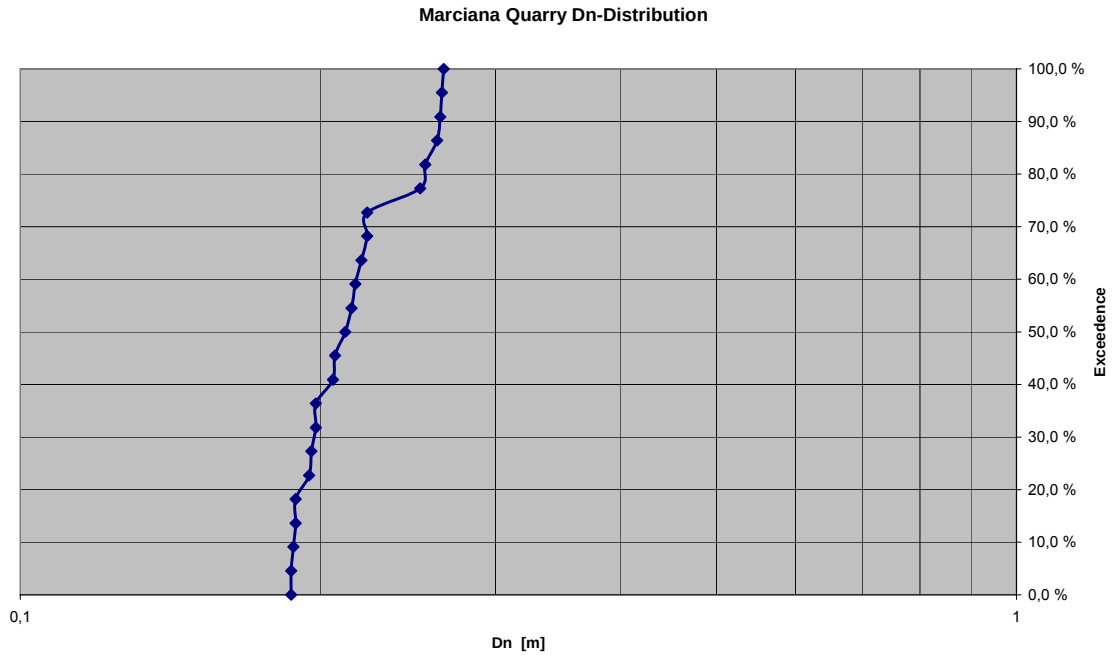

Log-normal graph of Dn-distribution of small rocks

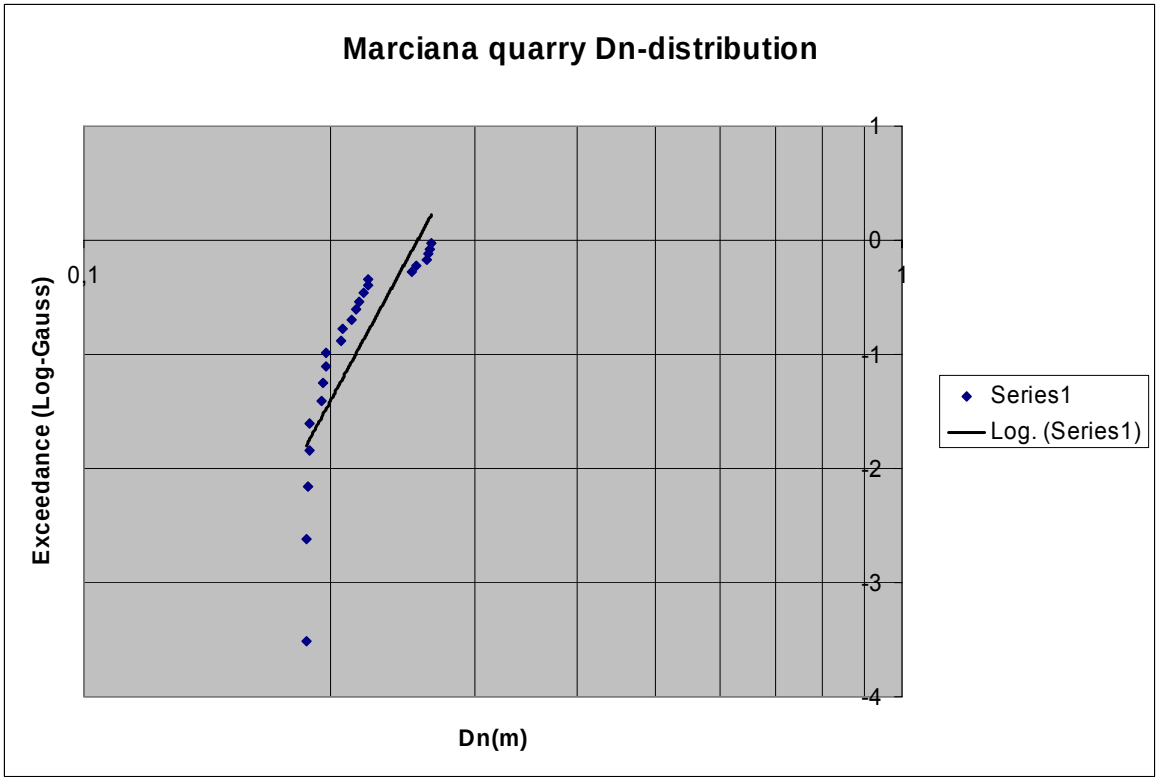

Log-gauss graph of D_n-distribution of small rocks

APPENDIX VIII: Data and Dn-distribution of large rocks at Marciana Quarry

	x (m)	y (m)	z (m)	l/d	BLx (est.)	Volume (m³)	Mass (kg)	D_n (m)
1	3.6	1.32	1.31	2.75	70%	4.36	10240	1.63
2	1.8	1.9	1.4	1.36	60%	2.87	6751	1.42
3	2.44	1.44	1.7	1.69	55%	3.29	7720	1.49
4	2.65	1.2	1.35	2.21	85%	3.65	8575	1.54
5	1.4	1.2	0.75	1.87	75%	0.95	2221	0.98
mean	2.38	1.41	1.30	1.83	69%	2.71	6359	1.36

Main characteristics of five large rocks at Marciana quarry

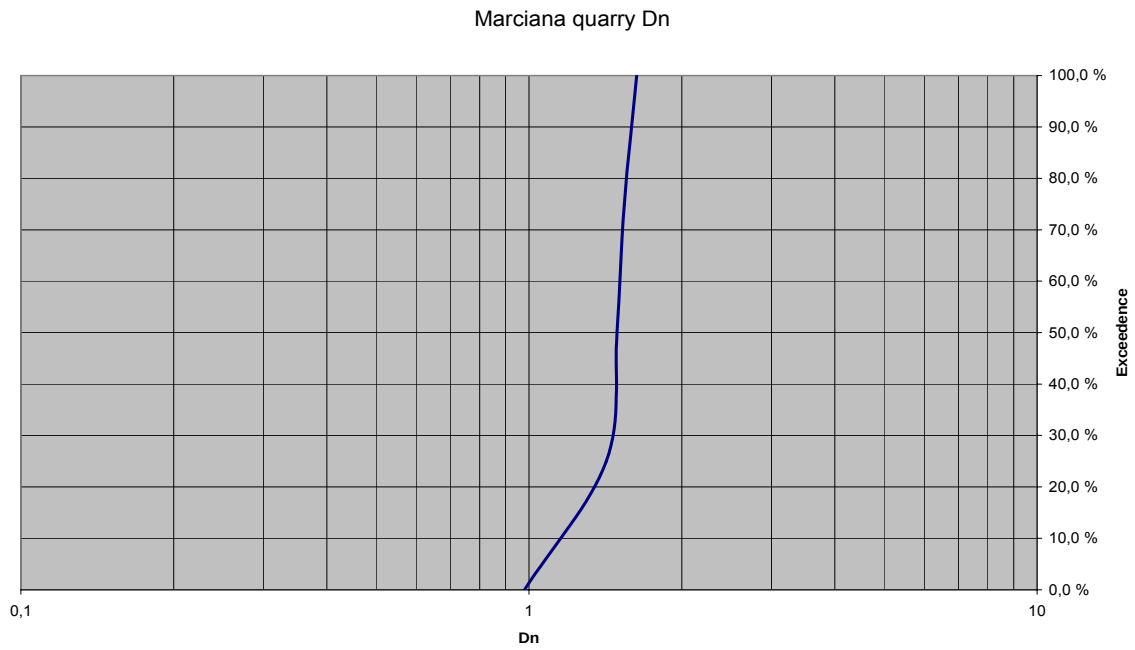

D_n-distribution of large rocks

On the horizontal axis the D_n values are plotted on a logarithmic scale from 0.1 to 1.
On the vertical axis the cumulative percentages (from 0 to 100%) are plotted.